PUBLIC LIBRARY
FEB 11 1941
DETROIT

JOURNAL OF APPLIED PHYSICS

FEBRUARY

1941

Vol. 12 No. 2

Plastic Properties of Solids. I

F. Seitz and T. A. Read

JOURNAL
OF
APPLIED PHYSICS

FEBRUARY, 1941 Vol. 12, No. 2

In This Issue

Page

Physics in the Electrical Industry 83

Physics in 1940 THOMAS S. OSGOOD 84

Theory of the Plastic Properties of Solids. I
FREDERICK SEITZ AND T. A. READ 100

Optical Properties of Rubber LAWRENCE A. WOOD 119

Contributed Original Research

Forced Oscillations in Cavity Resonators E. U. CONDON 129

Production of Proton Beams
E. S. LAMAR, W. W. BUECHNER AND R. J. VAN DE GRAAFF 132

Experimental Investigation of Ion Beam Focusing
W. W. BUECHNER, E. S. LAMAR AND R. J. VAN DE GRAAFF 141

Sparking of Oxide-Coated Cathodes in Mercury Vapor
D. D. KNOWLES AND J. W. MCNALL 149

General Theory of Three-Dimensional Consolidation
MAURICE A. BIOT 155

Field Emission X-Ray Tube
CHARLES M. SLACK AND LOUIS F. EHRKE 165

In Every Issue

Calendar of Meetings 118

Here and There 127

Contributors to This Issue 128

Innovations in Instruments iv

Index to Advertisers x

BOARD OF EDITORS

ELMER HUTCHISSON,
Editor

Associate Editors

FRANCIS BITTER
W. F. BUSSE
ROBLEY D. EVANS
MORRIS MUSKAT
B. E. WARREN
J. B. WHITEHEAD

Publication of the American Institute of Physics

ADMINISTRATIVE STAFF

HENRY A. BARTON,
Director

MADELINE M. MITCHELL,
Publications Manager

JOHN T. TATE,
Adviser on Publications

GOVERNING BOARD

PAUL E. KLOPSTEG,
Chairman
GEORGE B. PEGRAM,
Secretary
KARL T. COMPTON
WHEELER P. DAVEY
FLOYD A. FIRESTONE
HARVEY FLETCHER
R. C. GIBBS
ARTHUR C. HARDY
GEORGE R. HARRISON
A. STUART HUNTER
H. R. LILLIE
FREDERIC PALMER, JR.
W. B. RAYTON
JOHN T. TATE
WALLACE WATERFALL

The JOURNAL OF APPLIED PHYSICS, published monthly at Prince and Lemon Sts., Lancaster, Pa., is devoted to physics in its role as the science basic to other natural sciences and to the arts and industries. Previous to 1937 this publication was known as PHYSICS. It aims to be of service not only in physical laboratories, but also in the laboratories of industrial, chemical, geological, geophysical, meteorological, radio, and similar concerns. The JOURNAL OF APPLIED PHYSICS publishes editorials, news of physicists and reviews, as well as technical papers of applied physics.

Manuscripts should be submitted to Elmer Hutchisson, Editor, University of Pittsburgh, Pittsburgh, Pennsylvania.

Subscriptions and orders for back numbers should be addressed to Prince and Lemon Streets, Lancaster, Pa. or to the American Institute of Physics, 175 Fifth Avenue, New York, N. Y.

SUBSCRIPTION PRICE

	U. S. AND CANADA	ELSEWHERE
To members of scientific societies	$5.00	$5.70
To all others	7.00	7.70

Single copies are $.70 each.

Changes of address and proofs should be addressed to the Publications Manager.

Advertising rates supplied on request. Orders, advertising copy and cuts should be sent to the American Institute of Physics.

Entered as second class matter at the Post Office at Lancaster, Pennsylvania, under the Act of March 3, 1897. Accepted for mailing at the special rate of postage provided for in the Act of February 28, 1925, authorized May 2, 1932.

Copyright 1941, by the American Institute of Physics.

62 GALVANOMETERS

Anyone who uses electrical instruments must soon come in contact with the galvanometer. It confronts the freshman in physics. If he becomes a professor he may use an instrument so sensitive as to require a week to set it up. Or, as a field engineer, he may use one as simple as an alarm clock.

To meet these needs for galvanometers, we regularly list sixty-two. Fifty-three are D'Arsonval (moving-coil) instruments for d-c circuits. They range in sensitivity from 0.05 microvolt to 25; from 0.00001 microampere to 5; from 0.0003 microcoulomb to 0.01. The less sensitive of these can be dropped in a tool kit; the most sensitive require a vibration-free laboratory environment. Most of them, however, go to neither extreme, but are sensitive, relatively simple instruments, used under everyday conditions for research, teaching and testing.

D'Arsonval Galvanometer

One of our unique galvanometers is the Coblentz, which uses a moving magnet and is one or two decimals beyond even the most sensitive D'Arsonval. It can detect thermopile changes of a few microgram calories per sq. mm per second.

For a-c circuits we make three D'Arsonval galvanometers and three astatic dynamometers, of differing degrees of sensitivity and with impedances to suit the user's needs.

Many laboratory studies are facilitated by our Micromax recording or controlling galvanometers. These are integral parts of motor-driven, self-balancing null-type potentiometers and bridges. Highly dependable, they are available in various models and in several hundred ranges.

Astatic Dynamometer

Catalog ED will be sent on request.

New Possibilities In Analysis Offered By Electro-Chemograph

Difficult problems in chemical analysis are now being worked out with the help of L&N's Electro-Chemograph. Some users are speeding up routine chemical analyses. Others are making qualitative and quantitative tests which were never before practical. Some are investigating its possibilities as a guide to industrial process control. And still others are engaged in developing its applications in pure research. We hesitate to predict any limit to the uses which will be found for this L&N adaptation of the dropping mercury electrode principle.

This instrument requires no photographic process or dark room. Automatically inking a curve on its 10-inch chart, it offers all the many advantages of a potentiometer-type Micromax Recorder.

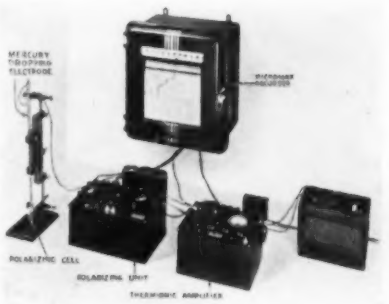

Already in use at the laboratories listed below, the Electro-Chemograph offers possibilities which few research departments can afford to ignore. A description of the equipment is contained in Technical Publication E-94(1) and Reprint E-94(1), both of which will be sent on request.

Location	No. of Instrs.
American Cyanamid Co.	1
Bryn Mawr College	1
University of Cincinnati	1
University of Delaware	1
Eastman Kodak Co.	1
E. I. duPont deNemours Co.	4
Harshaw Chemical Co.	1
Harvard University	1
Los Angeles Police Dept.	1
Memorial Hospital N. Y.	1
Merck & Co.	1
Michigan State University	1
Dr. C. S. Stephano	1
Texas Co.	1
Western Electric Co.	2

Single Contact and Short Circuit Key

Particularly useful in galvanometer circuits. In "open" position, galvanometer damping circuit is automatically closed for quick return to zero. When the key is depressed, shunt is removed, then galvanometer circuit is completed through lower contact. Bakelite base, tungsten contacts, brass springs.

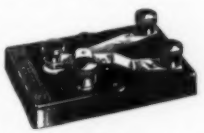

3702 SINGLE CONTACT AND SHORT CIRCUIT KEY . . $3.00
10% off for 6 or more; 20% off for 12 or more.

Jrl.Ad.E(11)

LEEDS & NORTHRUP COMPANY, 4978 STENTON AVE., PHILA., PA.

LEEDS & NORTHRUP

Measuring Instruments · Telemeters · Automatic Controls · Heat Treating Furnaces

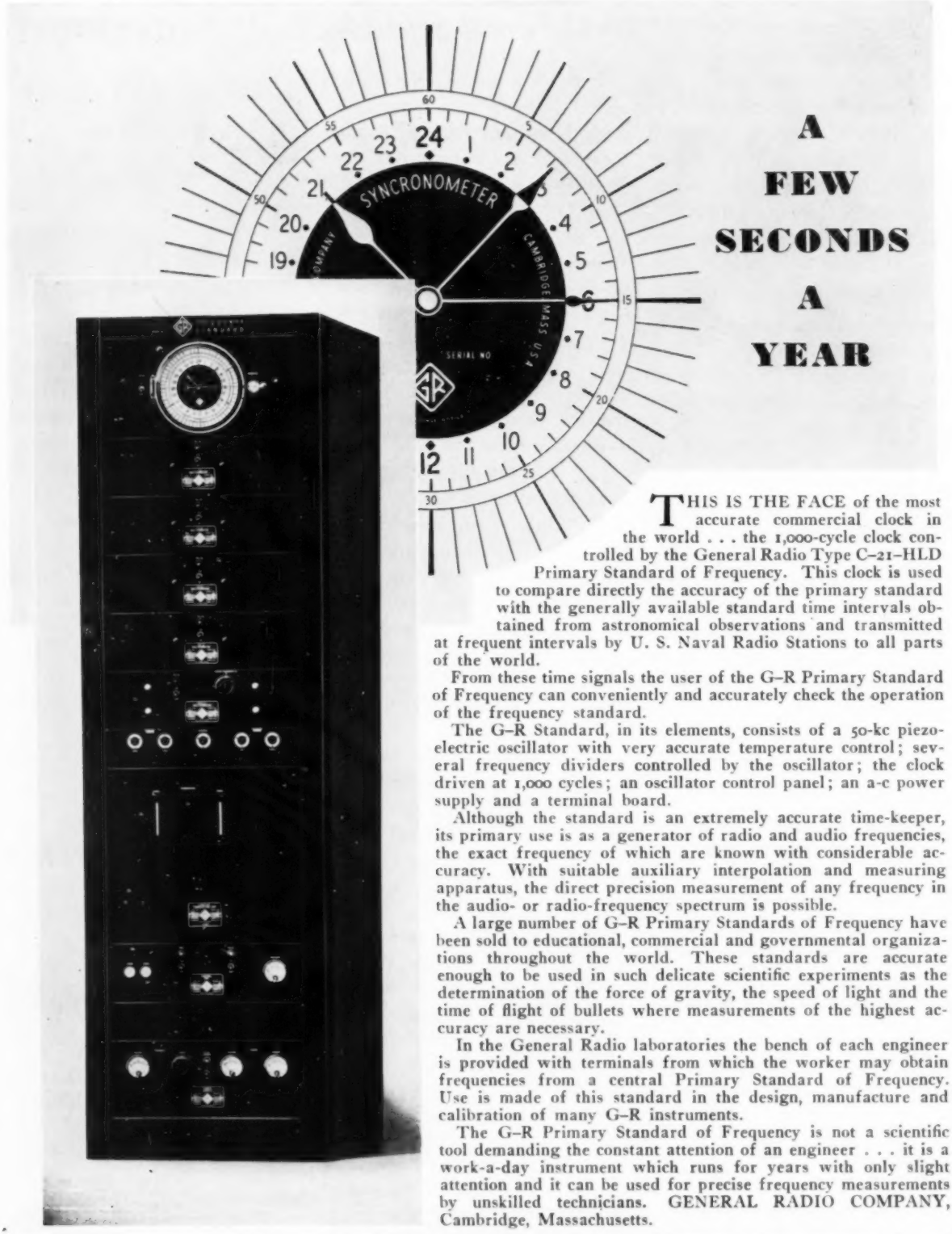

A FEW SECONDS A YEAR

THIS IS THE FACE of the most accurate commercial clock in the world . . . the 1,000-cycle clock controlled by the General Radio Type C–21–HLD Primary Standard of Frequency. This clock is used to compare directly the accuracy of the primary standard with the generally available standard time intervals obtained from astronomical observations and transmitted at frequent intervals by U. S. Naval Radio Stations to all parts of the world.

From these time signals the user of the G–R Primary Standard of Frequency can conveniently and accurately check the operation of the frequency standard.

The G–R Standard, in its elements, consists of a 50-kc piezo-electric oscillator with very accurate temperature control; several frequency dividers controlled by the oscillator; the clock driven at 1,000 cycles; an oscillator control panel; an a-c power supply and a terminal board.

Although the standard is an extremely accurate time-keeper, its primary use is as a generator of radio and audio frequencies, the exact frequency of which are known with considerable accuracy. With suitable auxiliary interpolation and measuring apparatus, the direct precision measurement of any frequency in the audio- or radio-frequency spectrum is possible.

A large number of G–R Primary Standards of Frequency have been sold to educational, commercial and governmental organizations throughout the world. These standards are accurate enough to be used in such delicate scientific experiments as the determination of the force of gravity, the speed of light and the time of flight of bullets where measurements of the highest accuracy are necessary.

In the General Radio laboratories the bench of each engineer is provided with terminals from which the worker may obtain frequencies from a central Primary Standard of Frequency. Use is made of this standard in the design, manufacture and calibration of many G–R instruments.

The G–R Primary Standard of Frequency is not a scientific tool demanding the constant attention of an engineer . . . it is a work-a-day instrument which runs for years with only slight attention and it can be used for precise frequency measurements by unskilled technicians. GENERAL RADIO COMPANY, Cambridge, Massachusetts.

MANUFACTURERS of PRECISION LABORATORY APPARATUS

Journal
of
Applied Physics

Volume 12 February, 1941 Number 2

Physics in the Electrical Industry

THE electrical manufacturing industry can boast of much progress during 1940. Some of the achievements are concerned almost exclusively with fundamental research and herald great things to come. Professor Osgood has covered these in his masterly review in this issue. Others, although bordering on engineering fields, emphasize the possibility of industrial application of recent fundamental research.

Most striking is the announcement of the rise in the output of fluorescent lamps from a quarter of a million per year in 1938 to seven million in 1940. These lamps are a direct result of fundamental research carried on many years ago on the discharge of electricity through high vacua, and of the more recent research on fluorescence and fluorescent materials. Fluorescent lamps are now on the market which are 60 inches long using only 100 watts and providing more than twice as much light as previous lamps of this wattage.

Among the new developments in the x-ray field are tubes which make use of heavy surges of current from a condenser in which electrical energy has been stored. These tubes can take pictures in one ten millionth of a second, such as that of a bullet passing through a block of wood. Even x-ray motion pictures now become possible, allowing detailed studies of the passage of the bullet through the gun barrel. Also announced are compact million-volt x-ray outfits capable of making photographs through four-inch metal castings in two minutes. The tube and the transformer are both contained in a metal can only three feet in diameter and four feet long. Freon gas instead of oil is used for insulation.

The distribution of current in a lightning discharge has been the subject of research which will make possible new methods of protecting power lines against damage from lightning. A record is made by allowing the current in the discharge to magnetize small steel fins which are mounted on the periphery of a rapidly-rotating disk. By this means, it is found that the current often amounts to as much as 160,000 amperes.

More accurate measurements of creep and relax in metals have provided better alloys for the electrical industry. New seals between glass and metals have been devised in which metal inserts are incorporated in bushings of cast glass. By the use of these bushings, hermetically sealed electrical equipment will soon come into common use. The rare metal, columbium, has found industrial application in an alloy of iron which is particularly suitable for high temperature steam turbines. Only a mention can be made of such applications as the use of high electrostatic fields for cleaning dust, pollen, and bacteria from the air and the installation of 1,400,000-volt x-ray equipment.

The applications mentioned here have been limited to the electrical industry. However, advances in any other industry tell the same story. *Progress demands fundamental research.* Now that free thought and scholarship are suppressed in continental Europe, America must take the initiative in supporting basic research. Let us all "shout this fact from the housetops" until research takes its rightful place in our American way of living.

Physics in 1940

By Thomas H. Osgood
The University of Toledo, Toledo, Ohio

IN the atmosphere of war which now envelops much of the civilized world, it is easy to imagine the mingled feelings with which many an academic physicist turns from his peaceful tasks to the field of martial science. Recent technical reports from Europe frequently present the results of incomplete studies, concluding apologetically with a remark that the work begun must be discontinued on account of the war, or more euphemistically, on account of the political situation. By force of circumstances, therefore, this annual summary is now, even more than it has been in the past, a record of what has been accomplished in the western hemisphere.

It would be presumptuous for any one writer to claim that his account of the year's events was a complete one. An attempt is made here to summarize, in language easily intelligible to an industrial or college physicist of moderate experience, the highlights of recent work in a few important fields. The emphasis on elementary points and the looseness of verbal expression as contrasted with mathematical rigor may irk the specialist, but it is hoped that even he will be able to find somewhere a suggestion which may lead him to wider but not less interesting reading.

I

Hahn and Strassmann's discovery of the splitting of uranium atoms into two fragments of roughly equal masses by neutron bombardment was news as sensational as scientific news is ever likely to be. Physicists were, therefore, well prepared in 1940 for the announcement[1] from the Westinghouse Research Laboratories that uranium and thorium atoms behaved in a similar fashion under the influence of energetic gamma-rays. Modern experiments on the transmutation of atoms are far from simple; they utilize as tools many processes which are themselves discoveries of recent date. In the particular case of the photo-fission of uranium and thorium, the primary requirement was an intense beam of gamma-rays of energies of the order of 5 Mev. This can be obtained by bombarding fluorine with protons. The Westinghouse electrostatic generator, an external view of which is shown in Fig. 1, provided a 0.5-microampere beam of protons of 2–3 Mev energy. These were made to fall on targets of CaF_2 and AlF_3, giving rise to gamma-radiation of the required energy, which in turn fell on some uranium placed inside an ionization chamber. The ruggedness and clean design of the target chamber shown in Fig. 2 will be particularly pleasing to those who were trained in research during the wax joint era.

Fission of a heavy atom is not, however, a frequent happening. In the particular experimental arrangement they used, Haxby, Shoupp, Stephens and Wells find that, with 2.9 Mev protons, about one such event occurs for every 3×10^{13} impinging protons. The proportions are: 3×10^{13} protons create 10^8 gamma-rays, which, falling on uranium, cause one atom to divide. Usually the numerical probability of such an occurrence is stated by ascribing an effective cross section to the uranium atom for the particular process under discussion. This turns out to be about 2×10^{-26} cm^2 for the case in question. Even this is ten times as great as the theoretical value estimated by Bohr and Wheeler. In other words, the chance that one quantum of gamma-rays per cm^2 will cause the fission of one atom of uranium is 2×10^{-26}. In comparable circumstances, the cross section of the uranium atom[2] for fission by slow neutrons would be about 3×10^{-24} cm^2. The latter process is, therefore, more than 100 times as probable as the photo-fission.

From the other side of the Atlantic there have come reports of the fission of uranium and thorium atoms by deuteron bombardment. After the preliminary experiments of Gant,[3] Krishnan and Banks[4] show that bombardment by 9-Mev

deuterons gives rise to fission products which are in several cases identical, both as regards chemical behavior and decay periods, with well-known fission products created when these heavy elements are bombarded with neutrons.

At the moment of writing, therefore, there are three methods of causing the fission of uranium and thorium: (a) by neutrons, (b) by gamma-rays, (c) by deuterons. Since (b) and (c) are very recent discoveries, there has hardly been time to investigate the energy relations of these processes, but some progress has been made in the detailed study of the neutron-uranium reaction. For example, a group of workers[5] at Columbia University, with the cooperation of Nier of the University of Minnesota, have investigated the fission of the partially separated isotopes 238, 235, 234 of uranium under neutron bombardment. Nier's mass spectrometer was capable of collecting the 238 isotope completely separated from the others, but preparations of

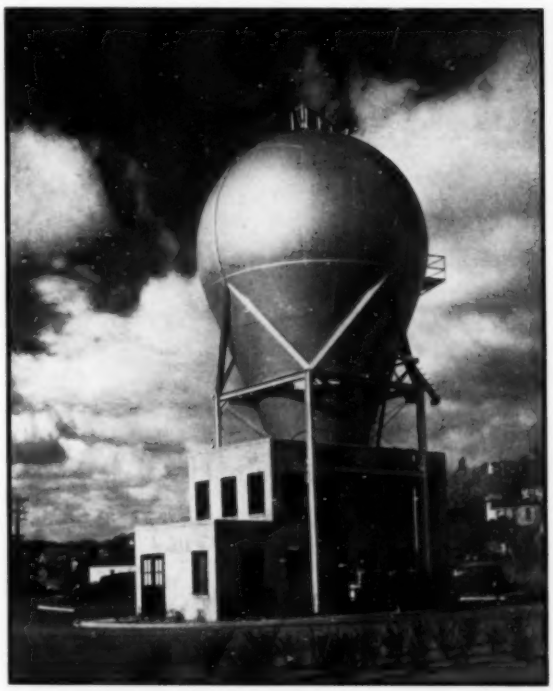

FIG. 1. The Westinghouse electrostatic generator. (Courtesy of E. U. Condon.)

the 234 and 235 varieties were limited in purity by the resolving power of his instrument. Specimens of U^{238} having masses of 3 or 4×10^{-6} g were obtained, those of partially pure U^{235} and U^{234} being smaller in the ratio of the natural abundances of the isotopes. As an indication of the frequency of fission, it is convenient to use the ratio of the number of fissions to the numbers of emitted alpha-particles. The three samples gave the following results under slow neutron bombardment: U^{238}, 0.1 fission per alpha-particle; U^{235}, 18; U^{234}, 2. It is clear that U^{235} is responsible for most of the slow neutron fission observed in unseparated uranium. On the other hand, under fast neutron bombardment, U^{238} appears to play the dominant part, for the observed fission/alpha ratio was large enough to account for all the fast neutron activity of unseparated uranium.

FIG. 2. Adjusting a target-holder at the bottom of the 40-foot accelerating tube of the Westinghouse electrostatic generator. (Courtesy of E. U. Condon.)

More and more known radioactive isotopes of elements in the middle of the periodic table are found to arise from the primary products of the fission of uranium. Grosse and Booth[6] have found radioactive Zr of 17-hour period which gives rise, by negative electron emission, to a (still radioactive) Cb. Since they observe that this continues to emit β-particles, it must decay to a form of Mo, but this Mo does not appear to be the same as that observed by other investigators. There need be no contradiction here, for it sometimes happens, along the chains of these decaying secondary products of fission, that the same chemical elements occur with nuclei in different excited states. The radioactive

decay periods would then be different, though the chemical behavior would be the same. Grosse and Booth point out that in the lightweight group of fission fragments and their descendants, there exists at least one radioactive isotope of each element numbered 35 (Br), 36 (Kr), 37, 38, 39, 40 (Zr), 41, 42, 43 (Ma); and in the heavyweight class are 51 (Sb), 52, 53 (I), 54 (Xe), 55, 56, 57 (La). The separating gap of seven elements remains unfilled.

To illustrate the occurrence of chemically similar elements with nuclei in different excited states in the sequences of radioactive products arising from fission, attention may be called to the work of Segrè and Wu.[7] These experimenters verified the existence of the already known chain

$$\mathrm{Sb} \xrightarrow[10\ \mathrm{min.}]{} \mathrm{Te} \xrightarrow[60\ \mathrm{min.}]{} \mathrm{I} \xrightarrow[22\ \mathrm{hr.}]{} \mathrm{Ce} \xrightarrow{5\ \mathrm{days}},$$

and also found a new chain

$$\mathrm{Te} \xrightarrow[15\ \mathrm{min.}]{} \mathrm{I} \xrightarrow[6.6\ \mathrm{hr.}]{} \mathrm{Xe} \xrightarrow{9.4\ \mathrm{hr.}}$$

Whether the latter represents a branching of the former, or whether the 15-minute tellurium is one of the primary products of fission remains an unanswered question.

There is good evidence[8] that the most probable fragments have masses 96 and 143 (for U^{239}), though rather wide variations in these numbers occur. One of the primary fragments always belongs to the 35–43 group, the other to the 51–57 group; but each of these fragments may thereafter follow one of several possible careers.

We may supplement these results by a condensed summary of the decay processes followed by some of the products arising from gases produced in the slow neutron fission of uranium. This table is taken from a recent paper by Glasoe and Steigman,[9] and is quoted as typical of the work of many investigators.

$$_{36}\mathrm{Kr}^{88} \xrightarrow{3\ \mathrm{hr.}} {}_{37}\mathrm{Rb}^{88} \xrightarrow[4.6\ \mathrm{Mev}]{17.8\ \mathrm{min.}} {}_{38}\mathrm{Sr}^{88}\ \text{probably stable},$$

$$_{36}\mathrm{Kr}^{89} \xrightarrow{1\text{–}5\ \mathrm{min.}} {}_{37}\mathrm{Rb}^{89} \xrightarrow[3.8\ \mathrm{Mev}]{15.4\ \mathrm{min.}} {}_{38}\mathrm{Sr}^{89} \xrightarrow{51\ \mathrm{days}} {}_{39}\mathrm{Y}^{89}\ (?),$$

$$_{54}\mathrm{Xe} \xrightarrow{17\ \mathrm{min.}} {}_{55}\mathrm{Cs} \xrightarrow[2.6\ \mathrm{Mev}]{32\ \mathrm{min.}} {}_{56}\mathrm{Ba}\ \text{probably stable},$$

$$_{54}\mathrm{Xe} \xrightarrow{\text{very short}} {}_{55}\mathrm{Cs} \xrightarrow{\text{very short}} {}_{56}\mathrm{Ba} \xrightarrow{300\ \mathrm{hr.}} {}_{57}\mathrm{La} \xrightarrow{40\ \mathrm{hr.}} {}_{58}\mathrm{Ce}\ (?).$$

The most detailed study yet available of primary fission fragments is that which has come from Bohr's laboratory[10] in Copenhagen. Tracks of such particles in a cloud chamber shown in Fig. 3 reveal deflections and spur tracks with a frequency far in excess of those observed when light particles traverse a gas. This is due to the large masses and high charges of the fragments. Most of the energy of (say) an alpha-particle is frittered away in its passage through matter by collisions with atomic electrons, and it is only rarely that another nucleus receives enough momentum to make it create a visible track. But when the mass of the flying particle is of the order of 100, close nuclear collisions become much more frequent. Unfortunately, the small deviations in the tracks, especially in a heavy gas like argon, become so frequent that even approximate deductions of the masses become unreliable. Brøstrom, Bøggild and Lauritsen say, for example, that "it seems impossible . . . to obtain any measure of the mass sufficiently precise to distinguish the two types of fragment." New problems arise, too, in the calculation of the ranges of such particles in terms of their initial velocities. In the case of alpha-particles, Bohr's 1915 theory accounted adequately for Geiger's empirical rule that the range is proportional to the cube of the initial velocity, a rule which holds within a few percent over all but

perhaps the last fifth of the range. By a timely modification of this theory, Bohr[10] finds that the rate of loss of velocity with distance of a heavy fission fragment should be quite different at different parts of the range. Near the beginning, the rate of velocity decrease should vary as the inverse cube of the velocity. Perhaps the most interesting point of all is that over most of the range, the rate of decrease of velocity should be approximately independent of the charge of the particle, and inversely proportional to its mass. It follows from this that initial momentum alone determines the range of a highly charged massive particle. Since the two fission fragments are bound to have the same momenta, their ranges should be equal, even though their energies differ by 30 percent. This is a matter that can be settled by experiment.

The information which is being gathered concerning the fission fragments is of fundamental importance in the theories of nucleus building. The reader who is interested in this and in the stability of nuclei should consult Turner's[11] recent paper. Its wealth of interesting detail defies abridgment.

II

More than a year ago several pretenders to the title of transuranic elements were comfortably disposed of and relegated to less exalted positions in the periodic table. They were the fission fragments of uranium and thorium. Now there are other claimants whose credentials, as far as they go, appear to be above suspicion. Nishina[12] and a group of his colleagues in Tokyo have bombarded uranium with fast neutrons for periods of a few days. From the activated material a uranium fraction was separated which showed a β-activity of period about one week. They suggested that this was $U^{237}{}_{\gamma}$ which, after decay, should become a transuranic element 93, with properties similar to rhenium. Thus a companion was found for the 2.3-day daughter of 23-minute uranium. The work from Japan was soon corroborated in very definite fashion by a report of independent experiments performed at the University of California. McMillan[13] stated that the β-period was 7 ± 0.2 days; that the maximum energy of the β-spectrum lay at 0.26 Mev.; that some gamma-rays were given off; and, that no internal conversion electrons were emitted. Thus he came to the same conclusion, *viz.* that the daughter product must be an element of atomic number 93. An attempted chemical separation of such an element gave a

FIG. 3. Tracks of fission fragments from a thick layer of uranium. The chamber, 25 cm in diameter, contains argon at a pressure of 8 cm of mercury, and water and alcohol vapors. (Courtesy of C. C. Lauritsen.)

residue which showed no definite α- or β-activity. It seems probable, therefore, that the period of this elusive substance is so long that its radiations are not intense enough to be detected by the methods yet available.

A corresponding uncertainty still exists in the identification of the 2.3-day substance which grows from 23-minute uranium. Indeed, because it does not have the similarity to Re^{75} which would be expected if it occupied a regular position in the periodic table next to uranium, McMillan and Abelson[14] have suggested that it may be the second of a new group of rare earths which starts at uranium.

Experiments a few years ago concerning the angular distribution of light disintegration particles created in a few well-established reactions with light elements showed that the distribution was spherically symmetrical. Now a recent group of papers[15] from the University of Iowa proves that the results of the earlier experiments were only roughly correct. The first reaction studied was $Li^7+H^1\rightarrow 2He^4$. With the improved technique now available, and at higher bombarding voltages than were formerly used,

a pronounced asymmetry appears in the distribution of the alpha-particles. At 100-kev bombarding potential, for example, asymmetry is just barely discernible; but at 400 kev the number of particles ejected in a forward direction is 1.5 or 2 times as great as the number counted at 90° to the incident beam of protons.

Now that the manufacture of radioactive isotopes of the elements has become almost a routine matter, the main interest in the field of artificial radioactivity has shifted from a mere cataloging of isotopes and their decay periods to an interpretation of their meaning in terms of nuclear structure. Any theory of nuclear structure must involve a knowledge of the energies of disintegration particles which may be emitted, and of the masses of the isotopes themselves. A paper by Perlow[16] may be taken as typical of the work being done by the Chicago group of nuclear physicists. The primary purpose of the experiments described was the accurate measurement of the energy released in the disintegration of Li^6 by protons, according to the following reaction

$$Li^6+H^1+\text{kinetic energy} \rightarrow He^3+He^4+\text{kinetic energy}.$$

This is a *nuclear* reaction, so that the letter symbols should be regarded as representing the masses of the nuclei alone, and the kinetic energy terms should be thought of as being expressed in mass units according to Einstein's equation. It must be remembered, however, that the masses of atoms quoted in tables in the literature are the masses of *neutral* atoms, so that corrections must be made before such values can be substituted directly into the equation above. To make the statement of the reaction more compact, the kinetic energy terms are taken together, so that the equation reads

$$Li^6+H^1 \rightarrow He^4+He^3+Q_1. \quad (1)$$

Although the Q_1 term, representing the energy of the reaction, is to be thought of strictly as mass, yet it is always expressed, for convenience, in Mev. Perlow's task was to measure the energy of the ejected He^4 alpha-particles. This was done by comparing their ranges in air with the ranges in air of the alpha-particles arising from the reaction

$$Be^9+H^1 \rightarrow Li^6+He^4+Q_2. \quad (2)$$

In this case the velocities and, therefore, the ranges of the He^4 nuclei are accurately known from earlier experiments[17] employing the electrostatic deflection method. It is not possible here to recount the experimental devices which were necessary to ensure, for example, that the right particles were being observed from the disintegration of the right Li^6 isotope. We give merely the result that with 370-kv protons, the He^4 nuclei had an energy of 1.802 Mev. Now since only two nuclei are formed in the reaction (1), and their masses are nearly in the ratio 4 to 3, they carry away approximately 3/7 and 4/7 of the energy, respectively. The total kinetic energy of the two He particles formed in the reaction is, therefore, 7/3 of 1.802 Mev, or 4.20 Mev. To find the value of Q_1 in the equation, the kinetic energy of the impinging proton (0.370 Mev) must be subtracted from this, leaving $Q_1=3.83$ Mev. For simplicity, approximate masses have been used here. Using the best available values for the masses, Perlow found $Q_1=3.95\pm0.06$ Mev, so the equation finally takes the shape,

$$Li^6+H^1 \rightarrow He^3+He^4+3.95\pm0.06 \text{ Mev}. \quad (3)$$

The main interests of the result still lie ahead, in its application to other nuclear reactions. A little manipulation of Eq. (3) along with two more which represent well-known processes,

$$D^2+D^2 \rightarrow H^3+H^1+3.98\pm0.02 \text{ Mev}$$
$$Li^6+D^2 \rightarrow 2He^4+22.20\pm0.04 \text{ Mev}$$

will show that

$$(2D^2-He^4)-(2H^1-D^2) = (H^3-He^3)+22.23 \text{ Mev}. \quad (4)$$

The mass differences in the brackets on the left of Eq. (4) have been well determined by measurements with the mass spectrograph; almost identical values have been found by Bainbridge and Aston. Both lead to a value about 0.1 ± 0.1 Mev for the quantity (H^3-He^3). The atoms H^3 and He^3 are isobars, that is, they have nearly the same mass, but different nuclear changes. Now H^3 has been found to be a β-rayer, in which case it must decay to He^3, emitting particles with energies given by the value of (H^3-He^3).

The value deduced above is in very satisfactory agreement with the observations of Alvarez and Cornog, and of others, who find that H^3 does emit β-particles with energies of about 0.01 Mev. The indirect approach to the question of the stability of H^3 thus gives a result which is consistent, within experimental error, with the direct observations.

Since the mass of H^3 has for some years been known with greater accuracy than that of He^3, it would appear from the above, at first glance, that the latter could now be calculated. No improvement in the accepted mass of He^3 can be made by this means, however, because the uncertainty in the value of the (H^3-He^3) difference is of the order of 0.1 Mev, which corresponds to 0.0001 atomic mass unit. So precise has the "weighing" of atoms become that such an uncertainty is now scarcely tolerable. The mass of He^3 can, however, be arrived at by a roundabout method involving simple nuclear equations containing the Q_1 evaluated above, and the masses of H^1, D^2, and He^4, which are all known to better than 0.0001 atomic mass unit. Such a calculation leads to $He^3 = 3.01688 \pm 0.00011$ as the best result at the present time.

The masses of elements heavier than those in the first period of Mendeléef's table are known, in many cases, with a smaller percentage error than those of the light elements. But since the most significant feature of atomic masses is the departure from the whole number rule, it is the absolute, rather than the relative error which must be taken as a measure of their precision. Among the intermediate elements, Pollard[18] has collected the available data to make a new table of atomic masses from Ne^{20} to Fe^{57}, and a new mass-deviation graph which demonstrates with admirable clarity (though not for the first time) three interesting facts. First, elements lighter than Ne^{20} have atomic masses somewhat greater than the corresponding atomic numbers, except the standard O^{16}; second, for elements heavier than Ne^{20}, the opposite is true; and third, in the progression from one element to the next, much more violent fluctuations in mass occur in the lighter than in the heavier group. Already these facts are beginning to receive logical explanations in the quantum language of theoretical atom builders.

III

When a particle such as a proton is scattered by a nucleus many times as massive, one of two things may happen. Either the particle is scattered elastically, in which case it comes away from the encounter with all but that small part of its original energy which it transfers to the scattering particle; or else the particle is scattered inelastically. In the latter case the sum of the kinetic energies of the two colliding masses after the collision is less than the total kinetic energy before collision; the balance has been retained in the form of potential energy by the scattering nucleus. Hence, after being scattered, the particle will have considerably less kinetic energy than it originally possessed. At the same time the scattering nucleus will be left in an excited state. The simplest case is that in which the scattering nucleus possesses only one excited energy state above its normal state. Since these two states are sharply defined, it follows that particles of original energy E_0 scattered in a particular direction by such nuclei will have energies E_1 or else E_1-W, where W represents the work required to change the scattering nucleus from its stable to its excited state, and E_1 is a little less than E_0 depending on the angle of scattering. The important point is that the scattered particles at any particular angle will divide into two groups differing in energy by W. Observations made on such scattered particles can therefore lead to an evaluation of W. Apart from its intrinsic interest, this quantity W is of importance in the detailed analysis of radioactive changes.

A group of investigators[19] in England have developed a simple and rapid method for making such studies of the scattering of protons by gases. Protons from the Liverpool cyclotron were passed along the axis of a small tube containing the gas. In the side of the tube, perpendicular to the axis, was a slit through which a wedge- or cone-shaped bundle of scattered protons could emerge, scattered at various angles from different parts of the gas along the axis of the tube. A photographic plate, placed a small distance away, and parallel to the slit and to the proton beam,

caught these protons. Tracks made by the protons in the emulsion of the plate could then be examined, and the energy distribution of the scattered protons could be found. Chadwick and his collaborators found only elastically scattered protons from oxygen, but from neon there came two groups, differing in energy by 1.4 Mev. The group of lower energy was attributed to inelastic scattering from Ne^{20}. Now Ne^{20} can be manufactured by bombarding fluorine with deuterons, in accordance with the equation:

$$F^{19}+H^{2}\rightarrow Ne^{20}+n^{1}.$$

Earlier studies of the neutron spectrum from this reaction led to the conclusion that Ne^{20} must have an excited state 1.4 Mev above its normal state, a fact which receives convincing support from the results of the Liverpool experiment.

IV

During the last year, mesotrons have almost if not quite monopolized the field of cosmic-ray studies. These particles, which formerly passed under several aliases such as meson, yukon, barytron and heavy electron, have masses about 150 times that of the negative electron, and carry a charge equal to that of an electron or of a positron. Their most remarkable property is their instability. With a lifetime of the order of 10^{-6} second they are presumed to disintegrate into an ordinary electron and a neutrino, but the latter is so elusive that convincing experimental evidence is difficult to find. Williams and Roberts[20] and Williams and Evans[21] have provided what is probably the best evidence to date. With a large cloud chamber 2 feet in diameter, they photographed some 50 kilometers of cosmic-ray track. On their negatives they found certainly one and probably two mesotron tracks which ended abruptly in the gas of the chamber, each giving rise at its end to the thinner track of a fast electron proceeding in an entirely different direction. One of these is shown, from two points of view, in Fig. 4. The observations are so important that we quote some of the reasons advanced by the authors for believing that these tracks are what they are claimed to be. In the first place, the slight curvature of the heavy track, produced by a magnetic field of 1200 oersteds leads to a mass of the order of two or three hundred electron masses; the lengths of the tiny branching δ-tracks, formed by the knocking-on of electrons, are much greater than they would be if they were caused by a proton; the directions of these δ-particles, like splashes of mud created as a wheel rolls forward, show that the assumed direction of flight of the heavy particle is correct (that is, the heavy particle has not been created by the lighter one); and the obvious kink near the end of the heavy track shows that the mesotron is slowing down, having at the kink an energy of only a few Mev. In the second place, the fine track has about the same linear density of droplets as other adjacent electron tracks; its curvature leads to an estimate of its energy compatible with half the annihilation energy of a mesotron (the neutrino would take the other half); the initial energy of the electron cannot have been supplied by the kinetic energy of the mesotron, and since it is so great, it can only be due to annihilation of mass.

More indirect evidence for the instability of the mesotron is provided by the experiments of Rossi, Hilberry and Hoag[22] which confirm and

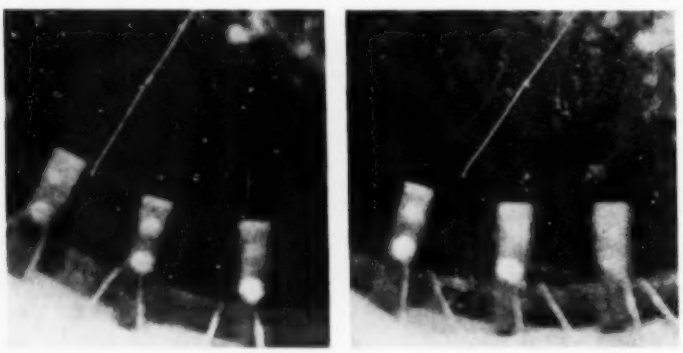

FIG. 4. Cloud-chamber photograph, taken by E. J. Williams and G. E. Roberts, showing two views of a mesotron track ending in the gas of the chamber, and giving rise to a disintegration electron. The mesotron track is the heavy one running diagonally from top right toward bottom left. The electron track is the thin line starting at the end of the mesotron track. Chamber is 2 ft. in diameter. (Reproduced from Nature **145**, 102 (1940).)

extend other similar work.[23] With an appropriately shielded triple Geiger-Müller counter they recorded the mesotrons at various altitudes from about 200 meters to 4300 meters, thus determining how the particles were absorbed during their long passage through the atmosphere. Then the manner of their absorption in carbon was determined by the simple use of graphite blocks. From a comparison of the counts it was clear that air was apparently a much better absorber, mass for mass, than graphite. The discrepancy is only an apparent one, however, for in their long passage through the atmosphere, a considerable fraction of the mesotrons have time to decay and hence appear to be absorbed, though they really just disappear. (The electrons to which they give rise have less penetrating power and a smaller specific ionization than their parents.) In a compact absorber like graphite, the time of passage is so small that only a negligible percentage of the particles decay. All the data, as well as those of Williams, lead to a value of the order of 2×10^{-6} sec. for the lifetime of the mesotron.

It may now be taken as definitely established that mesotrons are not a primary component of cosmic radiation, but that they are produced high up in the earth's atmosphere. Dymond's[24] experiments show that vertically moving mesotrons have a maximum intensity at a height of 16 km where the pressure is 80 mm of mercury. There the intensity is nine times the ground value, but it falls off rapidly on both sides of the peak. It is interesting to note that the position of the maximum is the same for all cosmic-ray particles taken together, that is, as they are recorded by unshielded counters. The maximum intensity in this case is, however, much more than nine times the ground value.

Dymond's results are in reasonably close numerical agreement with those found in what is probably a more accurate series of experiments carried out by Schein, Jesse and Wollan;[25] and the arrangement of counters used by this trio was such as to give definite evidence that the mesotrons were produced by non-ionizing particles, presumably photons, as Bhabha and others suggested on theoretical grounds about two years ago. We are able to reproduce in Fig. 5 a

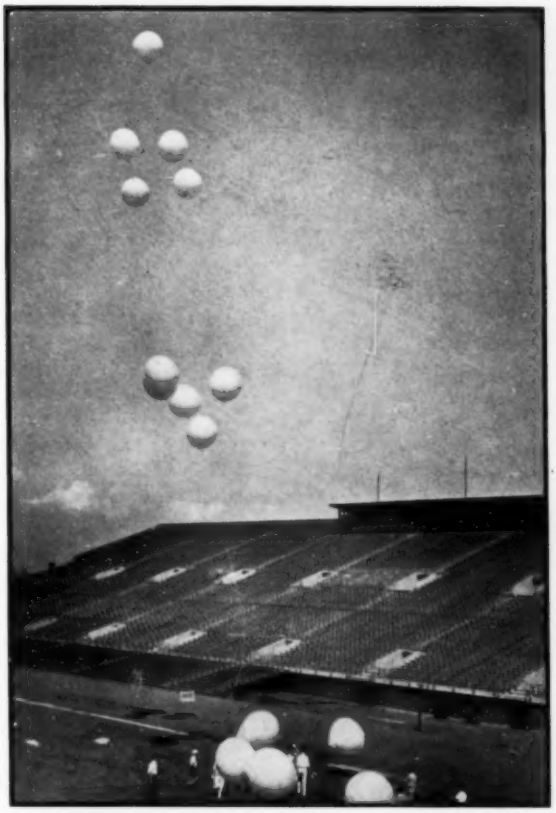

FIG. 5. Start of a cosmic ray balloon flight from Stagg Field, University of Chicago. (Courtesy of A. H. Compton.)

photograph showing the start of a high balloon flight from Stagg Field in Chicago. The balloons carry the counters and automatic radio transmitter weighing altogether nearly 40 lb. to a height of some 16 miles; there they remain in equilibrium for several hours, until at nightfall the balloons cool and begin to descend.

Swann and Ramsey[26] have brought forward more evidence to show that occasionally mesotrons do not come singly but in multiples. This discovery arose from the observation that some of the ordinary shower rays passed through several centimeters of lead without giving rise to further showers. The frequency of the occurrence was of the order of once per thousand ordinary showers. These small nonmultiplying showers are considered to consist of mesotrons. Somewhat similar experiments have been done by Jánossy and Ingleby[27] in England, and by Wataghin[28] and his collaborators in Brazil, all of them using electrical counting methods.

FIG. 6. Cloud chamber photograph of a pair of slow mesotrons, positive and negative, stopped by a thin copper plate which appears as a horizontal white band across the middle of the picture. Taken by Herzog and Bostick in an airplane at an altitude of 29,000 ft. (Courtesy of A. H. Compton.)

Josephson, Froman and Stearns[29] point out that their own slightly different arrangement of counters enables them to deduce that these small mesotron showers are not all produced high up in the atmosphere where most mesotrons are made, but may come from near the counting apparatus. A welcome graphic record of the phenomenon is found in the pictures of Powell,[30] of Braddick and Hensby[31] and of Herzog and Bostick.[32] Some of these authors interpret their work as establishing the existence of mesotron pairs. The pictures show, like Fig. 6, that the positive and negative particles which form a pair have initially the same direction.

There is a possibility, of course, that these pairs are merely small showers with an unusually narrow spread. It may be that very slightly diverging two-particle showers are more common that those at angles greater than a few degrees, for they would thus be photographed more frequently, and yet, in electrical counting experiments, they might well be recorded as single particles. Bose and Chowdhry[33] have found diverging mesotron tracks produced directly in the emulsion of photographic plates, but they have reported none so closely parallel as those which appear in the cloud-chamber pictures. Theory lags behind somewhat in the explanation of these small hard showers, but it seems to be definitely established on the experimental side that most are produced by photons, some by charged mesotrons, and a few by neutral mesotrons.

Now that the weather has been found to have an effect on the intensity of cosmic rays, the whole subject will probably begin to appear less abstruse to the layman. Blackett was the first to point out that the effect of atmospheric temperature on cosmic-ray intensity could be explained by considering the effect which temperature changes have on the mesotron component of the radiation. Mesotrons are produced, as we have said, near the outer fringe of the earth's atmosphere, after the primary radiation coming from outer space has traversed a small but definite amount of matter. If, now, the region where mesotrons originate is moved higher or lower, the mesotrons will reach the earth in a longer or in a shorter time, and this will cause changes in the numbers of them which decay before reaching sea level. This is exactly what happens when the mean temperature of the atmosphere changes. If a rise in temperature occurs, the air becomes less dense, and therefore in order that approximately the same barometric pressure may be exerted, the center of mass of a vertical column of the atmosphere must recede farther from the earth's surface, and a corresponding motion of the mesotron-producing region takes place. Most of the work on this topic is referred to in a paper by Loughridge and Gast[34] who themselves have investigated the effect of advancing warm or cold fronts on cosmic-ray intensity. A moving mass of cold air, tending to keep close to the ground, drives a wedge under the warmer air in front of it, in much the same way as an ordinary snow shovel does when used to clear away a light fall of snow from a concrete path. Just after the cold

front has passed, the average temperature is lower, the center of mass of air above a particular station is lower, the mesotron-producing layer is lower, and the cosmic-ray intensity shows an increase of the order of one percent. Loughridge and Gast find appropriate changes in intensity for both warm and cold fronts on the west coast of this continent, but observers[35] in Japan find the effect only for the warm fronts, because the cold fronts which move over that country are comparatively shallow, and are topped by warmer air masses.

V

Attention has been directed from time to time during the last twenty-five years to faint spots found on Laue x-ray pictures which are not immediately explicable as Bragg reflections from recognized internal planes in the crystal which is being examined. A revival of interest in this subject has been brought about recently by work in such widely separated places as Chicago and Bangalore. It will be remembered that in making a Laue photograph, a heterogeneous beam of x-rays is sent through a single piece of crystal. The ordinary spots are caused by reflection of those components of the beam which have the right wave-lengths to satisfy the conditions for Bragg reflection from fixed internal planes.

If a monochromatic beam of x-rays is allowed to fall in a fixed direction on a powdered crystal, the scattered radiation which is observed at various angles shows marked irregularities of intensity. The most prominent maxima are those which are formed by Bragg reflection from small crystals which happen to be orientated appropriately, but when these are allowed for there remains a varying intensity of scattered radiation. This more or less continuous background is caused by the process known as diffuse scattering. Long ago Debye showed that this diffuse scattering was due to thermal vibration of atoms in the crystal, which means that it should depend markedly upon the temperature. It is this diffuse scattering which is responsible for the extra spots on Laue diagrams. Debye's theory, modified and extended by many able workers, has been found valid in many experiments; but neither the theory nor the experiments seem to have possessed the delicacy which characterizes Zachariasen's[36] new work on this subject. His analysis of the standard procedure

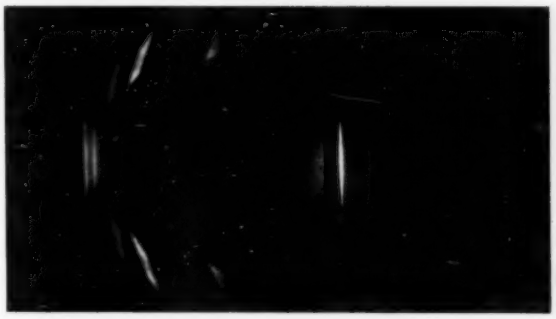

FIG. 7. Laue photograph of KCl showing a diffuse spot. The primary beam is rich in Cu $K\alpha$-radiation but contains also some continuous radiation. The direct beam, well collimated by two narrow slits, makes the image farthest to the right. The diffuse spot is the right-hand one of the two close images at the left, and is due to the monochromatic Cu $K\alpha$-radiation. All the other spots are regular Laue spots caused by the continuous part of the incident beam. Exposure time, 32 hours. (Courtesy of W. H. Zachariasen and S. Siegel.)

for taking Laue photographs shows that the radial streaks due to diffuse scattering found by many observers should be a general feature of all Laue pictures, but whether they occur or not is a question of exposure times, since their intensity is small particularly for crystals with high characteristic* temperatures. With monochromatic radiation these radial streaks show, as the theory predicts, a very rapid variation of intensity in the direction of their length, so rapid indeed, that the maxima appear as spots. Their positions are almost, but not quite identical with the Laue directions; and, therefore, in order that they may not be entirely masked by the many times more intense Laue spots, the crystal which is used to examine them must be set so as just to avoid[37] the regular Bragg reflections. A photograph taken by the Chicago workers is reproduced in Fig. 7 which shows one of these diffuse spots very close to a regular Laue spot which has been enormously reduced in intensity by the slight off-setting of the

* At very low temperatures the atomic heat (specific heat × atomic weight) has a low value, increasing rapidly with increase in temperature. The characteristic temperature of a substance is that temperature at which its atomic heat reaches the value 5.5. The Dulong and Petit value is about 6.0.

crystal. The incident beam was a filtered one, containing much copper $K\alpha$-radiation and a little continuous radiation. It is the latter which causes the regular Laue spots, but the extra spot is due to the diffuse scattering of the monochromatic copper $K\alpha$ line. One of the necessary conditions for the production of such photographs as these is a very small divergence of the incident beam. Zachariasen gives it as his opinion that this new effect was not discovered in earlier studies because the radiation used was too divergent, and the ionization chambers often used to detect the diffusely scattered radiation recorded merely an average value over a comparatively large angular range.

Broadly speaking, the new theory shows that these maxima of diffuse scattering are caused by temperature vibrations of the crystal lattice, the atoms moving as whole units. Raman and Nilakantan[38] have given a more pictorial idea of the process* by pointing out that temperature vibrations in the crystal, being reflected time and again from its boundaries like sound waves in a box, will set up a standing wave pattern in the crystal. This amounts to adding another periodicity to the crystal lattice, although it involves a dynamic, not a static, stratification. Furthermore, these stratifications will occur in many different directions, so that when monochromatic radiation is sent through the crystal the radiation picks out those planes of stratification which may appropriately reflect it, in the same way as a monochromatic x-ray pencil is reflected in Debye-Scherrer powdered-crystal photographs. Raman and Nilakantan add to the validity of this point of view when they report that upon passing a beam consisting mainly of both copper $K\alpha$- and $K\beta$-radiation through a diamond crystal, two extra diffuse spots are found, corresponding to the two important wave-lengths in the primary beam.

An interesting application of x-ray analysis to the study of diffusion in solids has been made by DuMond and Youtz.[39] A kind of artificial crystal was built up of alternate layers of gold and copper on a glass plate, the "grating space" being about 100A. $K\alpha$-radiation of molybdenum was reflected from this in the Bragg fashion, the main difficulty being that the glancing angles were so small (about 12 minutes of arc) that special precautions had to be taken to prevent the obliteration of the diffracted beam by the intense direct radiation. The first order was found easily, but higher orders were searched for in vain. This implies that the alternate layers of atoms of gold and copper, from the start, or at least by the time diffraction photographs could be made, lacked sharp boundaries; it implies further that the layers of gold already possessed a sinusoidal distribution of atoms, extending on both sides into the adjacent layer of copper. (The gold atoms are so much heavier than those of copper that the diffraction effects are due almost entirely to the former; the copper merely acts as a transparent spacer.) Only such a sinusoidal distribution will give a strong first-order reflection and a complete absence of higher orders.

From time to time as the artificial "crystal" aged over a period of a month, x-ray photographs were taken which showed changes in the shape and intensity of the first-order reflection. These changes the authors interpret for the time being in terms of the various harmonics which they consider to be present in the Fourier series representing the original distribution of gold atoms as they were laid down. The high harmonics, corresponding to highly localized irregularities of concentration, would naturally tend to disappear first, since the distances through which atoms would have to diffuse to smooth out these harmonics are quite small. The fundamental frequency, with the space periodicity of about 100A would persist for a longer time.

It appears from the absence of second and higher orders of reflection that within a day after the manufacture of such an artificial metal "crystal" the distribution of gold atoms in one gold layer loses its high harmonics and conforms to a simple sinusoidal variation of concentration. DuMond and Youtz think that on this account the method should prove valuable for the study of diffusion in solids, for it is then "a very simple matter to compute the diffusion coefficient from the grating constant and the time rate of decay of the diffracted intensity."

* *Added in proof:* The view presented here requires modification, for the effect found by Raman and Nilakantan is apparently not caused by diffuse scattering. See Raman and Nilakantan, Nature **146**, 686 (1940).

Among other important papers in the field of x-rays are those of Barrett and Geisler,[40] who photographed and interpreted streaks in Laue diagrams caused by a peculiar clustering of atoms which occurs during the aging of alloys; of Munier, Bearden and Shaw,[41] who have extended double crystal spectrometry to long wave-lengths; and of Abelson,[42] who has used x-ray spectra in the identification of products of radioactive decay.

VI

From time to time new experiments are performed which increase the accuracy with which atomic constants such as the charge of the electron, e, and the Avogadro number, N, are known. The value of e as determined by Millikan's original experiments has been considered uncertain for several years, mainly because of doubt as to the true value of the coefficient of viscosity of air. For example, the five best determinations of this coefficient in the years 1936–37–38 have an extreme variation of nearly one third of one percent. Their weighted mean is quoted by Bearden as $1833.1 \pm 1.3 \times 10^7$ in c.g.s. units at 23°C. The situation has been showing steady improvement, however, because eight or ten years ago there was a spread of nearly one percent in the results obtained by reliable workers.

About a year ago, Bearden[43] published an account of a new determination of the viscosity of air which far exceeds any other in precision. It is the first step toward a new measurement of the electronic charge by the oil drop method. Experience has shown that the most reliable methods are those involving a rotating cylinder, or flow through a capillary tube, but since the latter is subject to several corrections and one or two uncertainties, Bearden chose the rotating cylinder method. In essence, the experimental part consisted in measuring the torque transmitted through a layer of air about one cm thick from an inner cylinder rotating continuously, to an outer cylinder suspended by a torsion wire. Many quantities had to be known with high precision, and in obtaining the results listed below, valuable help was received from the physicists at the National Bureau of Standards. Here are five measurements made by them of the outside diameter of the inner cylinder: 12.44218, 12.44226, 12.44233, 12.44226 and 12.44218 cm. Since the measurements were made at different places on the cylinders, these figures speak for themselves in showing the geometrical perfection of the machining and grinding, and the accuracy of the observations. It happens that measurements of the inside diameter of a cylinder cannot be made with the same precision as outside measurements, so, in order to find the inside diameter of the outer cylinder with the necessary accuracy, Bearden closed the cylinder at both ends with flat plates and weighed it empty and then full of water. The density of water is known to two parts in a million, so that no troublesome uncertainty is introduced on that score. But the consistency of the volume determinations achieved by this method will come as a surprise to many readers, and will give them, as it gave the writer, a better understanding of what good technique can accomplish. The results of six trials are: 4573.831, 4573.807, 4573.843, 4573.783, 4573.779 and 4573.807 cm^3. The diameter of the cylinder is deduced as 14.95289 ± 0.00005 cm.

Probably the most uncertain quantity in this measurement of the viscosity of air was the torsion constant of the wire used to suspend the outer cylinder. This was determined in vacuum by the usual method of finding the period of oscillation of an object of calculable moment of inertia suspended by the wire. Different wires were found to give results of varying consistency but a technique was worked out for handling and treating specially made tungsten wires so that the torsion constant was practically independent of the period. The torsion constant of the wire used in the final experiments was known to about one part in a hundred thousand.

As a check on the precision of the experiment Bearden used two inner cylinders of different diameters. They gave results which agreed within two or three parts in a hundred thousand. It is, therefore, with some satisfaction that it can now be asserted that the viscosity of air at 23°C is $1834.12 \pm 0.06 \times 10^7$ c.g.s. units. This is 0.05 percent higher than the weighted average of other recent determinations which was quoted above. It is too soon yet to derive a new very

accurate value of e because there are available several sets of data from oil drop experiments which lead to the same number of values of e, differing among themselves by far more than the estimated experimental errors. Bearden reports, however, that he has a new oil drop experiment in progress, in which argon is to be used instead of air. We may soon learn whether or not this method gives the same value of e, $4.8025 \pm 0.0004 \times 10^{-10}$ e.s.u., as the x-ray method which has been relied on for several years.

In spite of the reliance which has been placed on this value, there has been a healthy skepticism concerning its validity. Two main criticisms have been leveled against the x-ray values of e and N. (Either constant can be derived from the other because their product Ne is equal to the faraday which is determined directly by electrolysis.) In the first place, if we write $N = M/\rho f$, where M is the molecular weight of a crystal, ρ its density and f the volume allocated to each molecule, it is clear that the value of N depends on one quantity, ρ, which must be found from sizable (though perhaps microscopic) fragments of crystal, and on another quantity, f, which is of atomic dimensions and can be determined only by x-ray diffraction or reflection. If crystals were geometrically perfect there would be no difficulty; but most of them are known to have a mosaic structure which introduces slight divergences from parallelism in the atomic planes, just as even in a well-built brick wall the bricks are not all in perfect alignment. In the second place, the Bragg reflection which is commonly used in the x-ray analysis gives information only about the surface layers of a crystal, and may not give true indications of the structure inside. Following others, Miller and DuMond[44] have recently looked into this question. The general scheme of their experiments was first to find the lattice constant and density of quartz (a crystal commonly used by earlier workers) by methods somewhat different from those ordinarily employed; and second to find the lattice constants and densities of well-annealed metallic crystals, and later to redetermine these constants after the metals had been mechanically worked by pressing, and then re-annealed. The lattice constants remained practically unchanged. No differences in densities were found greater than about one part in twenty thousand, which are hardly significant in the determination of e. However, when the metals were maltreated by hammering, the densities changed noticeably; that of silver increased by one part in three thousand, while that of aluminum decreased in about the same proportion. The authors conclude that if any correction ought to be applied to the x-ray value of e in view of the two criticisms mentioned above, this correction should be only on account of a mosaic effect, and should not exceed -0.04 percent.

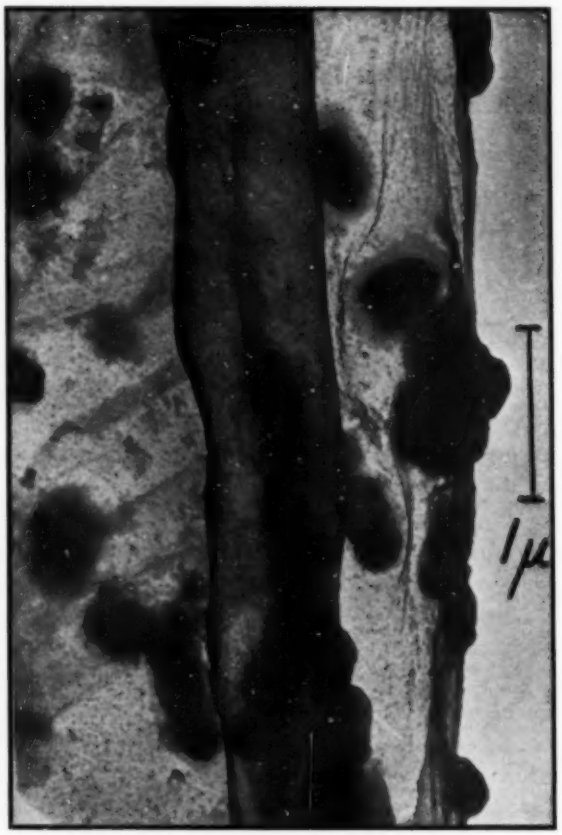

FIG. 8. Electron microscope picture of whooping cough bacteria on a thin collodion film which broke and curled up. Some of the bacteria are thus seen on the edge of the film in profile. Since they are the same size as other bacteria seen in transmission, it appears that neither the vacuum nor the electron bombardment causes them to collapse. (Courtesy of L. Marton.)

VII

During the last decade there has been an interesting challenge to technique in the hy-

pothesis that if the well-established rules of physical optics apply to the matter waves associated with particles such as electrons, then a microscope which employs these matter waves in place of those of light should have a theoretical limit of resolution of the order of 10^{-8} cm. Now, after several years of development, the electron microscope is emerging from the state of being a scientific curiosity into being a powerful tool with immediate applications (to mention only one) in the field of medicine. In such a microscope the image is produced by a stream of electrons which pass through the specimen just as light passes through an ordinary microscope slide. Carefully designed coils carrying steady currents act as "lenses" for this stream of electrons. So close is the analogy between the behavior of light and of electrons that much of the optical theory requires little modification to make it fit the electronic case.

The literature of the year gives accounts[45] of the performance of two recently completed microscopes, one at the RCA Research Laboratories, the other at the University of Toronto. Both are provided with such refinements as devices for changing specimens and photographic plates and for making adjustments without breaking the vacuum, causing only a few minutes' interruption in the operation of the instruments. Photographs can be taken at a direct magnification of the order of 20,000, and the limits of resolution of the instruments (estimated at about 5×10^{-7} cm) are so low that these photographs can afterwards be enlarged so as to bring the total magnification to something approaching 200,000. Since the electron stream must penetrate the object being examined, very thin specimens are required; bacteria, for example, can be supported on delicate films of nitrocellulose. Already the RCA instrument has shown the details of internal structure of germ cells which are themselves so small as to be almost at the limit of resolution of the ordinary optical microscope. And the end has not yet been attained, for the Toronto workers state that at the present time the resolving power of their instrument seems to be set more by the nature of the specimens than by instrumental limitations. Figure 8 is a picture taken with the RCA instrument showing whooping cough bacteria. The adjoining print, Fig. 9, is a high power micrograph of the same type of bacteria taken with an optical microscope. The reader may draw his own conclusions regarding the possibilities of the new instrument.

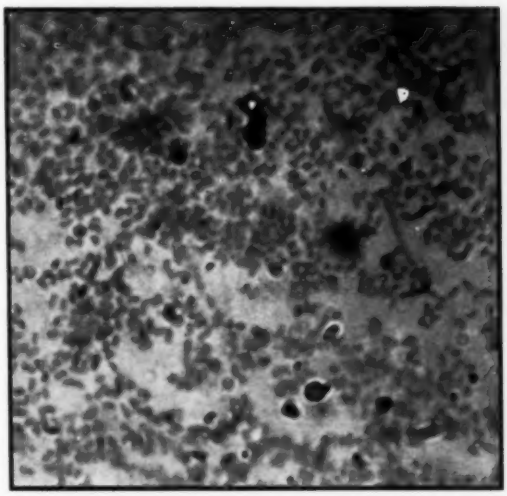

FIG. 9. Optical microphotograph of whooping cough bacteria. Over-all magnification, 1900. The bacteria are the numerous specks about as long as the commas on this page. Compare with Fig. 8. (Courtesy of A. N. Solberg.)

Electrons moving more slowly than those used in electron microscopes have been used extensively to study the structure of surface films. Here the thickness of material to be penetrated is quite small, and the structure of the film is deduced from the diffraction pattern formed by the reflected electrons. Several years ago[46] studies were made by this and by other methods of the growth of films on slowly oxidizing metals like Al, but the speed and sensitivity of the electron diffraction method enable investigations[47] to be made now on fast-corroding metals like lithium, sodium, potassium and calcium. These films can be examined by electron diffraction at a much earlier stage than they can be by chemical means, and so it is possible that the report of Yamaguchi that CaO is formed first in air on metallic calcium does not render entirely invalid the statement formerly found in chemistry textbooks that the metal tarnishes in air owing to the formation of nitride.

Once a very thin oxide film has been formed on a metal, the question may well be asked, How does it grow thicker? It is reasonable to suppose that it grows either at the metal-oxide interface, or else at the outer surface of the film which is in contact with an oxidizing atmosphere; but not at the middle of the oxide film, where there is a dearth of free metal and of oxygen atoms.

This means that the metal or the oxygen must be soluble in the oxide, or both. In any case the thickness of the film formed can be shown to be proportional to the square root of the time of growth—a prediction which is well borne out by observations which have been made, for example, on copper. But the explanation is not always so simple, for on certain metals, notably aluminum, chromium and stainless steels, protective films grow to a small but definite thickness and then practically stop. Hence these metals do not, to the eye, appear to tarnish. Mott's theory[46] of the process "starts from Wagner's hypothesis that metal atoms diffuse through the oxide film in the form of metal ions and electrons separately. Since the films do not grow beyond a thickness of some 40A on aluminium, for example, it follows that either the ions or the electrons cannot pass through a thicker layer." Experiments can be recalled which show that aluminum ions can pass through very thick layers of oxide, so that it must be the electrons which are unable to penetrate it. Now the electrons are supposed to leave the metal at the metal-film interface by thermionic emission, but if the work function is high this cannot happen at ordinary temperatures. Here Mott invokes the aid of the "tunnel effect" which has been used successfully by Gurney and Condon in explaining the emission of alpha-particles from naturally radioactive atoms. He calculates the rate at which electrons can "tunnel" through a thin film in terms of its thickness. The number of electrons will, of course, determine the number of molecules which can be built up as oxide, which will in turn be a measure of the increasing film thickness. He finds that when the oxide film on aluminum is of the order of 40A thick, it grows at the rate of about 1 atomic layer per year; and this may, with no undue stretch of the imagination, be described as a permanent protective film of constant thickness.

Before we leave the subject of thin films we call attention to a new and promising method of investigating molecular structure. In infra-red spectroscopy, an absorbing layer containing some 10^{19} molecules/cm^2 is ordinarily required to produce worth-while spectra. A monomolecular layer contains only about 5×10^{14} molecules/cm^2, and even though polymolecular films can be built up to a thickness of 1000 molecules, the number of atoms in such layers still falls far short of 10^{19}. Sutherland and Tutte[48] were surprised to find, however, that a double transmission through a film of methyl stearate only 700 molecules thick was enough to give an easily detectable absorption spectrum, and that absorption was even observable with 200-molecule layers. Molecules apparently absorb much better when they are part of a surface film, than when they have a purely random arrangement.

VIII

The investigations which are known as pure scientific research are usually so far removed from the problems of the everyday world that it is often a long time before their results are, if ever, applied to commercial devices. At the present time, for example, it is somewhat fanciful to count soon upon the convenient production of power by the fission of uranium, though improvements may be expected in the separation of isotopes, perhaps by thermal diffusion, in order to concentrate the active U^{235}. Our preoccupation with armaments and defense will undoubtedly act as a spur to studies such as have recently been published in this journal on klystron oscillators and on the phenomena of lubrication, but it will at the same time prevent many innovations in instrument design from reaching the widely circulated literature. Nevertheless, the main problems of the rearmament program will be the skilful application and coordination of techniques already known; and the flourishing condition of our technical societies shows that the United States has men enough with the ability to cope with this pressing problem.

Bibliography

1. R. O. Haxby, W. E. Shoupp, W. E. Stephens and W. H. Wells, Phys. Rev. **58**, 92 (1940).
2. A. O. Nier, E. T. Booth, J. R. Dunning and A. V. Grosse, Phys. Rev. **57**, 546 (1940).
3. D. H. T. Gant, Nature **144**, 707 (1939).
4. R. S. Krishnan and T. E. Banks, Nature **145**, 860 (1940).
5. A. O. Nier, E. T. Booth, J. R. Dunning and A. V. Grosse, Phys. Rev. **57**, 748 (1940).
6. A. V. Grosse and E. T. Booth, Phys. Rev. **57**, 664 (1940).
7. E. Segrè and C. S. Wu, Phys. Rev. **57**, 552 (1940).
8. M. H. Kanner and H. H. Barschall, Phys. Rev. **57**, 372 (1940).
9. G. N. Glasoe and J. Steigman, Phys. Rev. **58**, 1 (1940).
10. K. J. Brostrøm, J. K. Bøggild and T. Lauritsen, Phys. Rev. **58**, 651 (1940); N. Bohr, Phys. Rev. **58**, 654 (1940).
11. L. A. Turner, Phys. Rev. **57**, 950 (1940).
12. Y. Nishina, T. Yasaki, H. Ezoe, K. Kimura and M. Ikawa, Phys. Rev. **57**, 1182 (1940)
13. E. McMillan, Phys. Rev. **58**, 178 (1940).
14. E. McMillan and P. H. Abelson, Phys. Rev. **57**, 1185 (1940).
15. V. J. Young, A. Ellett and G. J. Plain, Phys. Rev. **58**, 498 (1940); W. B. McLean, A. Ellett and J. A. Jacobs, Phys. Rev. **58**, 500 (1940).
16. G. J. Perlow, Phys. Rev. **58**, 218 (1940).
17. S. K. Allison, L. S. Skaggs and N. M. Smith, Jr., Phys. Rev. **57**, 550 (1940).
18. E. Pollard, Phys. Rev. **57**, 1186 (1940).
19. C. F. Powell, A. N. May, J. Chadwick and T. G. Pickavance, Nature **145**, 893 (1940).
20. E. J. Williams and G. E. Roberts, Nature **145**, 102 (1940).
21. E. J. Williams and G. R. Evans, Nature **145**, 818 (1940).
22. B. Rossi, H. Van N. Hilberry and J. B. Hoag, Phys. Rev. **57**, 461 (1940).
23. For example, M. Ageno, G. Bernardini, N. B. Cacciapuoti, B. Ferretti and G. C. Wick, Phys. Rev. **57**, 945 (1940); W. M. Nielson, C. M. Ryerson, L. W. Nordheim and K. Z. Morgan, Phys. Rev. **57**, 158 (1940).
24. E. G. Dymond, Nature **144**, 782 (1939).
25. M. Schein, W. P. Jesse and E. O. Wollan, Phys. Rev. **57**, 847 (1940).
26. W. F. G. Swann and W. E. Ramsey, Phys. Rev. **57**, 1051 (1940).
27. L. Jánossy and P. Ingleby, Nature **145**, 511 (1940).
28. G. Wataghin, M. D. de S. Santos and P. A. Pompeia, Phys. Rev. **57**, 339 (1940).
29. V. Josephson, D. K. Froman and J. C. Stearns, Phys. Rev. **57**, 335 (1940).
30. W. M. Powell, Phys. Rev. **58**, 474 (1940).
31. H. J. J. Braddick and G. S. Hensby, Nature **144**, 1012 (1939).
32. G. Herzog and W. H. Bostick, Phys. Rev. **58**, 278 (1940).
33. D. M. Bose and B. Chowdhry, Nature **145**, 894 (1940).
34. D. H. Loughridge and P. F. Gast, Phys. Rev. **58**, 583 (1940).
35. Y. Nishina, Y. Sekido, H. Simamura and H. Arakawa, Phys. Rev. **57**, 1050 (1940).
36. W. H. Zachariasen, Phys. Rev. **57**, 597 (1940); Nature **145**, 1019 (1940). See also K. Lonsdale, I. E. Knaggs and H. Smith, Nature **146**, 332 (1940).
37. S. Siegel and W. H. Zachariasen, Phys. Rev. **57**, 795 (1940).
38. C. V. Raman and P. Nilakantan, Nature **145**, 667 (1940).
39. J. DuMond and J. P. Youtz, J. App. Phys. **11**, 357 (1940).
40. C. S. Barrett and A. H. Geisler, J. App. Phys. **11**, 733 (1940).
41. J. H. Munier, J. A. Bearden and C. H. Shaw, Phys. Rev. **58**, 537 (1940).
42. P. H. Abelson, Phys. Rev. **56**, 753 (1939).
43. J. A. Bearden, Phys. Rev. **56**, 1023 (1939).
44. P. H. Miller, Jr. and J. W. M. DuMond, Phys. Rev. **57**, 198 (1940).
45. L. Marton, Phys. Rev. **58**, 57 (1940); E. F. Burton, J. Hillier and A. Prebus, Phys. Rev. **56**, 1171 (1939).
46. See summary by N. F. Mott, Nature **145**, 996 (1940). Quotations are from this article.
47. S. Yamaguchi, Nature **145**, 742 (1940).
48. G. B. B. M. Sutherland and W. T. Tutte, Nature **144**, 707 (1939).

Theory of the Plastic Properties of Solids. I*

BY FREDERICK SEITZ,
Randal Morgan Laboratory, University of Pennsylvania, Philadelphia, Pennsylvania
AND
T. A. READ,**
Westinghouse Research Laboratories, East Pittsburgh, Pennsylvania

Introduction

FROM the standpoint of direct experimental observation,[1] the plastic properties of solids may be classified into five categories, namely: (a) slip, (b) creep, (c) twinning, (d) rupture, and (e) fatigue.

Slip is one of the fundamental ways in which crystals may deform inelastically. It consists, at least from the gross experimental standpoint, of the displacement of one part of a given crystal relative to another along a definite crystallographic plane (Fig. 1). What actually is observed in a practical experiment with a single crystal is as follows. Let us suppose that the specimen is placed under stress in a tension machine and that its elongation is measured, the machine being able to detect a certain minimum rate of elongation of the order of 10^{-5} cm/sec. Starting with very small stresses, it is found that the elongation initially occurs practically instantaneously, is proportional to the stress, and is exactly reversed when the load is removed. This is the region of stress in which Hooke's law is valid. When the stress reaches a critical value, about which more will be said later, the elongation continues relatively slowly after the first instantaneous rise. If the stress is released after such a deformation, only a part of the elongation is reversed and the specimen has received a permanent increase in length. Within limits (Section 2), this increase in length is greater the longer the load is applied and the further the stress lies above the critical value for which it began. An examination of a single crystal specimen which has undergone an elongation of a percent or so shows that parts of the crystal have been displaced relative to one another along particular crystallographic planes (Fig. 2). These planes may be detected by the presence of step-wise discontinuities on the surface of the specimen which are called *slip-bands*. In many instances these bands run continuously around the crystal, their spacing and orientation depending greatly upon the conditions surrounding the experiment. In the simplest cases they are parallel to one another and are spaced by distances of the order of a micron. We shall defer additional discussion of the details of the slip process until Section 2.

Creep is a temperature dependent type of plastic flow that occurs when the solid is stressed below the critical stress mentioned in the preceding paragraph. Its detection generally requires a more sensitive type of instrument than that used in detection of slip. A separate designation for this more gradual type of flow was introduced originally because of the fact that its measurement required a particularly designed apparatus. Actually, it appears that the fundamental atomic motions occurring during slip and creep are identical in single crystals of many substances. As we shall see in Section 3, the

* The writers wish to express their deep indebtedness to Dr. C. S. Barrett of the Carnegie Institute of Technology and to Drs. A. Nadai and S. Siegel of the Westinghouse Research Laboratories for many informative discussions on this topic.

** Westinghouse Research Fellow.

[1] Extensive accounts of experimental work in this field may be found in the following books and periodicals:
C. F. Elam, *The Distortion of Metal Crystals* (Oxford University Press, 1936).
E. Schmid and W. Boas, *Kristallplastizität* (Springer, Berlin, 1936).
A. Nadai, *Plasticity* (McGraw-Hill Book Company, New York, 1931).
Reports of the International Conference in Physics 1934 (Cambridge University Press, 1935), Vol. II.
"Report of a conference on internal strains in solids," Proc. Phys. Soc. **52**, 1 (1940).
S. L. Hoyt, *Metals Progress*, **38**, 659 (1940).

continuity between creep and slip has been established fairly definitely in zinc, cadmium and tin.

Twinning resembles slip in that it is another of the fundamental ways in which plastic deformation can occur. As in the case of slip, the end result of twinning is the relative displacement of neighboring planes of atoms. However, the important difference is that in twinning millions of successive, neighboring planes may be displaced relative to another by a fixed distance that is not an integer multiple of a lattice spacing, whereas in slip parts of the original crystal appear to move relative to one another with a transition region whose width is less than the resolving power of optical microscopes (about a micron). Thus the end result of twinning in a single crystal is the production of a region, namely that in which the relative motion has occurred, in which the atoms have perfect crystalline arrangement, but in which the crystalline orientation is usually very different from that of the parent crystal. The end result of slip in an ideal case is the

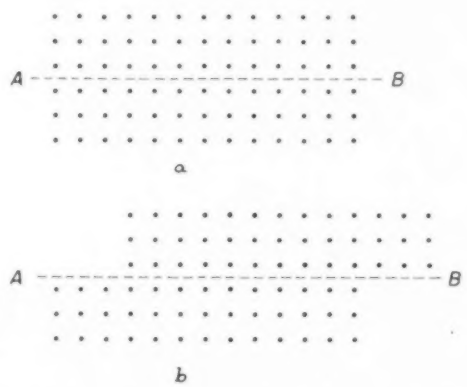

FIG. 1. Schematic representation of the atomic displacements resulting from slip. The lines of atoms shown in (a) are displaced in the manner shown in (b) as a result of slip in the plane A–B.

production of a polycrystal consisting of a number of identically oriented single crystals that are separated by the slip bands.

Rupture is the process by which solids break when placed under static stress, whereas fatigue is the breaking induced by periodic stress. This division of the topic of breaking is important because solids will break under periodic stressing for smaller maximum load than in static stressing.

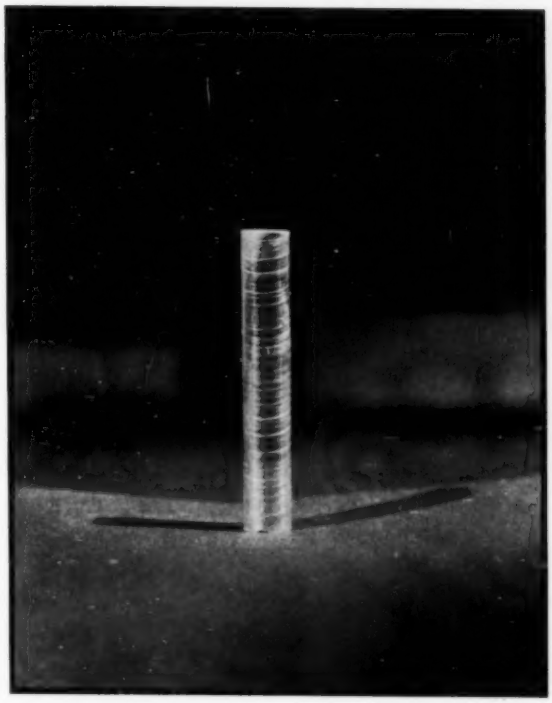

FIG. 2. A photograph of a zinc single crystal which shows slip bands. The slip bands are ellipses formed by the intersections of the slip planes, which are perpendicular to the hexagonal axis of the crystal, and the cylindrical surface of the crystal.

In treating each of these topics, we may recognize four types of crystalline textures, namely pure single crystals, single crystals of alloys, pure polycrystalline materials, and polycrystals of impure materials and alloys. The last two types of texture have the greatest practical interest and naturally have been used most extensively in experimental testing. Unfortunately only a very minor part of the results of this work seems to have value for understanding the fundamental mechanisms involved in the plastic properties of solids. In fact this fraction of the work dealing with polycrystals is relatively small compared with the work on single crystals in which we shall be interested. For this reason the largest part of this article will deal with the properties of single crystals.

We shall proceed with a concise discussion of the experimental material relating to the plastic properties of solids and accompany this with a presentation of the theory suggested by this experimental work. This procedure will be fol-

lowed first for single crystals and then for polycrystalline materials. It should be borne in mind that in its present state of development, this theory is far less complete than the theories of many other properties of solids. For this reason the present series of articles should be viewed entirely as an attempt to plot an orderly course in a field in which extensive changes in viewpoint will undoubtedly prove necessary.

Part A. Single Crystals

1. The Elastic Range*

Before proceeding with the plastic behavior of solids, it is appropriate to survey the relationships in the range of stress and strain in which Hooke's law is valid. Careful experimental work seems to indicate that a certain amount of plastic flow occurs at all stresses. However, it is unquestionably true that for sufficiently small stresses and sufficiently low temperatures the stress-strain relation is practically linear and reversible. Since such topics as internal friction and plasticity may be introduced by discussing deviations from this idealized linear relation, it may be said to be the foundation of all discussions of stresses and strains in solids.

Let us consider a homogeneous medium that is under stress. In order to describe its state of stress completely, we should know the stresses acting on each infinitesimal component. To do this conveniently, we may refer the medium to a Cartesian reference system and subdivide it into rectangular parallelepipeds whose faces are defined by the coordinate planes of the Cartesian system. The state of stress at a given point is then completely described by giving the forces that act across each of the faces of the infinitesimal rectangular cell surrounding this point and having edge-lengths dx, dy and dz parallel to each of the coordinate axes (Fig. 3). Since the cell is infinitesimally small, by assumption, the forces on opposite faces will be equal to within infinitesimals if the stress variation is continuous. Hence there are no more than nine independent components of force; these correspond to the forces acting on three mutually perpendicular faces of the cell. We shall designate the three components of the force per unit area acting on the cell across the x face by σ_{11}, σ_{12}, σ_{13} in an obvious notation in which the subscript 1 refers to the x component, 2 to the y component and 3 to the z component. Similarly the components of the force per unit area acting on the cell across the other two faces will be designated by σ_{21}, σ_{22}, σ_{23} and σ_{31}, σ_{32}, σ_{33}, respectively. These nine quantities constitute the *stress tensor*, the individual components being the *stress components*. It is clear from Fig. 3 that σ_{11}, σ_{22}, σ_{33} correspond to forces normal to each of the three faces of the cell and hence are compression or tension stresses, whereas the other six stress components correspond to forces lying in the plan faces and hence are shearing stresses.

Now it is easy to show[2] that in ordinary static stress distributions the shear components satisfy the following relations, which imply that the stress tensor is symmetric,

$$\sigma_{12}=\sigma_{21}, \quad \sigma_{23}=\sigma_{32}, \quad \sigma_{13}=\sigma_{31}. \tag{1}$$

Thus there are only six independent stress components. For simplicity these are usually designated by a one-subscript symbol $\sigma_i (i=1, 2, \cdots, 6)$ in accordance with the following relations

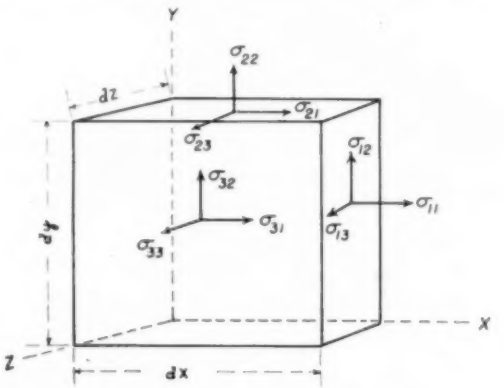

Fig. 3. The infinitesimal parallelepiped in terms of which the stress components are defined.

$$\begin{aligned} &\sigma_1=\sigma_{11}, \quad \sigma_2=\sigma_{22}, \quad \sigma_3=\sigma_{33}, \\ &\sigma_4=\sigma_{12}, \quad \sigma_5=\sigma_{23}, \quad \sigma_6=\sigma_{13}. \end{aligned} \tag{2}$$

The strains in a medium may be described in a manner analogous to that used for stresses. Let us suppose that in the strain-free state the points of the medium are designated by coordinates

* This section should merely be skimmed for its qualitative content by a reader not interested in the details of elasticity theory.

[2] See, for example, A. E. H. Love, *The Mathematical Theory of Elasticity* (Cambridge University Press, 1927).

x, y, z relative to a Cartesian reference system, and that after straining has occurred the point previously at x, y, z has been displaced to the point x', y', z'. We may assume for simplicity that the point at the origin of coordinates has not been displaced for we could always translate the origin of coordinates to the new position if it had. Since Hooke's law is valid for small deformations, we may consider this special case and write the relation between x, y, and z and x', y', and z' in the form

$$\begin{aligned} x'-x &= S_{11}x+S_{12}y+S_{13}z, \\ y'-y &= S_{21}x+S_{22}y+S_{23}z, \\ z'-z &= S_{31}x+S_{32}y+S_{33}z. \end{aligned}$$

In general the S_{ij}, which are known as the components of the strain tensor, are functions of position; however, the homogeneous case, in which they are constant, is an important one.

As in the case of the stress tensor, the practically interesting situations correspond to symmetric strain tensors, that is to tensors in which the shearing strains are related by the equations

$$S_{12}=S_{21}, \quad S_{23}=S_{32}, \quad S_{31}=S_{13}. \tag{3}$$

Thus there usually are only six independent components of the strain tensor. It is frequently convenient to designate these by the six one-subscript symbols $S_i (i=1, 2, \cdots, 6)$ in accordance with the relations

$$\begin{aligned} &S_1=S_{11}, \quad S_2=S_{22}, \quad S_3=S_{33} \\ &S_4=S_{12}=S_{21}, \quad S_5=S_{23}=S_{32}, \quad S_6=S_{31}=S_{13}. \end{aligned} \tag{4}$$

In this case the components S_{11}, S_{22}, S_{33} give the fractions by which the medium is extended or compressed along the three coordinate directions, respectively, whereas the other six components give a corresponding measure of the relative amounts by which coordinate planes are displaced parallel to themselves along the coordinate axes (i.e., sheared).

In the region in which Hooke's law is valid, the stress and strain components are proportional to one another, that is the following relations are satisfied

$$\begin{aligned} \sigma_i &= \sum_{j=1}^{6} c_{ij}S_j \\ & \qquad (i=1, 2, \cdots, 6). \\ S_i &= \sum_{j=1}^{6} C_{ij}\sigma_j \end{aligned} \tag{5}$$

TABLE I. *The elastic constants of crystals. (The values are given in units of 10^{-12} cm²/dyne.)*

METAL	C_{11}	C_{12}	C_{44}
Face-centered cubic			
Al	1.59	−0.58	3.52
Au	2.33	−1.07	2.38
Ag	2.32	−0.993	2.29
Cu	1.49	−0.625	1.33
Pb	9.30	−4.26	6.94
Body-centered cubic			
Fe	0.757	−0.282	0.862
Na	48.3	−20.9	16.85
K	83.3	−37.0	38.0
W	0.257	−0.073	0.660

	HEXAGONAL				
	C_{11}	C_{12}	C_{13}	C_{33}	C_{44}
Mg	2.23	−0.77	−0.45	1.98	5.95
Zn	0.84	+0.11	−0.78	2.87	2.64
Cd	1.23	−0.15	−0.93	3.55	5.40

	LOWER SYMMETRY					
	C_{11}	C_{33}	C_{44}	C_{12}	C_{13}	C_{14}
Sb	1.77	3.38	4.10	−0.38	−0.85	−0.80
Bi	2.69	2.87	10.48	−1.4	−0.62	+1.6
Sn	1.85	1.18	5.70	−0.99	−0.25	$C_{66}=13.5$

	ALLOYS		
ALLOY	C_{11}	C_{12}	C_{44}
100 Ag– 0 Au	2.32	−0.993	2.29
75 Ag– 25 Au	2.07	−0.891	2.05
50 Ag– 50 Au	1.97	−0.852	1.97
25 Ag– 75 Au	2.05	−0.909	2.06
0 Ag–100 Au	2.29	−1.04	2.34
Cu_3Au	1.34	−0.565	1.508
72 Cu–28 Zn	1.94	−0.84	1.39
50 Cu 50 Zn	3.88		
95 Al 5 Cu	1.5	−0.69	3.7

	IONIC CRYSTALS		
SALT	C_{11}	C_{12}	C_{44}
NaCl	2.27	−.476	7.89
KBr	3.17	−.462	16.1

The c_{ij} and C_{ij} are not independent, of course, for the two sets of Eqs. (5) are simply algebraic inverses. We need not be concerned with the detailed relations here. Since there are six σ_i and six S_i, it follows that at most thirty-six constants enter into either of the sets of equations. Not all of these *elastic constants* are independent however, for it may be proved by means of the first law of

thermodynamics[2] that the following relationships exist

$$c_{ij}=c_{ji},$$
$$C_{ij}=C_{ji}.$$

Thus only twenty-one elastic constants are independent at most.

Further relationships occur in crystals having particular symmetry. For example, there are only three independent constants in the case of cubic crystals such as copper, iron, rocksalt, etc., and

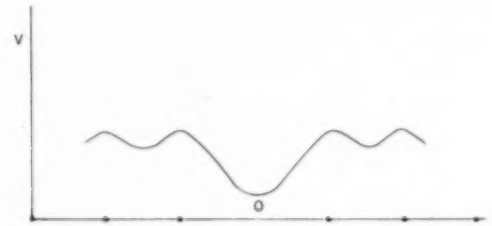

FIG. 4. Schematic form of the potential energy of an atom in a lattice. The abscissae represent the positional coordinates of the atom. This potential is essentially parabolic in the vicinity of the minimum 0, which is the normal equilibrium position of the atom.

there are only five in hexagonal crystals such as zinc, cadmium, wurtzite, etc. Experimental values of some of the measured C_{ij} are given in Table I for several well-known crystals. We shall find these constants useful in the following sections for making estimates of stresses for which plastic flow should begin in solids. It should be added that they are independent of the previous history of a specimen to within a factor of about one percent.

It is interesting at this point to consider the facts concerning the interatomic forces that give rise to Hooke's law. Any atom in a solid is under forces exerted on it by its neighbors, and in an ideally perfect crystal, translationally equivalent atoms are under identical forces. The form of the potential well in which an atom moves is shown schematically in Fig. 4, the minimum point being the equilibrium position at absolute zero of temperature when the crystal is not under external stress. At temperatures above absolute zero, the atom will oscillate about this equilibrium point with varying amplitude in accordance with the laws of statistical mechanics. Since the potential energy is a quadratic function of displacement relative to the position of minimum energy, in first approximation, the forces restoring the atom to its equilibrium position will be proportional to the displacement for small displacements. Thus if the ideal crystal is placed under stress, we may expect the atoms to be displaced relative to one another by an amount proportional to the stress as long as the displacement is small compared with interatomic distances; that is, we should expect Hooke's law to be obeyed. Elastic constants computed on the basis of this atomic mechanism[3] with the use of quantum mechanics and the assumption of ideal lattices are in excellent agreement with experimental values in a number of cases.

Now these computations, and similar ones involving molecules rather than solids, show that the quadratic approximation is usually accurate for displacements of the order of ten percent of the interatomic distance, so that we should expect Hooke's law to be valid in an ideal crystal for stresses in which the strain is less than one-tenth. Thus, using values of the elastic constants given in Table I, we should expect the law to be valid in the materials listed for stresses at least as high as 10^{10} dynes/cm^2 (or 100 kg/mm^2). As we shall see below, large deviations from Hooke's law actually occur for stresses a thousand times smaller than this in carefully grown, well-annealed single crystals of practically all pure metals and many salts, even at temperatures in the vicinity of absolute zero. Thus, although the elastic constants are determined by the bulk properties of the ideal solid, we must conclude that deviations from the ideal state occur and are in some way responsible for deviations from Hooke's law.

2. THE THEORIES OF SLIP

a. Basic concepts

The most easily detected phenomenon associated with breakdown of Hooke's law is the process of slip. As was mentioned previously, this is characterized by the irreversible motion of one part of a crystal relative to another along a definite plane (Fig. 1). The motion is usually made evident by the appearance of bands on the

[3] See, for example, the survey of this topic in F. Seitz, *The Modern Theory of Solids* (McGraw-Hill Book Company, New York, 1940).

exterior of the specimen which correspond to the intersection of the slip planes with the boundary surface. An actual representation of the slip bands in a single crystal in which slip has occurred along a number of parallel planes is given in Fig. 2. This situation is typical of both zinc and cadmium in which slip occurs most prominently in planes normal to the hexagonal axis (basal planes). The slip system is usually not as simple in cubic crystals since symmetrically equivalent planes are not necessarily parallel. Before interpreting slip in the light of the remarks made at the end of the preceding section, we shall summarize several of the laws obtained as a result of the rather extensive experimental work on slip.

(1) The rate at which slip occurs in a given plane in a given specimen is determined primarily by the component of shearing stress in the plane. In general, the slip rate is very slow for a range of shearing stress extending from zero to a more or less definite value (for the particular specimen and plane) at which it becomes measurable in somewhat standardized laboratory equipment. A readily measurable rate of shearing strain is 10^{-6} sec.$^{-1}$. In practical work, this stress at which the rate of slip becomes readily measurable with comparatively crude equipment is called the *critical shearing stress*.

We shall find it very convenient to follow the practical procedure in the present section and reserve the word "slip" for the plastic flow occurring for stresses at least as large as the critical shearing stress. The less rapid flow for smaller stresses will be treated in the next section under the heading "creep." As was mentioned in the introduction, the two types of flow are intimately connected so that this division of the topic is mainly one of convenience.

(2) The critical shearing stress is different for different types of crystallographic planes. In some cases, such as zinc and cadmium, cited above, the critical value is so much lower for one set than for all others that slip is observed almost exclusively in that system of planes. It seems to be a general rule in the case of metals that the planes of easiest slip are the most nearly close-packed ones. Thus the basal planes are the easiest in close-packed hexagonal crystals, whereas the four types of (111) planes (octahedral planes) are easiest in face-centered cubic lattices, such as copper and aluminum. Moreover, when slip is observed in other planes, such as in the (100) planes of aluminum, these are also planes of relatively high atomic density. There are several planes of nearly equal atomic density both in the body-centered cubic lattice and in white tin. Andrade[4] and his co-workers have found slip in the (112), (110) and (123) planes in several body-centered cubic crystals, whereas Obinata and Schmid[5] have found slip in the (100), (110), (101), and (121) planes of tin for nearly equal shearing stresses.

In addition to this rule that the planes of easiest slip are the most highly packed planes in simple substances, it is found that the direction of slip is usually in the direction of lines of greatest atomic density. Thus slip occurs in the (101) direction in the (111) planes of face-centered metals and in the (1120) direction in zinc and cadmium. Andrade[4] has suggested that this rule is even of more fundamental importance than the rule concerning the density of atoms in the slip plane, for whereas there are several slip planes in body-centered cubic lattices, the slip direction is along the body diagonal in all cases. A list of easy planes and directions in metals is given[6] in Table II, along with measured shearing stresses.

Among the salts, slip has been investigated most fully in those having the sodium chloride structure and it is found that in all of these cases the slip planes are the six systems equivalent to (110) and the slip direction is $(1\bar{1}0)$. A few other salts whose properties have been investigated less thoroughly, are not listed in the table. Although the (110) planes in the sodium chloride lattice are not the most close-packed planes, the slip direction is that of greatest atomic density.

It is clear from the values of the critical shearing stress given in the table that slip usually occurs in pure metals and salts for stresses not appreciably larger than 10^7 dynes/cm^2, which is smaller than the value to be expected for ideal lattices by a factor of about a thousand. As we

[4] E. N. daC. Andrade, Proc. Phys. Soc. **52** (1940);—and Y. S. Chow, Proc. Roy. Soc. **175**, 290 (1940);—and L. C. Tsien, Proc. Roy. Soc. **163**, 1 (1937).

[5] I. Obinata and E. Schmid, Zeits. f. Physik **82**, 224 (1933).

[6] These data are taken principally from the references of footnote 1. A careful treatment of the geometry of slip is given by M. J. Buerger, Am. Minerologist **15** (1930).

mentioned at the end of the preceding section, we must conclude that actual solids do not possess ideal structures and that the imperfections are in some way responsible for this type of weakness. Before continuing the discussion of slip, we shall survey the present evidence for lattice imperfections.

b. Types of lattice imperfections

There is considerable evidence for the following types of lattice imperfections in single crystals.

(1) Thermal oscillations. The fact that the atoms in crystals oscillate about their equilibrium positions at temperatures above absolute zero is indicated by so many sources of evidence that we need not discuss them in detail. In addition, atoms undergo the quantum-mechanical "zero-point" oscillations even at the absolute zero of temperature. However, these quantum-mechanical fluctuations are so very small for the heavier atoms, with which we shall be almost exclusively concerned, that we need not be concerned with them here.

(2) Defects extending over regions of the order of atomic dimensions. There is abundant evidence[7] from investigations of diffusion and ionic conduction in solids that all crystals have many small-scale imperfections. In the simplest cases these consist of interstitial atoms not present in a perfect crystal and vacant lattice sites (Fig. 5). It is believed that these defects are generated as a consequence of the thermal fluctuations and play an essential role in many types of transport phenomena in solids. We shall have occasion to consider special types of defects of this kind in part *c* of the present section.

It should be mentioned at this point that small scale defects of this type do not give rise to observable x-ray diffraction patterns because of their small size. Or expressed in another way, their patterns are so diffuse because of their small size, that they appear in the general background of the Laue or Hull-Debye-Scherrer x-ray patterns of crystals and are not measureable. They do scatter x-rays, however, and in consequence should detract from the intensity of the ordinary diffraction lines. We shall be concerned with this effect in another part of the present section.

[7] See, for example the book referred to in footnote 3, and the book by N. F. Mott and G. W. Gurney *The Theory of Ionic Crystals* (Oxford University Press, 1940).

(3) The mosaic structure.[8] The widths of the x-ray lines scattered from small regions of crystals

TABLE II. *Data concerning slip in solids.*

Metal	Impurity Content	Slip Plane	Direction	(kg/mm²) Critical Stress
Pure Metals				
Cu	0.001	(111)	$(10\bar{1})$	0.10
Ag	0.0001	(111)	$(10\bar{1})$	0.060
Au	0.0001	(111)	$(10\bar{1})$	0.092
Ni	0.002	(111)	$(10\bar{1})$	0.58
Mg	0.0005	(0001)	$(11\bar{2}0)$	0.083
Zn	0.0004	(0001)	$(11\bar{2}0)$	0.094
Cd	0.00004	(0001)	$(11\bar{2}0)$	0.058
		(1100)		>0.03
Na		(110)		
		(112)	(111)	
		(123)		
Mo		(112)	(111)	
		(110)		
K		(123)	(111)	
W		(112)	(111)	
K		(123)	(111)	
Fe		(110)		
		(112)		
		(123)		
β-Sn	0.0001	(100)	(001)	0.19
		(110)	(001)	0.13
		(101)	$(10\bar{1})$	0.16
		(121)	$(10\bar{1})$	0.17
Bi	~0.001	(111)	$(10\bar{1})$	0.221
Hg	$\sim 10^{-6}$	Complex		0.007
Alloys				
Composition		Slip Plane	Slip Direction	Critical Stress (kg/mm²)
99.4 Zn 0.006 Cd		(0001)	$(11\bar{2}0)$	2.7
6.8 Al 93.2 Mg		(0001)	$(11\bar{2}0)$	1.4
85 Al 15 Zn		(111)	$(10\bar{1})$	8
72 Cu 28 Zn		(111)	$(10\bar{1})$	1.5
$AuCu_2$ (ordered)				2.2
$AuCu_2$ (disordered)				4.4
Ionic Crystals				
NaCl		(110)	$(1\bar{1}0)$	~0.2
AgCl		(110)	$(1\bar{1}0)$	~0.1
KCl, KBr, KI, RbCl		(110)	$(1\bar{1}0)$	

[8] Evidence for the mosaic structure is surveyed in the *Report of the International Conference on Physics, 1934* (University of Cambridge Press, 1935), Vol. II. Additional evidence has been given by A. B. Focke, Phys. Rev. **46**, 623 (1934), who showed that polonium precipitates from bismuth on planes separated by about 1μ.

indicate that the size of the coherent domains of actual lattices are of the order of 10^{-4} cm. Similarly, microscopic examinations of the etch patterns of crystal surfaces indicate that most crystals consist of a mosaic of blocks of the order of one micron in size. Beyond these facts, there is very little experimental information concerning the nature and origin of the mosaic structure. The most reasonable interpretation[9] is that of Smekal and of Buergers, namely that the blocks arise as a result of accidents of growth during the formation of the single crystals, the block boundaries being either places where some of the impurities present in the melt congregated during solidification or boundaries between regions that started from different points on the growing crystal surface and have become slightly out of line by accident. In agreement with this picture is the fact that some natural crystals that undoubtedly required geological times for growth show practically no evidence of mosaic structure.[10] The factors leading to imperfections should be a minimum in such cases because there is ample time for the forming crystal to be at complete equilibrium with its melt at all stages of growth.

(4) Slight variations in lattice spacing either from domain to domain or over regions comparable with the domain size. The contribution to line widths arising from this type of variation in lattice spacing can be separated from that arising from the actual existence of domains by studying the change in width from one order of the x-ray diffraction pattern to another.[11] The magnitude of these variations is greatly dependent upon the amount of mechanical working the specimen has received, as we shall see below.

(5) A coarser texture extending over regions of a millimeter or more. Simple observations[8] of the optical reflection of fresh cleavage faces of most single crystals show that such faces are rarely perfectly flat and that variations take place over regions of the area of one square millimeter. X-ray examination shows that this is not a superficial effect, but the crystallographic axes are rotated in passing from one of these regions to another, the angle of rotation commonly being as much as several minutes. The amount of distortion of this type does not seem to be directly related to the existence of mosaic blocks, for it may appear strongly even in cases in which the domain broadening is almost absent. Thus even though the distortion may arise in a manner closely resembling the origin of the mosaic structure, the determining factors are probably different in the two cases. For example, the coarser structure may be related to impurity or concentration gradients in the melt whereas the mosaic structure may be related to temperature gradients.

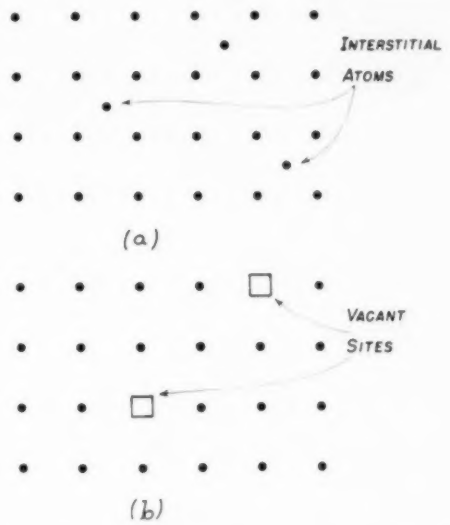

FIG. 5. Types of lattice imperfections that play an important role in atomic transport phenomena in solids such as diffusion and ionic conductivity. (a) Interstitial atoms; (b) vacant lattice sites.

c. Three hypothetical mechanisms of slip

Three outstanding mechanisms for the slip process have been suggested in the course of development of the theory of this topic. We shall discuss each of these and attempt to evaluate them critically.

1. Becker's theory.—Since atoms in crystals are continually oscillating at temperatures above absolute zero, it is natural to consider the possibility that these oscillations influence the shearing strength. A theory of this type was first given by Becker.[12] He pointed out that the stress at any point in the crystal will not be constant at

[9] See footnote 8; also M. J. Buerger, Zeits. f. Krist. **89**, 195 (1934).
[10] R. M. Bozorth and F. E. Haworth, Phys. Rev. **45**, 821 (1934).
[11] This topic is surveyed by U. Dehlinger and A. Kochendörfer, Zeits. f. Metallkunde **31**, 231 (1939).
[12] R. Becker, Physik. Zeits. **26**, 919 (1925).

finite temperatures, but will fluctuate as a result of thermal oscillations. Occasionally the local fluctuations should become sufficiently large to cause groups of atoms to slip past one another and produce a small amount of slip locally. Thus the observed slip could be explained as the end result of many such local slips.

A criticism of this theory requires that we look into its quantitative aspects. The elastic energy per unit volume in a region where the shearing stress is σ is equal to

$$\sigma^2/2C_s, \tag{6}$$

where C_s is the shear modulus. Thus in the absence of an externally applied stress, the relative probability that a given small volume V of the crystal will be under the stress σ as a result of thermal fluctuations is,[13] according to Boltzmann's theorem,

$$\exp(-V\sigma^2/2C_skT). \tag{7}$$

If the atomic planes can slip past one another in time τ when the stress reaches a critical value σ_0, the rate r at which slip will occur in the volume V is approximately

$$r=\frac{1}{\tau}\exp(-V\sigma_0^2/2C_skT). \tag{8}$$

For an otherwise perfect lattice, we should expect σ_0 to be of the order of 10^{10} dynes/cm^2. We need not be concerned with the numerical value of τ in the following, although we might expect it to be of the order of an atomic oscillation period, that is, about 10^{-13} sec.

Now let us consider the case in which the average applied stress is σ'. For slip to occur in the direction of the applied stress, it is only necessary that fluctuations add a stress of amount $(\sigma_0-\sigma')$, if it is assumed that the external stress acts constantly on all atoms. Hence (3) is changed to

$$r(\sigma')=\frac{1}{\tau}\exp(-V(\sigma_0-\sigma')^2/2C_skT). \tag{9}$$

This equation was derived by Becker in a manner essentially equivalent to that employed here.

[13] This equation is only approximate, for its use involves the implicit assumption that the entropy of the crystal in the stressed state is the same as in the normal state.

In spite of its exponential character, Eq. (9) predicts that the critical shearing stress should vary relatively slowly with temperature, for in ordinary static slip tests, slip is said to occur when r reaches a more or less constant observable value (see part *a* of this section). The condition for this is

$$(\sigma_0-\sigma')/T^{\frac{1}{2}}=a,$$

where a is a constant. Thus the critical shearing stress σ_c should vary with temperature in accordance with the equation

$$\sigma_c-\sigma_0=-a(T)^{\frac{1}{2}}. \tag{10}$$

As we might have expected, σ_0 should be the value of the critical shearing stress at the absolute zero of temperature. The temperature dependence predicted by (10) is in qualitative agreement with the observed dependence in zinc and cadmium, as may be seen from Fig. 6. Unfortunately, the value of σ_0 obtained by extrapolating the observed points to absolute zero is of the same order of magnitude as the values of σ_c at room temperature, namely 10^7 dynes/cm^2. As a result, we may conclude that the imperfections introduced by thermal fluctuations are not sufficient to account for the low values of the shearing strength.

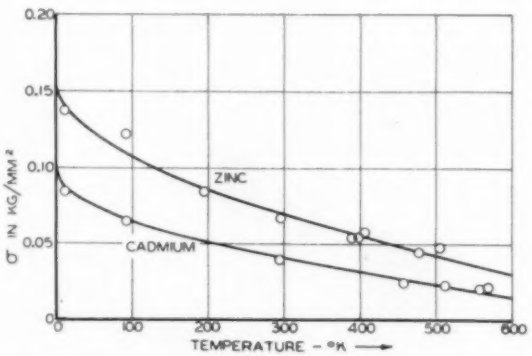

FIG. 6. Temperature dependence of the critical shearing stress for slip in zinc and cadmium (after Schmid and Boas). The relatively slow dependence is in qualitative agreement with equation (5). The ordinates are given in units of kg/mm^2.

2. Smekal's theory.—Smekal[14] has suggested that the weakness of actual crystals is intimately related to the existence of the mosaic structure.

[14] This work is reviewed by Smekal in the reference of footnote 8. See also *Handbuch der Physik*, vol. XXIV 2.

According to his picture the mosaic boundaries are essentially weaker than the interior of the blocks and this weakness is the source of the low plastic strength of solids. In general this weakness has two mutually assisting effects: (a) The blocks may move relative to one another more easily than parts of the material within the blocks and (b) the variations in structure allow for variations in stress from one region to another when the crystal is placed under stress, so that the values at some regions may be considerably higher than the average value. The second point may be fully appreciated by considering a simple example first considered by Griffith.[15] If a bar containing a long cylindrical crack with an elliptical cross section is placed under tension so that the direction of the applied force is normal to the cylinder axis and the major axis of the ellipse (Fig. 7), the stress at the edge of the major axis is larger than the average value by the factor $2a/b$, where a is the major diameter and b the minor diameter of the ellipse. Thus the stress magnification at the edge of a long thin crack may be very large. Even if the correctness of Smekal's viewpoint were to be granted, it would seem very difficult to develop these ideas into a systematic theory of plasticity, for our reliable knowledge concerning the mosaic structure is extremely small. In its most elementary form, a theory of this type would presumably go as follows: Slip takes place along the block boundaries which have an inherent shearing strength about a thousand times lower than that of perfect crystals; this type of slip may be aided by temperature fluctuations in a manner similar to that postulated in Becker's theory, so that an equation similar to (10) is valid. Although the evidence against a simple picture of this kind is by no means overwhelming, it does face several difficulties, which may be summarized:

(a) It is difficult to understand why the slip bands can extend as uniformly through single crystal specimens as they appear to do. This difficulty may be associated with our ignorance of the nature of the mosaic pattern, of course, for it is possible that it is very regular.

(b) It is difficult to interpret the fact that crystals soften with annealing, for we should expect the weak regions to become more nearly perfect as a result of heating and the crystal to be strengthened thereby.

(c) Crystals may be hardened by the addition of soluble impurities, whereas insoluble ones have

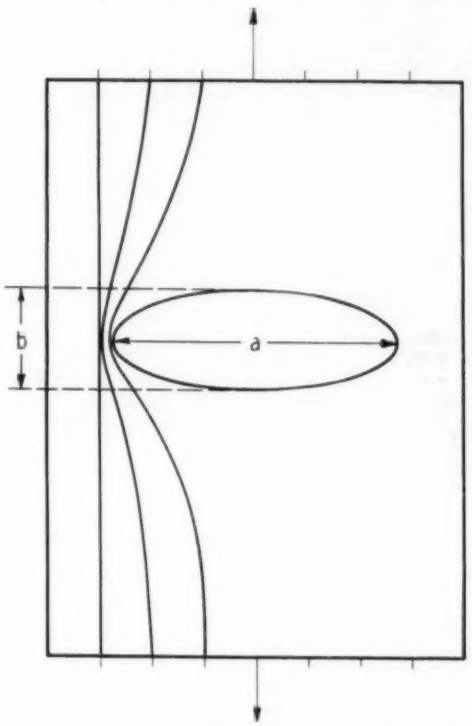

FIG. 7. The concentration of stress at the edges of an elliptical crack in a solid. In avoiding the crack, the lines of stress concentrate at the edges, the stress magnification factor being $2a/b$.

a much smaller effect [see a later part of this section (next installment) for additional details]. Since the soluble impurities enter the interior of the blocks, whereas insoluble ones presumably should tend to congregate near the block boundaries, one would expect the latter to have a greater influence if the simple picture given above is valid.

(d) As we shall see in a later section, the boundaries between crystal grains in polycrystals appear to furnish resistance to shear rather than to aid it. Unless the block boundaries have entirely different nature from intercrystalline boundaries, it is difficult to reconcile this fact with the foregoing picture.

For these reasons, or at least until our knowledge of the mosaic structure is more complete, it seems most fruitful to assume that the role

[15] A. A. Griffith, Trans. Roy. Soc. **221**, 163 (1921).

played by block boundaries is at least secondary, if not actually minor.

Masing[16] has pointed out that one of the major objections to Becker's theory, namely the fact that it does not explain the weakness at absolute

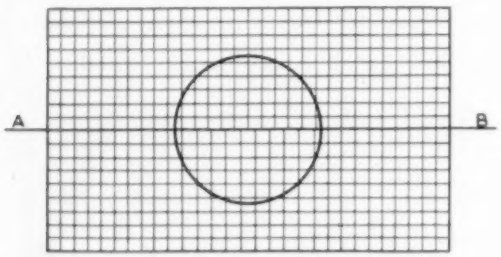

FIG. 8. A schematic picture of a dislocation of the type considered in the theory of slip (after Orowan). Within the circular region there is one more atom in the line of atomic cells above A–B than in the line below. In the text it is assumed that the region of dislocation extends indefinitely in a direction normal to the plane of the paper, so that this figure represents a normal cross section of a line dislocation.

zero of temperature, is removed if we postulate that the block boundaries operate to furnish a stress magnification factor of about a thousand at some point of the solid, for then Becker's slip processes could start at these regions for values of the mean applied stress much lower than σ_0. In the formal equations derived above, this would mean that, in all of the equations in which it appears, the applied stress σ' is to be multiplied by a factor q equal to about a thousand. Equation (10) would then become

$$\sigma_c=\frac{1}{q}[\sigma_0-a(T)^{\frac{1}{2}}]. \qquad (11)$$

Although this result of the juxtaposition of the Smekal and Becker concepts has fewer objections than either scheme alone, it leaves unexplained the mechanism by which slip travels from the regions of high stress magnification to those of low magnification and why soluble impurities play an important role.

(3) *The theory of dislocations.*—A theory of slip that appears to meet many of the strongest objections of the preceding theories has been developed as a result of independent contributions of a number of workers. We shall present the essential points of this theory from a unified viewpoint and then scrutinize it from several different angles.

Let us postulate the existence of a type of lattice imperfection having the following three properties:

(a) The region of imperfection may move through a large part of the lattice without a given atom shifting by more than a single lattice distance. (b) The end result of the motion of the imperfection across a crystal is to translate the part of the crystal on one side of a plane by a unit lattice distance relative to the other part. (c) In an otherwise perfect crystal, the shearing stress required to make the region of imperfection move is about a thousand times lower than the stress required to cause slip in an ideal lattice.

If such imperfections can occur, it is clear that any amount of slip can be produced as a result of the motion of a sufficiently large number of them.

A type of imperfection that possesses the properties (a) and (b) was apparently first considered by Prandtl[17] in connection with a theory of internal friction in solids and later by Dehlinger[18] in a theory of recrystallization. The

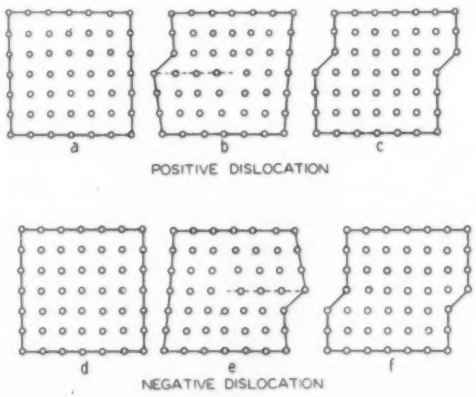

FIG. 9. Generation of dislocations at crystalline boundaries (after Taylor). In cases (a), (b) and (c) a positive dislocation is generated at the left-hand side of the crystal and moves to the right, whereas in cases (d), (e), and (f) a negative dislocation moves to the left. The end result is identical in the two cases.

credit for its use for the theory of slip belongs to Orowan,[19] Polanyi,[20] and Taylor.[21] Let us con-

[16] G. Masing, Zeits. f. Metallkunde **31**, 235 (1939).

[17] L. Prandtl, Zeits. f. angew. Math. Mech. **8**, 85 (1928).
[18] U. Dehlinger, Ann. d. Physik **2**, 749 (1929).
[19] E. Orowan, Zeits. f. Physik **89**, 634 (1934).
[20] M. Polanyi, Zeits. f. Physik **89**, 660 (1934).
[21] G. I. Taylor, Proc. Roy. Soc. **145**, 362 (1934).

sider the type of lattice distortion shown in Fig. 8. In this case, the part of the lattice above the line $A-B$ contains one more atomic cell within the region indicated by the circle than the part below the line. We shall call this type of imperfection a *dislocation*. Taylor has pointed out that dislocations of this type may be generated at the surface of a lattice in the manner shown in Fig. 9. In the upper set of figures, the dislocation starts at the left-hand side of the lattice with the compressed region above and the extended region below and moves to the right, whereas the converse occurs in the lower set of figures. It is clear that the end result of the motion of the first of these types of dislocation from left to right and of the second from right to left is slip by a unit distance along the plane containing the dislocation. The direction of slip would be reversed if the dislocation moved in the opposite directions in the two cases. Following Taylor, we shall call a dislocation of the first kind positive and one of the second kind negative.

In addition, Orowan has pointed out that dislocations of the same type may be generated pairwise in the interior of a crystal in the manner

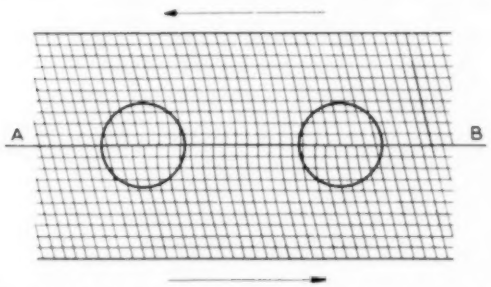

FIG. 10. If dislocations are generated in the interior of crystals, it is necessary that pairs of this type be generated simultaneously. If the members of this pair move out of the lattice in opposite directions, the end result is the same as that shown in Fig. 9.

shown in Fig. 10. If the members of a pair of this type move to the surface in opposite directions, it is clear that the lattice will undergo a unit of slip. Since this type of generation of dislocations requires the production of pairs simultaneously, whereas generation at surfaces requires only single production, it seems almost beyond question that surface production requires least energy.

It should be clearly understood that in the

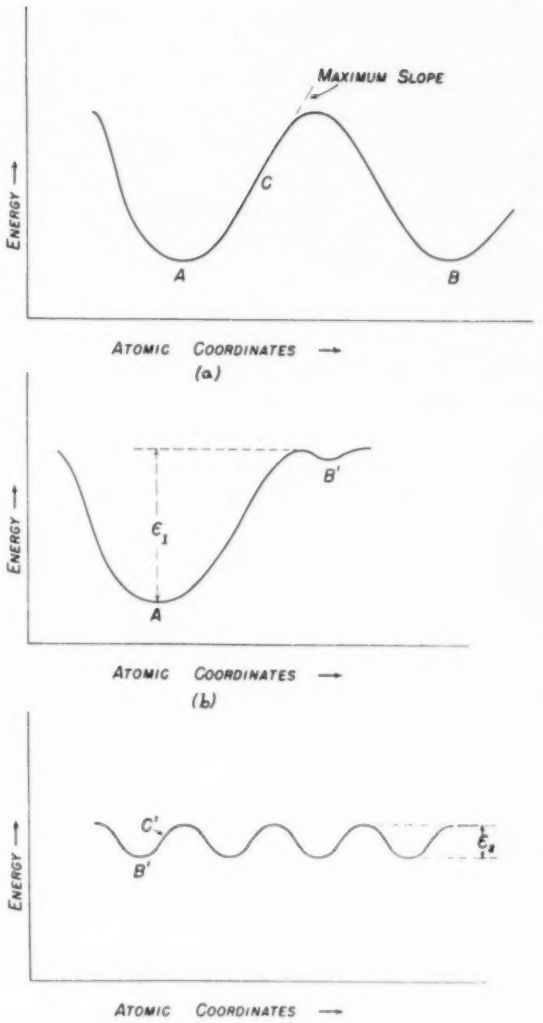

FIG. 11. Curves showing the change in energy of a lattice (a) during shear in an ideal lattice; (b) during formation of a dislocation; (c) during the motion of a dislocation. The abscissae represent schematically the atomic coordinates that are changed during these processes. In case (a) two parts of an ideal crystal move past one another along a slip plane. The point A represents one equilibrium position, the point B another in which one unit of slip has occurred. The critical shearing stress (at absolute zero) is determined by the maximum slope, that is, the slope at C. Figure (b) represents the change in energy during the formation of a dislocation. A corresponds to the perfect crystal, whereas B' is the equilibrium state in which a dislocation is present. The maximum energy change ϵ_1 in going from A to B' is the activation energy for formation of the dislocation. This is dependent on where the dislocation is formed. Figure (c) shows the periodic changes in energy during the motion of a dislocation through the lattice. The shearing stress required to move the dislocation (at absolute zero of temperature) is determined by the slope at C', which should be much smaller than the slope at C in (a), if dislocation theory is valid. The energy ϵ_2 is the activation energy for motion of a dislocation.

models of dislocations shown in Figs. 8, 9 and 10, it is implied that the dislocation extends indefinitely in a direction normal to the plane of the paper and that this entire line of dislocation moves as a unit. We shall refer to these as *line dislocations*. More will be said concerning the actual length of dislocations in a later paragraph.

The change in energy induced in a crystal by the presence of dislocations is illustrated schematically by means of Fig. 11 in which the energy of a portion of the crystal is shown as a function of the atomic coordinates. Naturally a many-dimensional diagram would be required to represent the effect of moving all atoms in the crystal, so, for convenience, the atomic coordinates are represented by a single variable. In an ideal crystal, these coordinates possess values corresponding to an absolute minimum of energy such as the point A. If the atoms are displaced relative to one another from these values, the energy rises, the change in energy varying quadratically with change in relative spacing for small displacements. If two parts of the ideal crystal are sheared past one another along a slip plane by an amount equal to a lattice spacing, the energy will rise to a maximum and then fall to another absolute minimum B as the atoms again come into perfect lattice positions. The critical shearing stress σ_i required to bring about this change is measured by the maximum slope of the curve leading from A to B, that is, the slope at the point C. The energy of the crystal is raised in the manner shown in Fig. 11(b) when a dislocation is formed, for the atomic configuration is no longer that of an ideal crystal. The system is still relatively stable, however, since the energy has the relative minimum value B'. We shall call the energy ϵ_1 required to form a dislocation the *activation energy* for the dislocation. This energy will depend, of course, on whether the dislocation is formed near a surface or in the interior of the crystal. As the dislocation moves through the crystal from one equilibrium position to another, its energy will pass through successive maxima (Fig. 11(c)). The critical shearing stress σ_d required to induce this motion is again measured by the maximum slope. The success of dislocation theory requires that σ_d be many powers of ten lower than σ_i.

The question of the ease with which dislocations of the type considered above can move through the lattice has not yet been investigated with a degree of thoroughness worthy of the problem; however, there is little question that they can move far more easily than atomic planes in a perfect crystal. A qualitative way of seeing this fact is given in Fig. 12. We consider a schematized lattice consisting of two lines of atoms in which there is the dislocation shown. For simplicity, we shall assume that the forces exerted on the lower row of atoms by the upper row may be represented in terms of the sinusoidal energy curve. In an ideal lattice the atoms in the lower row would be opposite the minima of this curve; in the dislocation they are not. However, they are still at equilibrium under the combined action of the forces exerted by the atoms in the upper row and the forces they exert on one another. It may be seen from the figure that the forces exerted on atoms 2 and 8 by the upper row of atoms are in opposite directions, as are those on atoms 3 and 7, and on 4 and 6. Hence these forces tend to compensate one another when the dislocation moves from one equilibrium position to another. The situation obviously would be very different in a perfect lattice, for then the forces exerted on all of the atoms in the lower line would be identical and there would be no compensation during slip.

It should be emphasized at this point that different amounts of energy generally will be

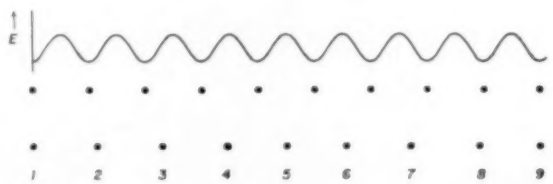

FIG. 12. Illustration of the fact that the critical shearing stress for motion of a dislocation is less than that for an ideal lattice (see text). The upper curve represents the interaction energy of the lower row of atoms in the field due to the upper row.

required to produce dislocations that move in different planes, and that the shearing stress required to make dislocations move in different planes should be different. The easy plane of slip presumably is that for which this shearing stress is lowest.

Peierls[22] has made a rough attempt to estimate the size and critical shearing stress for a dislocation using a simplified model in which the forces between atoms on a given side of the slip plane were treated by regarding the material as continuous and isotropic, and the interaction forces between the two sides were approximated by a sinusoidal function, the amplitude of this function being determined approximately from the shear modulus. The results of this work indicate that the dislocated region extends over only a few atomic distances in the direction normal to the line of the dislocation. In addition, it was found that the ratio R of the shearing stress required to move the dislocation to the stress required to cause slip in a perfect lattice is given by the equation

$$R=\frac{4\pi}{1-\rho}[5.8-\log(1-\rho)]\exp(-4\pi/(1-\rho)),$$

where ρ is Poisson's ratio for the material. This leads to values of R of the order of 10^{-6} or smaller for values of ρ applicable to continuous media.

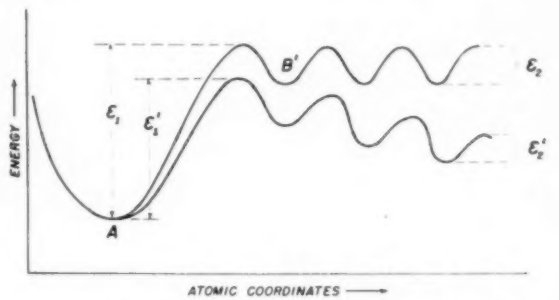

FIG. 13. Schematic illustration of the effect of an applied stress on the activation barrier for production of a dislocation. The upper curve represents the energy in the absence of a stress; the lower curve represents the energy in the presence of one. It may be seen that both activation energies are lowered from values ϵ_1 and ϵ_2 to ϵ_1' and ϵ_2', respectively.

More accurate computations of this type based on more rigorous principles of atomic mechanics are well within the range of feasibility at the present time. It is to be hoped that such computations will be carried out in the near future.

Although the energy required to form a dislocation has not been computed even for a simple hypothetical lattice, we may expect values of the order of one electron volt[23] per atomic plane along the length of the dislocation since the energies associated with interstitial atoms and vacancies (Fig. 5) are of this order of magnitude.

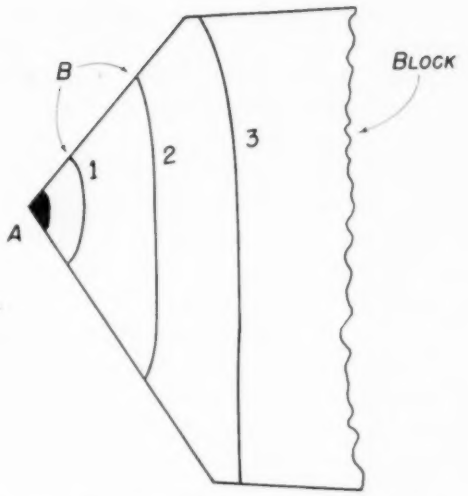

FIG. 14. Schematic representation of the "nucleation" and growth of a dislocation. The dislocation starts as a small slip at A, and grows by elongation in successive stages to a full length dislocation 3. At stages 1 and 2, work must be done at regions such as B, where the dislocation meets the surface in order to elongate the dislocation line.

An important obstacle to dislocation theory seems to arise at this point. If the previous expectation concerning the formation energy per plane in a line dislocation is correct, the total energy in a dislocation that runs through a block about 10^{-4} cm long is about 10^{4} ev. This energy is so enormous when compared with the activation energy for ordinary atomic processes that it is out of the range of possibility to expect such line dislocations to be generated spontaneously by temperature fluctuations. There are two factors that could operate to remove this difficulty:

(a) The activation energy for formation of a dislocation could be much smaller in the presence of an applied stress than in the unstressed crystal.

(b) It is easily conceivable that dislocations start over very small regions near the surface of crystals and become elongated as they proceed through the crystal. In this event, the activation energy required to produce the initial dislocation

[22] R. Peierls, Proc. Phys. Soc. **52**, 34 (1940).

[23] One electron volt is equal to $1.60\cdot10^{-12}$ erg.

could be far smaller than the energy of the final dislocation.

The principles behind the first of these possibilities are illustrated in Fig. 13. The upper curve of the pair shown illustrates schematically the variations in the energy of the crystal during the formation and migration of a dislocation in an unstressed crystal, and is a combination of Fig. 11(b) and (c). Now since the external forces do work on the crystal as a result of the strain occurring during the formation and migration of a dislocation, it follows that the energy curve for the system is altered when stress is applied. This effect may be taken into account by superimposing on the upper curve of Fig. 13 a curve giving the variation of energy with strain due to the external forces. If the stress acts in such a direction as to cause the system to move from left to right in the sense of the diagram, the added function decreases uniformly from left to right and leads to the second curve shown. Thus both the activation energy for the production of dislocations and that for their motion are lowered. The second effect was postulated previously, of course, when we assumed that a dislocation could be made to move even at the absolute zero of temperature for stresses of the order of magnitude of 10^7 dynes/cm^2, for this effect corresponds to lowering the activation energy to zero.

Now it is only reasonable to suppose that the stress required to produce a change in the activation energy ϵ_1 (Fig. 11) for the production of dislocations that is comparable with ϵ_1 should be of the same order as the stress required to produce slip in a perfect lattice. This follows from the fact that the strain involved in producing a dislocation is closely like that occurring during this kind of slip, as may be seen from Fig. 9. Since the applied stresses required to move dislocations are only of the order of 10^7 dynes/cm^2, we must conclude that they are not sufficient to affect the barrier ϵ_1 appreciably unless large stress magnifications occur at some regions of the crystal.

The possibility that the original dislocated area covers only a few atomic dimensions seems to be well within the range of reasonableness, particularly if dislocations start at block boundaries where the surfaces of the blocks may be somewhat irregular (Fig. 14). Once the dislocation has started, it will prefer to move in the direction determined by the applied stress since the system gains energy when it does so. There will then be two retarding factors: (a) The activation energy required for motion of the dislocation without extension of its length; (b) the activation energy required for extension of length. According to the previous discussion, the first of these is very small. There is no reason for supposing that the second is nearly as large for an extension by an atomic length as the activation energy for production of the first small dislocation area. Nevertheless, there is no reason for expecting it to be as small as (a). Moreover, there is no reason for expecting a particularly large stress concentration at the end of the dislocation, at least for the model of a dislocation we are using. Hence it appears to be necessary to postulate that thermal fluctuations supply the activation energy required to extend the length of a dislocation. Thus the process of forming a full-length dislocation would appear to be analogous to the process of forming a crystal of a new phase during the transformation of a metal from one phase to another. That is, the process of forming the first small dislocated area is analogous to the formation of the nucleus of the crystal, whereas the process of extension of the length of this region is analogous to the growth of the crystal from the nucleus. In the present case the driving force for the "reaction" is the applied stress, whereas it is the difference in free energy of the new and old phase in the case of the phase change.

Thus we see that even if stress magnification of the type postulated by Smekal were to play a role in the formation of the first dislocated region (our knowledge of mosaic structure seems to be too fragmentary to argue this point one way or another at present), there is no reason for supposing that such stress magnification could play an equally important role during the elongation of the dislocation. We seem to be forced to the conclusion that dislocations probably cannot be formed at absolute zero of temperature and that any slip that occurs at extremely low temperatures must involve the use of dislocations formed

before cooling. Moreover, according to our picture, the formation of a full length dislocation also requires the presence of an applied stress to direct the process of elongation and supply the free energy for the reaction.

We now pause to summarize the foregoing discussion by giving the following outline:

(a) It seems most probable that slip takes place through the volume of blocks rather than simply at their surface.

(b) The properties of line dislocations seem to be sufficient to provide us with a mechanism for the slip process, provided their existence can be made plausible.

(c) It seems most probable that dislocations are nucleated in small regions near the crystal surface or at block boundaries by the production of small regions of slip, and that line dislocations grow from these by extension. It is perhaps worth adding at this point that there are reasons for supposing that dislocations would be most efficiently produced in pairs at block boundaries. These reasons will be discussed in part (e) of this section.

(d) The initial slip-nuclei may be produced almost entirely as a result of thermal fluctuations; stress can play a primary role in this process only if stress magnification factors of the order of 10^3 are possible.

(e) Even if stress plays a primary role in the formation of slip nuclei, it seems most probable that an appreciable activation energy is required for extension of these nuclei and that this energy is provided by thermal fluctuations. The applied stress plays a guiding role during extension by providing a preferential direction in which the extension-process should take place[24] and furnishing the free energy required for the process.

One of the fundamental problems concerning slip that does not receive an obvious or satisfactory answer in the foregoing picture of the slip mechanism is the fact that the slip bands are separated by distances equal to many lattice spacings. Andrade[4] has pointed out, for example, that the slip bands of many metals are separated by distances of the order of 5 microns. A possible explanation of this fact is that each of the observed slip planes is formed by dislocations generated from a single weak spot. However, if this were true, and if the weak spots were more or less randomly distributed, we should expect the slip bands to be closer in large crystals than in small ones because of the greater number of weak spots. There seems to be no evidence bearing on this point. We shall return to this question later on.

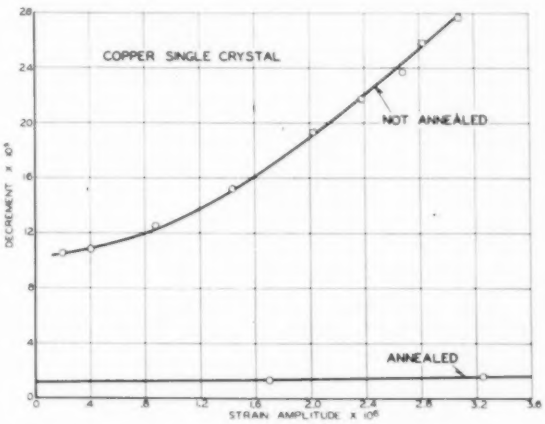

FIG. 15. The decrement as a function of amplitude of oscillation in a single crystal of copper before and after annealing. These curves are reversible functions of strain at room temperature.

d. Internal friction

If any solid is set into oscillation, it will eventually dissipate its vibrational energy even if it is so completely isolated from its surroundings that sound loss and similar effects are negligible. Since the elastic energy reappears as heat in the crystal, this dissipative effect is called internal friction. It is very convenient to express the magnitude of the internal friction in terms of the *decrement* Δ, defined by the relation

$$\Delta = \Delta W / 2W,$$

where ΔW is the energy dissipated per cycle and W is the total vibrational energy.

As we shall see in a later section, one of the largest sources of internal friction in polycrystals is the intercrystalline thermal currents arising from temperature differences between crystals which, as the work of Zener shows, originate as a

[24] The electrostatic field plays a similar role in the case of ionic conductivity in solids. The conducting particles are made mobile as a result of thermal fluctuations, and the field simply provides a preferential direction for their motion.

result of the thermoelastic effect.[25] This type of internal friction is apparently not observed in well-made single crystals at frequencies in the kilocycle range for which measurements are ordinarily made. Instead it is found that a type of internal friction having very different characteristics occurs. In brief, the decrement resulting from the observed internal friction of a specimen is dependent upon amplitude instead of being constant as is the decrement arising

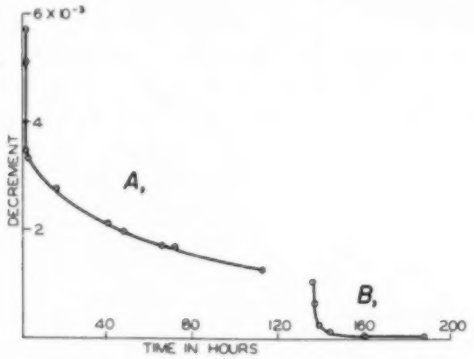

FIG. 16. The variation of the decrement with time for a single crystal of zinc. Curve A: before annealing; Curve B: after annealing.

from thermal currents. In addition the decrement decreases with frequency in a manner unlike that of the friction related to the thermoelastic effect. From the nature of its behavior, which will be described presently, Read[26] has concluded that the internal friction of single crystals is closely related to slip and has its origin in plastic flow within the crystal as a result of the stresses present during vibration. If this interpretation is correct, we should expect to explain some of the properties of the decrement with the aid of the theory of dislocations developed above.

Let us begin by considering the internal friction in a single crystal of copper. The variation with strain amplitude of the decrement before and after annealing is shown[27] in Fig. 15. The first striking fact is that the internal friction decreases very much as a result of anneal. In addition, the decrement increases with increasing strain amplitude. This change with amplitude is completely reversible in the range of strain shown, although it would not be if the strain were larger by a factor of a hundred or so.

These results may be simply explained in a qualitative manner with the following assumptions:

(a) The internal friction arises from the motion of dislocations already present in the crystal under the action of the stresses that occur during oscillation. It is clear that the stresses do irreversible work on the dislocations when the dislocations move, for the elastic energy of the solid is decreased without a corresponding rise in the mutual potential energy of the atoms. It is also clear that the decrement should increase with increasing number of dislocations if we assume that the stress required to make them move does not increase proportionally with their number, for then there are more dissipating centers.

(b) The number of dislocations in the unannealed specimen is higher than in the annealed one because some of the dislocations diffuse out of the crystal during the heat treatment. With this, we must assume, of course, that the dislocations present before anneal were introduced as a result of handling. If this concept is true, we should expect the decrement of the annealed specimen to rise when strained sufficiently, as is the case.

(c) Not all dislocations move with the same ease in the range of stress employed in these experiments. If we grant this, the increase in

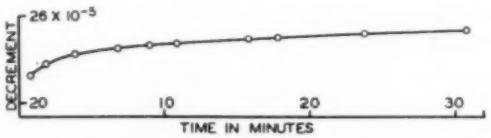

FIG. 17. The increase of the decrement with time for an annealed single crystal of zinc during oscillation at constant strain amplitude (about 10^{-6}). This indicates that dislocations are produced in zinc at room temperature by very small stresses.

decrement with increasing amplitude is easy to understand since dislocations will move as the amplitude of oscillation increases. This postulate is entirely reasonable, for as we shall see below, dislocations may impede one another so that the

[25] C. Zener, Phys. Rev. **52**, 230 (1937), *et seq.*; Proc. Phys. Soc. **52**, 152 (1940). The thermoelastic effect, as its name implies, is the phenomenon in which the temperature of solids is changed as a result of the application of stress.
[26] T. A. Read, Phys. Rev. **58**, 371 (1940).
[27] Based on unpublished work by T. A. Read.

ease with which they move should be different in regions of differing dislocation density. In addition, the stress for which dislocations that are in the process of formation move should be higher than that for fully formed ones (see the preceding part of this section).

The fact that the decrement of single crystals can be raised by stressing them sufficiently at room temperature implies, according to our picture of internal friction, that dislocations can be generated in copper at room temperature. Now we saw in the previous part of this section that there is good reason for believing that dislocations can form completely only if assisted by temperature fluctuations. Thus a good test both of this picture of internal friction and of the picture of dislocation formation would be obtained by studying the effect of stresses on the decrement at very low temperatures where thermal processes in metals and ionic solids are practically halted. Evidence from the study of work hardening of metals, to be discussed later, indicates that dislocations are not formed under these conditions, but measurements of internal friction should provide a much more sensitive test.[28]

On the other hand, the fact that the internal friction of copper does not vary with time at room temperature when the crystals are not stressed implies that the dislocations in this metal are not sufficiently mobile at this temperature to migrate completely out of the crystals of their own accord.

The situation that occurs in zinc at room temperature seems to be very different from that in copper. In the first place if the decrement of a previously annealed single crystal of zinc is measured as a function of time for relatively small but constant vibrational amplitude (say, a strain amplitude of 10^{-7}), and if the measurements are started soon after the crystal has received the strain incident to ordinary handling and cutting, it is found that the decrement continuously decreases. This effect is shown by curve A in Fig. 16. It may be seen that the decrement asymptotically approaches a very small value, the initial rate of decrease being rapid compared with that attained at the end of several hours. If the specimen is removed before it has reached a steady state and is annealed, the decrement then rapidly drops to a very small value, as is shown by curve B in Fig. 16. It is not possible to say whether the asymptote of curve A is the same as that of curve B. The fact that the decrement at the start of run B was nearly as high as at the completion of run A is related to handling received during mounting prior to taking measurements.

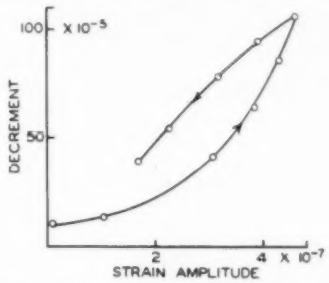

FIG. 18. The variation of the decrement of a single crystal of zinc with amplitude. The lower curve represents measurements made at successively increased strain amplitudes. The upper curve was obtained by making the measurements in the reverse order.

We may interpret the facts contained in Fig. 16 very easily by assuming that the dislocations present when the measurements were started gradually diffuse out of the crystal. The fraction that are in process of formation would naturally diffuse out more rapidly since they are nearest the surface, and would thereby account for the initial rapid decrease in decrement. This exodus of dislocations is greatly speeded by annealing although a comparatively small number of dislocations are produced when the specimen is mounted. These are near the surfaces, however, and disappear very rapidly.

That there should be a large difference in the room temperature internal friction of zinc and copper is not at all surprising for many changes take place in zinc at room temperature that normally occur in copper only at temperatures of the order of 200°C. For example the effects of work hardening disappear in zinc at normal temperatures whereas a high temperature anneal is required for copper.

An extension of these experiments on zinc shows that the internal friction of a well-annealed specimen increases with time when the

[28] In such an experiment it would be necessary to cool the specimen sufficiently slowly to avoid the high stresses that accompany thermal gradients.

crystal oscillates at constant amplitude (Fig. 17). This implies that very small stresses are required to promote the growth of dislocations at room temperature. In accordance with this, it is found that the increase of decrement with amplitude, such as is illustrated in Fig. 15 for copper, is not reversible in the case of zinc if measurements are made in a time comparable with that required to induce the change shown in Fig. 17. Decrement *versus* amplitude curves obtained during increase and subsequent decrease of amplitude are shown in Fig. 18.

It should be mentioned in passing that experiments with variously oriented zinc crystals show that for given amplitude of oscillation, the larger the decrement the larger the shearing stress in the slip plane. This fact illustrates further the close correlation between the type of internal friction considered here and the slip properties.

Thus we may summarize this discussion by saying that experiments on the internal friction of single crystals may be satisfactorily correlated in a qualitative way on the basis of dislocations of the type postulated in the previous section.

We shall continue with a discussion of the theory of dislocations and its applications in the next installment of this series of articles.

Calendar of Meetings

February

21–22 American Physical Society, Cambridge, Massachusetts
21–22 Optical Society of America, Cambridge, Massachusetts

March

3– 7 American Society for Testing Materials, Washington, D. C.
4– 5 Inter-Society Color Council, Washington, D. C.
30–April 5 American Ceramic Society, Baltimore, Maryland

April

1– 3 American Society of Mechanical Engineers, Atlanta, Georgia
4– 5 Southeastern Section of American Physical Society, Vanderbilt University, Nashville, Tennessee
7–11 American Chemical Society, St. Louis, Missouri
16–19 Electrochemical Society, Inc., Cleveland, Ohio
23–25 American Society of Civil Engineers, Baltimore, Maryland
28–30 National Academy of Sciences, Washington, D. C.
30–May 3 American Geophysical Union, Washington, D. C.

May

1– 3 American Physical Society, Washington, D. C.
5– 7 Acoustical Society of America, Rochester, New York
5– 7 Society of Motion Picture Engineers, Rochester, New York
12–15 American Foundrymen's Association, New York, New York
12–21 American Institute of Chemical Engineers, Chicago, Illinois
19–23 American Society for Metals, Los Angeles, California
27–29 American Society for Refrigerating Engineers, Cincinnati, Ohio

June

20–21 American Physical Society, Providence, Rhode Island
23–27 American Association for the Advancement of Science, Durham, New Hampshire

The Optical Properties of Rubber*

BY LAWRENCE A. WOOD

National Bureau of Standards, Washington, D. C.

The optical properties of rubber are discussed under four main headings: absorption, scattering, refractive index, and double refraction. A general survey of the results of previous work in each of these fields is given. Some of the possibilities for future investigation are indicated. New experimental data are presented for the transmission values of milled pale crepe and a soft vulcanized rubber compound at wave-lengths from 400 to 750 mμ. The results of some measurements on scattering are also included. The variation of refractive index with wave-length is given, as calculated from unpublished measurements of the angles of minimum deviation of prisms of unvulcanized and of vulcanized rubber.

I. Introduction

THE potentially-extensive field of research embracing the optical properties of rubber, in comparison with the study of its mechanical, thermal, and electrical properties, has been relatively neglected. It is possible, therefore, even within the limits of the present paper, to give a fairly complete general survey of this field, with brief indications of theoretical consequences and practical applications, as well as some possibilities for future research. Principal consideration is given to four optical properties—absorption, scattering, refractive index, and double refraction. Previous work on each of these topics is summarized, and, in the case of absorption and refractive index, the results of hitherto unpublished measurements made at the National Bureau of Standards are included. No discussion is given regarding the microscopy of rubber, since the topic is complex and somewhat distinct from those treated here.

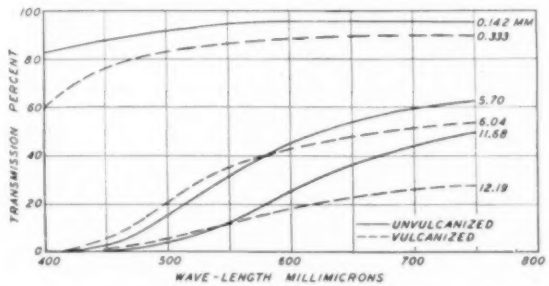

FIG. 1. Transmission of specimens of different thickness as a function of wave-length.

* Paper presented at the symposium on the Physics of Rubber, held at Akron, Ohio, October 12, 1940, under the auspices of the Ohio Section of the American Physical Society.

II. Absorption

The transmission of light by a material is of course a property of fundamental importance in the study of almost any of its optical properties. The purified rubber hydrocarbon, like all the other hydrocarbons with a few exceptions, has been found to have no absorption bands in the visible region of the spectrum. Consequently this material appears colorless and transparent. Commercial raw rubber, on the other hand, possesses a distinctly amber or orange-yellow color. The color is readily evident in rubber prepared by drying latex or by coagulating latex and drying the coagulum, after washing. In smoked sheets the natural color is also evident, although darkened by constituents of the smoke. In pale crepe, on the other hand, it is usually obscured by the white appearance arising from minute air bubbles or tiny surface irregularities, but is readily noticeable after milling.

Since measurements of the transmission of rubber as a function of wave-length do not seem to have been reported, the results of unpublished measurements made at the National Bureau of Standards using the General Electric automatic recording spectrophotometer are here included. Data on six specimens of different thickness are shown in Fig. 1. The solid curves are for milled 1-X pale crepe, and the broken curves for a vulcanized compound made from it. In all cases the data have been corrected by the usual relation for reflection at the surfaces. This relation, based on theoretical considerations, assumes that the ratio of intensities of reflected and incident beams at each surface is equal to $(n-1)^2/(n+1)^2$, where n is the refractive index of the material.

In the computation, use was made of the values of the refractive index given in a later section. The corrections in all but one case amounted to between 8 and 9 percent of the observed values.

These curves should not be regarded as possessing any absolute significance, especially since the absorption seems to be caused by an impurity and not by the rubber hydrocarbon itself. The transmission and color of raw rubber vary considerably from one bale to another, as every rubber technologist knows. The color of a vulcanized compound is also dependent on the nature and amounts of vulcanizing ingredients, particularly the accelerators. The results are, however, typical of the transmission which can be obtained from unpurified, commercial rubber.

If one calculates from the data values of the apparent absorptive index at a given wave-length, the magnitude of the apparent index is found to decrease with increasing thickness of the specimen. From this fact one would conclude that there are surface effects which diminish the intensity of the transmitted beam, and which are of course relatively less important with the thicker specimens. Such effects were not noted by Hock and Müller,[16] in observations with red light on specimens ranging from 1.3 to 5.4 mm in thickness.

According to the work of Eaton and Fullerton[8] the pigment responsible for the color of raw rubber is the yellow hydrocarbon carotene[23] (one of the exceptions to the general rule previously mentioned). They found the amount of carotene in most samples of rubber to be only of the order of 0.002 percent. Bondy and Lauer[5] have found strong anti-oxidant activity in the presence of light, either in the pigment itself or in some material which they could not separate from it. They found, however, that carotene from other sources showed no anti-oxidant activity.

The crystallization of a sheet of rubber is found to reduce the transmission very considerably,[48] and to give the sheet a white appearance. These effects are presumably caused primarily by the heterogeneity of the mixture of amorphous and polycrystalline material and not necessarily to an absorption within each crystal.

The transmission of the vulcanized specimens, as shown by the broken curves, shows the same general features as that of the unvulcanized. However, for specimens of nearly the same thickness a crossing of the curves is evident. For the particular compound used, vulcanization actually increased the transmission at the shorter wave-lengths, while decreasing it at the longer. The specimens therefore appear a greenish-yellow, while the raw rubber from which they were made is distinctly more orange-yellow. It is not obvious whether the increased transmission at the shorter wave-lengths is the result of some chemical reaction of the pigment during vulcanization or of some other cause.

In compounding rubber to obtain a vulcanizate of high transmission, it is desirable to add only enough compounding ingredients to obtain good vulcanization, especially avoiding any excesses of materials which might crystallize out. In order to keep the sulfur content low, an "ultra-accelerator" is almost invariably used. In our work it has been found desirable to use rather low temperatures of vulcanization, with correspondingly lengthened times.

The transmission curves in Fig. 1 were obtained in experiments on vulcanizates of the compound given in Table I.

TABLE I.

	PARTS BY WEIGHT
Pale crepe No. 1–X	100.
Sulfur	1.5
Tetramethylthiuram monosulfide	0.188
Zinc oxide (Kadox)	0.5
Acrin	0.5
AgeRite gel	0.25
Total	102.938

Vulcanization: 90 minutes at 103°C

Fillers having nearly the same refractive index as rubber may be incorporated into a compound in considerable volume without impairment of the transmission. Magnesium carbonate, the best-known example of such a filler, has been studied by several observers.[3, 4, 37] In amounts up to 15 percent the addition of one variety of the carbonate actually increased the transmission. This effect was ascribed to the dilution of the rubber by the carbonate, which has a relatively higher transmission.

The ultraviolet absorption of purified rubber in solution has been studied,[22, 28, 31] and no appreciable absorption is found at wave-lengths longer

than about 270 mμ. Below this point the absorption increases, becoming very strong at about 200 mμ. The increase of absorption appears to be uniform, without the superposition of any observable fine structure. Somewhat similar results have been obtained with thin films of rubber.[2, 21]

The infra-red absorption of rubber has been measured by a number of investigators.[6, 35, 45–47] Since the subject is being discussed by Dr. Sears in another paper,[30] it needs merely be stated here that a number of absorption bands have been found, and some of them have been identified in terms of atomic vibrations. No absorption bands have been observed at wave-lengths shorter than 2μ.

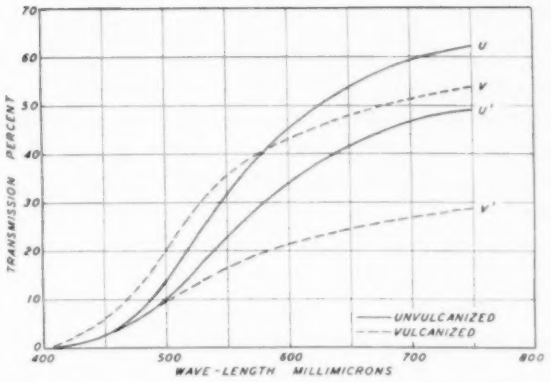

FIG. 2. Transmission as affected by scattering. For curves U and V, light scattered at all angles less than about 38° with the incident beam was included. For curves U' and V', light scattered at all angles less than about 8° with the incident beam was included.

III. Scattering

It can be observed that light is scattered very considerably in its passage through rubber. A considerable portion of the decreased transmission of rubber at shorter wave-lengths is caused by scattering rather than by actual absorption by a pigment. The nature of the particles responsible for the scattering has not been established.

Some idea of the magnitude of the scattering at different wave-lengths may be gained from Fig. 2. The upper curves U and V are the curves already shown in Fig. 1 as the values of the transmission of unvulcanized rubber 5.70 mm thick and of the vulcanized rubber 6.04 mm thick. The optical system, as with all the measurements already discussed, was such that light scattered by the specimen at angles as large as about 38° with the axis was included and measured as transmitted light. When the specimens were moved farther away from the collecting aperture so that only light making angles of about 8° or less, with the axis, was included in the measurement, the lower curves, U' and V', were obtained. In the former position a considerable amount of scattered light was included, since the solid angle subtended was about 20 percent that of a full hemisphere. In the latter position relatively little scattered light was included, since the solid angle subtended was about one percent that of the hemisphere. Some indication of the amount of light scattered at angles less than 38°, then, may be obtained from the difference in ordinates of the corresponding curves U and U', and V and V'. The values obtained vary somewhat with wave-length, but are of the order of one-third that included in the direct beam, in the case of the unvulcanized rubber. For vulcanized rubber, the scattered light is very approximately equal to that in the direct beam. The larger scattering in the vulcanized rubber is probably caused by the presence of uncombined, undissolved compounding ingredients.

Some observations regarding the effect of stretching on the scattering of light in rubber have been made by Schwarzenbach.[29] He discovered several striking optical effects, which are as yet unexplained. A beam of light, circular in cross section, was found to be scattered by stretched rubber in such a way that the section was no longer circular, but consisted of several crossed bands of light.

The scattering of light by rubber solutions has been the subject of extensive studies by Gehman and Field.[10–12] In other work[13] the scattering of light by filler particles in rubber has been made the basis of a method of measuring their size.

The Raman effect—the change of wave-length on scattering—has been the subject of several investigations dealing with rubber solutions. A number of characteristic frequencies were observed by Gehman and Osterhof,[14] and some were identified in terms of the atoms involved. Reasonable agreement between these results and those obtained from infra-red absorption bands was obtained in several cases.

IV. Refractive Index

Of all the optical properties of rubber, the refractive index has probably received the most attention.[25] In fact it seems to be the only optical property of the different varieties of synthetic rubber which has been discussed in the literature.[19] For natural rubber, its value is found to depend but little upon the origin, preparation, or purification of the rubber. Most observers[19, 24] have used the Abbe or the Pulfrich refractometers to measure the index. These instruments, while convenient and rapid in operation, depend upon measurement of the critical angle of total reflection, and are inherently somewhat less precise and accurate than the best spectrometers. Accordingly in some work, as yet unpublished, at the National Bureau of Standards, a number of rubber prisms were made for use with a spectrometer. Complete details of their construction are included in a paper which is now in preparation.

Pale crepe rubber was milled and molded against small plates of glass, the effective surfaces of which were optical plane parallels. For vulcanized rubber prisms, two compounds were employed, one containing about 1.5 percent sulfur and the other about 1.9 percent sulfur, together with accelerators and other ingredients in very small amounts. The specimens were molded or vulcanized, as the case might be, in the form of prisms having refracting angles of about 10° in some cases and about 20° in others. The glass plates were not removed, but, of course, their presence did not alter the direction of the light beam, since they were optically plane parallel, as determined by a method involving the interference of light from the two surfaces. The glass plates served to keep the rubber surfaces clean and to prevent distortion of the rubber.

Measurements of the angles of minimum deviation for light refracted by these prisms were made, in cooperation with Mr. L. W. Tilton, by the use of a spectrometer in the usual manner. The refracting angles of the prisms were measured with the spectrometer and, from these data, refractive indices could be calculated. Measurements were made at five different wave-lengths, corresponding to the *C*, *D*, and *F* lines of Fraunhofer, as well as the *e* and *g* mercury lines. The light sources were a mercury arc, a hydrogen discharge tube, and a sodium flame. Measurements were made at several temperatures, the temperature coefficient thereby determined, and the results finally computed at a standard temperature of 25°C. The results are shown in Fig. 3. The curve for ordinary crown glass is given for comparison.

The dispersion, defined as the difference between indices at two arbitrary wave-lengths, usually the Fraunhofer *F* and *C* lines of the hydrogen spectrum, is seen to be somewhat higher for rubber than for the glass. Its value for unvulcanized rubber at 25°C is 0.01315. This is not far different from that found for unconjugated diolefin hydrocarbons of low molecular weight.[44]

The results show good agreement with the measurements of previous observers, who with a single exception obtained values of the index only for the sodium *D* line. McPherson and Cummings,[24] studying an extensive series of rubber compounds vulcanized with sulfur alone, have shown that the refractive index increases by 0.0037 for each percent of combined sulfur. Assuming the continued validity of this result when accelerators are employed, one may conclude that 1.6 percent and 1.9 percent of combined sulfur are present in the two specimens of vulcanized rubber. There is good correspondence between these values and the 1.5 percent and 1.9 percent used in the compounds. It is to be expected that, under the conditions of the experiment, practically all of the sulfur would become combined.

It is common practice to calculate the molecular refractivity R from the refractive index n_D, density ρ, and molecular weight M, of a substance. The formula usually used is that of Lorenz and Lorentz, namely:

$$R=\frac{n_D^2-1}{n_D^2+2}\frac{M}{\rho}.$$

It is found that for many organic compounds, particularly hydrocarbons, the molecular refractivity is an additive function of terms called atomic refractivities depending on the nature of the atoms and bonds present. The values of the atomic refractivities given by Eisenlohr[9] were

based on studies of a great number of compounds, and have been extensively used. More recent work has led to the suggestion of somewhat different values for the atomic refractivities of carbon and hydrogen, but not to any new value for the refractivity to be associated with a double bond. By the use of Eisenlohr's value, 1.733, for the refractivity to be associated with the double bond, and the various suggested values for the atomic refractivities of carbon and hydrogen, the values of molecular refraction of a C_5H_8 unit containing one double bond have been calculated. The following results were obtained, corresponding to the values for the atomic refractivities suggested by the respective authors: Eisenlohr,[9] 22.62; Swientoslawski,[36] 22.71; van der Hulst,[41] 22.88; and Alsopp and Willis,[1] 22.65. All of these are in sufficiently good agreement with the experimentally determined value of 22.82 to afford optical confirmation of the chemical observation of the existence of a C_5H_8 unit containing one double bond, as the unit group in rubber.

The incorporation of coarse filler particles in rubber, while usually accompanied by a diminution in light transmission, is found to be without influence on the refractive index. Zinc oxide and whiting, however, when present in rubber as particles a few tenths of a micron in diameter, or smaller, are found to raise the value of the refractive index. This effect was first observed by McPherson and Cummings[24] and further investigated by Jones.[17] Its explanation is probably closely associated with the fact that the size of the particles involved is smaller than the wave-length of the light used.

The refractive index of mixtures of unvulcanized rubber and sulfur has been found by McPherson and Cummings[24] to bear a linear relation to the amount of sulfur, with an increase in index n_D^{25} of 0.0016 for each percent of sulfur. The measurements in this case were taken within an hour after mixing on a hot mill. Measurements on mixtures containing up to 4 percent of sulfur were made one month and fourteen months later. They reproduced the first measurements only up to an index corresponding to 1.2 percent of sulfur. Above this point the index in the later measurements showed no further increase. This effect was ascribed to the presence of a supersaturated solution of sulfur in rubber during the first observations. Crystallization of the excess sulfur had occurred during the interval of a month between the first set and the second set of observations. The value 1.2 per-

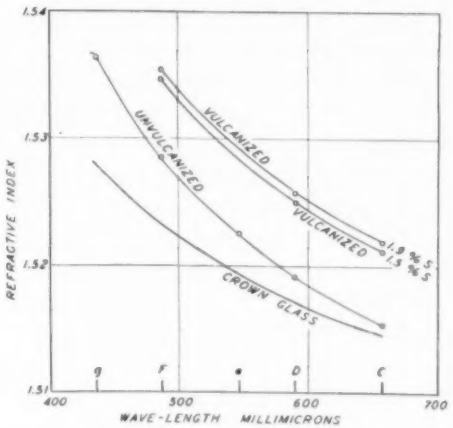

FIG. 3. The variation of refractive index at 25°C with wave-length.

cent, for the amount of sulfur in a saturated solution in rubber at 25°C, is in very good agreement with that very recently obtained by Kemp and his co-workers[18] in an extended investigation by a method involving direct visual observation of the crystallized sulfur. Observations of refractive index can be utilized in a similar manner to measure the solubility of other compounding ingredients in rubber, provided that the refractive indices are appreciably different from that of rubber. The solubility of phenyl-beta-naphthylamine is found by this method to be also 1.2 percent at room temperature.[24]

V. Double Refraction

Rubber appears to be normally isotropic, and the speed of light in it is normally the same in all directions. When it is stretched, however, this is no longer true, and double refraction occurs. A beam of light passing through it emerges as two plane-polarized rays, the ordinary and extraordinary rays. The velocities of these rays, as evidenced by the corresponding indices of refraction, differ, so that there is a phase difference between the rays as they emerge. The amount of phase difference, or retardation of one ray with respect to the other, has been shown

by Thibodeau and McPherson[38] to be usually proportional to the thickness of the rubber and to the stress, provided that the stress is uniform over any section of the sheet and shearing stresses are absent. The proportionality constant is the stress-optical coefficient. The value found for the stress-optical coefficient of soft vulcanized rubber is about 2100 brewsters, a brewster being 10^{-13} cm²/dyne. Most other materials[7] have stress-optical coefficients below 50 brewsters. Gelatine apparently is the only material for which values higher than that for rubber have been reported. The retardation is usually measured by means of the arrangement of displaceable quartz wedges commonly known as the Babinet compensator. It is found that the ordinary ray is faster than the extraordinary ray, and is polarized so that its vibrations are at right angles to the direction of stress.[20, 27]

Double refraction may be used as a means of evaluating the actual stresses in rubber, when it is difficult to measure them directly. In this manner structural changes during the processing of rubber have been studied,[15] and the complex stresses around a rigid inclusion have been evaluated.[39]

The double refraction thus far discussed is similar to that observed with many noncrystalline materials, and has been considered to have no connection with crystallization of the rubber. The conditions that double refraction is present at low elongations and that it bears a linear relation to stress do not correspond to those involved in the formation of crystals, as studied by other methods of observation. However, if the conditions are such that crystals of rubber are formed, a crystalline double refraction appears, and may be superposed on that caused by stress alone.

One method of inducing the formation of crystals is by stretching the rubber. Elongations of at least 100 percent are found to be required. The crystals in this case have one direction fixed, and a fiber axis is found along the direction of stretching. There is random orientation of the crystalline axes in the plane at right angles to this axis. Double refraction has been used in conjunction with a parallel study by x-rays to investigate the conditions of formation of crystals in stretched rubber.[26, 40, 42, 48, 50]

Unstretched rubber may also be crystallized at temperatures from about 15°C to −40°C, or at room temperature at pressures greater than atmospheric. The crystals which are formed in this manner are usually, if not always, very small and oriented at random.[32] The crystals are not isotropic, and double refraction occurs in each crystal.[31, 33] Because of the random orientation, it is often impossible to make quantitative measurements of double refraction in this case. However, if the rubber is crystallized from solution[31, 33] or from very thin films formed by evaporation of a rubber solution,[32] it is sometimes possible to obtain needle-like single crystals which may be observed under the microscope. From crystals obtained in this manner ϵ and ω, the two refractive indices corresponding, respectively, to vibrations along and at right angles to the axis of a uniaxial crystal, were determined at −5°C. The values obtained[31, 33] were $\epsilon = 1.535$ or 1.533, and $\omega = 1.583$.

VI. Conclusions

The general survey which has been presented here shows that, while a number of the optical properties of rubber have been investigated, the measurements of most of them have been more or less preliminary or exploratory in nature and often directed towards some immediately practical application. There appears to be ample opportunity for extended, systematic research on the optical properties for their own sake.

The results to be expected from such study may lead in two directions, each of them illustrated in a very preliminary fashion, by examples given in the present paper. The one direction is that of more fundamental knowledge of the constitution of rubber, especially when optical methods are used in conjunction with other types of measurement. An illustration already mentioned is the use of molecular refractivity to confirm the existence of a C_5H_8 unit containing one double bond as the unit group in rubber. Such work might well be extended, in order to be of assistance in elucidating the constitution of vulcanized rubber. Another illustration is the use of infra-red spectra or Raman spectra to determine the types of chemical bonds present in rubber.

The other direction in which a study of the optical properties of rubber may lead is toward the direct solution of practical problems without regard for the theoretical significance of the measurements. Problems of control or analysis might be approached in this manner, since optical methods usually require only small amounts of material, and are often easily adaptable to rapid and precise measurements. Such applications have already been illustrated in preliminary form by the use of refractive index to determine amounts of combined or dissolved sulfur. The solution of practical problems by optical methods is also illustrated by the use of the photoelastic method for the analysis of stresses in rubber.

Optical measurements in the past have been restricted in most cases to samples having fairly high light transmission. On this account the work has included only unvulcanized rubber and vulcanized compounds of the "pure gum" type. By the use of very thin sections or by employing methods which are based on the reflection of light rather than its transmission, it should be possible to extend the measurements to many practical rubber compounds which appear to be opaque, but which in reality are dispersions of filler particles in a matrix of transparent rubber.

VII. Bibliography

1. C. B. Allsopp and H. F. Willis, "Refractive dispersion of organic compounds. VII Refractive indices of hexane and the refractivities of hydrogen and carbon," Proc. Roy. Soc. London **A153**, 379 (1935).
2. K. Asano, "The action of light on rubber," India-Rubber J. **70**, 307, 347 and 389 (1925).
3. W F. Bixby and H. I. Cramer, "Transparency of rubber compounds containing magnesium carbonate II." Paper presented at Detroit meeting of American Chemical Society, Sept. 1940. Abstract in Rubber Age **47**, 317 (1940).
4. W. F. Bixby and E. A. Hauser, "Transparency of rubber compounds containing magnesium carbonate I," Rubber Chem. Tech. **10**, 299 (1937).
5. H. F. Bondy and G. G. Lauer, "The anti-oxidants of rubber latex I," Ber. deut. chem. Gesell. **66**, 1611 (1933); Rev. gen. Caoutchouc **11**, No. 106, 9 (1934); translated in Rubber Chem. Tech. **7**, 23 (1934).
6. W. F. Busse, "Physics of rubber as related to the automobile," J. App. Phys. **9**, 438 (1938).
7. R. B. Carleton, "Suitability of materials for photoelastic investigations," Rev. Sci. Inst. **5**, 30 (1934).
8. B. J. Eaton and R. G. Fullerton, "The identification and quantitative estimation of the yellow pigment of raw rubber," Quarterly J. Rubber Res. Inst. Malaya **1**, 135 (1929).
9. F. Eisenlohr, "A new calculation of atomic refractions," Zeits. f. physik. Chemie **75**, 585 (1910).
10. S. D. Gehman and J. E. Field, "Colloidal structure of rubber in solution," Ind. Eng. Chem. **29**, 793 (1937), reprinted in Rubber Chem. Tech. **10**, 643 (1937).
11. S. D. Gehman and J. E. Field, "Colloidal structure of rubber in solution. Effect of precipitants," Ind. Eng. Chem. **30**, 1031 (1938), reprinted in Rubber Chem. Tech. **11**, 663 (1938).
12. S. D. Gehman and J. E. Field, "Colloidal structure of rubber in solution. Colloidal aspects of vulcanization," Ind. Eng. Chem. **32**, 282 (1940), reprinted in Rubber Chem. Tech. **13**, 275 (1940).
13. S. D. Gehman and T. C. Morris, "Measurement of average particle size of fine pigments," Ind. Eng. Chem. Anal. Ed. **4**, 157 (1932), reprinted in Rubber Chem. Tech. **5**, 202 (1932).
14. S. D. Gehman and H. J. Osterhof, "Raman spectrum of rubber and some related hydrocarbons," J. Am. Chem. Soc. **58**, 215 (1936), reprinted in Rubber Chem. Tech. **9**, 275 (1936).
15. E. A. Grenquist, "Structural changes during the processing of rubber," Ind. Eng. Chem. **22**, 759 (1930). Reprinted in Rubber Chem. Tech. **3**, 716 (1930).
16. L. Hock and H. J. Müller, "Application of photometry in rubber technology," Kautschuk **8**, 79 and 92 (1932).
17. H. C. Jones, "Refractometer studies on rubber-pigment mixtures," Ind. Eng. Chem. **32**, 331 (1940), reprinted in Rubber Chem. Tech. **13**, 649 (1940).
18. A. R. Kemp, F. S. Malm, G. G. Winspear and B. Stiratelli, "Diffusion of sulfur in rubber. Relation to vulcanization," Ind. Eng. Chem. **32**, 1075 (1940).
19. F. Kirchhof, "Refractometry of rubber and gutta-percha hydrocarbons," Kautschuk **8**, 137 (1932), translated in Rubber Chem. Tech. **6**, 92 (1933).
20. M. Kröger, "The double refraction of rubber in the undeformed and in the deformed state," Kolloid Zeits. **45**, 52 (1928).
21. M. Kröger and H. Staude, "The light absorption of stretched and unstretched rubber and of isoprene," Gummi-Ztg. **43**, 22 (1928).

22. S. J. Lewis and B. D. Porritt, "Preliminary note on the absorption of light by caoutchouc," J. Soc. Chem. Ind. **40**, 18T (1921).
23. H. J. McNicholas, "The visible and ultra-violet absorption spectra of carotin and xanthophyll and the changes accompanying oxidation," Bur. Stand. J. Research **7**, 171 (1931).
24. A. T. McPherson and A. D. Cummings, "Refractive index of rubber," J. Research Nat. Bur. Stand. **14**, 553 (1935), RP 786. Reprinted in Rubber Chem. Tech. **8**, 421 (1935).
25. T. H. Messenger, "The refraction of light by raw rubber," J. Research Assoc. British Rubber Mfrs. **5**, 49 (1936).
26. L. S. Ornstein, J. G. Eymers and J. Wouda, "Thermodynamics of rubber. I. Rubber as a system of two phases," Proc. Roy. Soc. Amst. **32**, 1235 (1929), reprinted in Rubber Chem. Tech. **3**, 397 (1930).
27. B. W. Rowland, "Some aspects of double refraction and structure in rubber," Ind. Eng. Chem. **22**, 1182 (1930), reprinted in Rubber Chem. Tech. **4**, 83 (1931).
28. G. Scheibe and R. Pummerer, "The absorption of rubber and gutta-percha in the ultraviolet region of the spectrum," Ber. deut. chem. Gesell. **60**, 2163 (1927).
29. H. A. Schwarzenbach, "Light scattering in stretched rubber." Helv. Phys. Acta **12**, 270 (1939), translated in Rubber Chem. Tech. **13**, 285 (1940).
30. W. C. Sears, "Infra-red spectra of rubber," J. App. Phys. **12**, 35 (1941).
31. W. H. Smith and C. P. Saylor, "Ether-insoluble or gel rubber hydrocarbon, its solution, crystallization, and properties," J. Research Nat. Bur. Stand. **13**, 453 (1934), RP 719. Reprinted in Rubber Chem. Tech. **8**, 214 (1935).
32. W. H. Smith and C. P. Saylor, "Optical and dimensional changes which accompany the freezing and melting of Hevea rubber," J. Research Nat. Bur. Stand. **21**, 257 (1938), RP 1129. Reprinted in Rubber Chem. Tech. **12**, 18 (1939).
33. W. H. Smith, C. P. Saylor and H. J. Wing, "Preparation and crystallization of pure ether-soluble rubber hydrocarbon: composition, melting point, and optical properties," Bur. Stand. J. Research **10**, 479 (1933), RP 544. Reprinted in Rubber Chem. Tech. **6**, 351 (1933).
34. P. S. Srinivasan, "Ultraviolet irradiation of rubber," Proc. Ind. Acad. Sci. **10**, 186 (1939), reprinted in Rubber Chem. Tech. **13**, 549 (1940).
35. R. Stair and W. W. Coblentz, "Infrared absorption spectra of plant and animal tissue," J. Research Nat. Bur. Stand. **15**, 295 (1935), RP 830.
36. W. Swientoslawski, "Atomic refraction," J. Am. Chem. Soc. **42**, 1945 (1920).
37. Y. Tanaka, "Magnesium carbonate and the transparency of vulcanized rubber," Trans. Inst. Rubber Ind. **2**, 330 (1927).
38. W. E. Thibodeau and A. T. McPherson, "Photoelastic properties of soft vulcanized rubber," J. Research Nat. Bur. Stand. **13**, 887 (1934), RP 751. Reprinted in Rubber Chem. Tech. **8**, 183 (1935).
39. W. E. Thibodeau and L. A. Wood, "Photoelastic determination of stresses around a circular inclusion in rubber," J. Research Nat. Bur. Stand. **20**, 393 (1938), RP 1083.
40. P. A. Thiessen and W. Wittstadt, "Forced and spontaneous changes in the arrangement of the molecules in stretched rubber. Crystals and fused phase in stretched rubber," Zeits. f. physik. Chemie **B41**, 33 (1938), translated in Rubber Chem. Tech. **12**, 736 (1939).
41. L. J. N. van der Hulst, "A new determination of atomic refractions." Rec. trav. chim. **54**, 518 (1935)
42. W. C. van Geel and J G. Eymers, "The double. refraction of stretched rubber," Zeits. f. physik. Chemie **B3**, 240 (1929), translated in Rubber Chem. Tech. **2**, 545 (1929).
43. A. van Rossem and J. Lotichius, "The freezing of raw rubber," Kautschuk **5**, 2 (1929), translated in Rubber Chem. Tech. **2**, 378 (1929).
44. A. von Grosse and R. C. Wackher, "Quantitative determination of aromatic hydrocarbons by a new method," Ind. Eng. Chem. Anal. Ed. **11** , 614 (1939).
45. A. J. Wells, "Infra-red transmission of thin films of various organic materials," J. App. Phys. **11**, 137 (1940).
46. D. Williams, "An application of infra-red spectroscopy to rubber chemistry," Physics **7**, 399 (1936), reprinted in Rubber Chem. Tech. **10**, 249 (1937).
47. D. Williams and R Taschek, "Effects of elastic stretch on the infra-red spectrum of rubber," J. App. Phys. **8**, 497 (1937), reprinted in Rubber Chem. Tech. **10**, 697 (1937).
48. W Wittstadt, "External influence and the internal state of rubber," Kautschuk **15**, 11 (1939), translated in Rubber Chem. Tech. **12**, 488 (1939).
49. L. A. Wood, "Synthetic rubbers: a review of their compositions, properties, and uses," Nat. Bur. Stand. Circular C427. (U. S. Government Printing Office, Washington, D. C., 1940.) Also in India Rubber World **102**, No. 4, 33 (1940).
50. H. Zocher and H. J. von Fischer, "Optical anisotropy of stretched rubber," Kautschuk **5**, 173 (1929).

Here and There

Physicists Needed for National Defense Work

The civil service examinations announced on November 14, 1940, for physicists have not produced enough applicants, according to a statement issued by the United States Civil Service Commission, Washington, D. C. The announcements have been amended by the Commission to extend the closing dates for receipt of applications for nearly a year—until December 12, 1941. Only one application need now be filed at the Commission's Washington office by persons wishing to apply for two or more positions, and no written test is required for any grade.

The positions to be filled include the following grades: physicist (any specialized branch), $3,800 a year; also principal, $5,600; senior, $4,600; associate, $3,200; and assistant, $2,600 a year. These salaries are subject to a 3½ percent retirement deduction.

Applicants for all grades must have completed a 4-year college course; for the three higher grades they must have had major study in physics; and for the two lower grades they must have completed at least 24 semester hours in physics. They must have had professional experience in physics, but partial substitution of graduate study in a specialized branch of physics may be made. Applicants will not be required to report for examination—they will be rated on their qualifications as shown in their applications and on corroborative evidence.

Further information regarding the examination, and the proper application forms, may be obtained from the Secretary of the Board of U. S. Civil Service Examiners at any first- or second-class post office, or from the U. S. Civil Service Commission, Washington, D. C.

★

Cyclotron Equipment on Order

Electric equipment to operate the University of California's new 100,000,000-volt cyclotron has been ordered from the General Electric Company, according to a recent announcement from the company's News Bureau in Schenectady. This electrical equipment, including transformers, capacitors, rectifiers and switchgear, will occupy the space of a two-story house, and engineers estimate that more than a year will be required for the building of it. They explain that the machinery will take 2500 kva supplied at 12,000 volts, 3-phase, 60-cycle alternating current, at constant voltage, and will rectify it to 25,000 volts, direct constant current, which will be fed into the oscillator of the cyclotron, operating at 10,000,000 cycles.

Construction of the University of California's supercyclotron, under the direction of Professor E. O. Lawrence, was made possible through a $1,150,000 grant by the Rockefeller Foundation, to be augmented by an additional $250,000 from other sources.

A. Cressy Morrison Prize

The A. Cressy Morrison prize of $500 of the New York Academy of Sciences has been divided between Dr. Hans A. Bethe, Professor of Physics at Cornell University, and Dr. Robert E. Marshak, Instructor in Physics at the University of Rochester, for a joint paper entitled "The sources of stellar energy."—*Science*.

★

University of Pittsburgh Cyclotron

A gift of $50,000 for the construction of a cyclotron has been given to the University of Pittsburgh Medical School by Mrs. Alan M. Scaife. Construction, which will begin immediately, will be under the general supervision of Dr. Alexander J. Allen, Associate Professor of Physics.

★

Royal Society Awards Medals

Recommendation made by the Council of the Royal Society for the award of a Royal Medal to Professor P. M. S. Blackett, F.R.S., has been approved by King George, according to a recent announcement in *Nature*. Professor Blackett has been chosen for this honor in recognition of his studies of cosmic rays and the showers of particles which they produce, for his share in the discovery of the positive electron, for his work on mesons, and for many other experimental achievements.

Of particular interest to physicists are the following announcements of awards made by the President and Council of the Society:

The Copley Medal to Professor P. Langevin, For. Mem. R.S., for his pioneer work in the electron theory of magnetism, his fundamental contributions to discharge of electricity in gases, and his important work in many branches of theoretical physics.

The Rumford Medal to Professor K. M. G. Siegbahn for his pioneer work in high precision x-ray spectroscopy and its applications.

The Davy Medal to Professor H. C. Urey for his isolation of deuterium, the heavy hydrogen isotope, and for his work on the use of this and other isotopes in following the detailed course of chemical reactions.

The Hughes Medal to Professor A. H. Compton for his discovery of the Compton effect, and for his work on cosmic rays.

Contributors to This Issue

J. W. McNall

J. W. McNall received his B.S. degree in 1936 from the Case School of Applied Science. Since that time he has been connected with the Westinghouse Electric and Manufacturing Company Research Laboratories. He is now on leave of absence at Massachusetts Institute of Technology where he is pursuing his graduate studies in physics under the Westinghouse B. G. Lamme Scholarship.

Thomas A. Read

Thomas A. Read received his A.B. and Ph.D. degrees from Columbia University. Since June, 1939, he has been a Westinghouse Research Fellow, working at the Westinghouse Research Laboratories on the damping of mechanical vibrations in metal single crystals.

D. D. Knowles

Dewey Deforest Knowles is a member of the research engineering staff of the Special Products Department of the Westinghouse Lamp Division, Bloomfield, New Jersey. Mr. Knowles, inventor of the grid glow tube and a number of other electronic devices, is a graduate of Baldwin-Wallace College, Berea, Ohio, and of Purdue University, Lafayette, Indiana.

Lawrence A. Wood

Lawrence A. Wood has been a member of the Rubber Section of the National Bureau of Standards since 1935. He received the Ph.D. degree from Cornell University, where he was Instructor in Physics from 1928 to 1935 and was engaged in research work on blocking-layer photo-cells.

The following contributors have received mention in earlier issues of the *Journal of Applied Physics:*

Thomas H. Osgood, p. 73, Vol. 11, No. 1, 1940.
Maurice A. Biot, p. 36, Vol. 9, No. 1, 1938.
E. U. Condon, p. 563, Vol. 11, No. 8, 1940.
L. F. Ehrke, p. 128, Vol. 11, No. 2, 1940.
C. M. Slack, p. 128, Vol. 11, No. 2, 1940.

Edward S. Lamar

Edward S. Lamar received his A.B. and A.M. degrees at George Washington University in 1926 and 1928, and his Ph.D. degree at Princeton University in 1934. He is now an Assistant Professor of Physics at the Massachusetts Institute of Technology.

William W. Buechner

William W. Buechner received his B.S. and Ph.D. degrees at the Massachusetts Institute of Technology. He is now a Research Associate in Physics at that institution.

Robert J. Van de Graaff is an Associate Professor of Physics at the Massachusetts Institute of Technology. He received the B.S. degree from the University of Alabama in 1922 and the Ph.D. degree at Oxford in 1928. From 1928 to 1931 he was a National Research Fellow, first at Oxford and then at Princeton. Dr. Van de Graaff's picture appeared in the *Journal of Applied Physics* on p. 602, Vol. 8, No. 9, 1937.

Frederick Seitz is Assistant Professor of Physics at the University of Pennsylvania. He has participated in the past three Summer Sessions at the University of Pittsburgh, and spent the past two summers as visiting physicist at the Westinghouse Research Laboratories. Dr. Seitz received his Ph.D. degree from Princeton University in 1934. His picture appeared in the *Journal of Applied Physics*, p. 72, Vol. 8, No. 1, 1937.

Contributed Original Research

Forced Oscillations in Cavity Resonators

E. U. Condon
Westinghouse Research Laboratories, East Pittsburgh, Pennsylvania
(Received October 17, 1940)

Formulas are developed for calculation of the impedance of a cavity resonator when excited by a coupling loop or by a capacitative coupling.

THERE is a rapidly growing appreciation of the importance of cavity resonators in ultra-high frequency work especially where the frequencies are of the order of 300 megacycles/sec. or greater. The theory for the resonant modes for simple shapes is well known from the classical work[1] and has recently been restated in convenient form for practical use.[2] This paper discusses the coupling of a transmission line to a cavity resonator.[3]

General Ideas

The cavity resonator is assumed to be bounded by highly conducting walls, so the Q values of the various resonant modes are large. The resonator will have a number of resonant frequencies, ν_a, associated with each of which there is a standing wave field derivable from the vector potential, $\mathbf{A}_a$ by the formulas

$$\mathbf{E}_a = -\frac{1}{c}\frac{\partial \mathbf{A}_a}{\partial t}, \quad \mathbf{H}_a = \text{curl } \mathbf{A}_a.$$

It is convenient to normalize the $\mathbf{A}$'s in such a way that they are dimensionless,

$$\int \mathbf{A}_a(\mathbf{r}) \cdot \mathbf{A}_b(\mathbf{r}) dV = \begin{cases} 0 & a \neq b \\ V & a = b. \end{cases} \tag{1}$$

An arbitrary electromagnetic field inside the resonator which satisfies the boundary conditions can be expanded in terms of the resonant wave patterns, $\mathbf{A}_a(\mathbf{r})$,

$$\mathbf{A}(\mathbf{r}, t) = \sum_a p_a(t) \mathbf{A}_a(\mathbf{r}). \tag{2}$$

Suppose we are given the time and space distribution of current density $\mathbf{i}(\mathbf{r}, t)$ inside the resonator and wish to calculate what resonant modes are excited. First we assume that $\mathbf{i}$ can be expanded in terms of the $\mathbf{A}_a(r)$ functions

$$\mathbf{i}(\mathbf{r}, t) = \sum_a I_a(t) \mathbf{A}_a(\mathbf{r}). \tag{3}$$

The coefficients $I_a(t)$ are easily found formally in view of (1)

$$I_a(t) = \frac{1}{V} \int \mathbf{i}(\mathbf{r}, t) \cdot \mathbf{A}_a(\mathbf{r}) dV. \tag{4}$$

The equation for the $p_a(t)$ is found by substituting in the Maxwell equation

$$\text{curl } \mathbf{H} - \frac{1}{c} \dot{\mathbf{E}} = 4\pi \mathbf{i}, \tag{5}$$

which leads at once to the following equations, one for each resonant mode,

$$\ddot{p}_a + (2\pi\nu_a)^2 p_a = 4\pi c^2 I_a(t). \tag{6}$$

The theory leading to this equation is approximate in that it neglects damping. If damping is small and is measured by the quantity Q_a in the usual way, then (6) can be replaced by

$$\ddot{p}_a + \frac{2\pi\nu_a}{Q_a} \dot{p}_a + (2\pi\nu_a)^2 p_a = 4\pi c^2 I_a(t). \tag{7}$$

This equation permits the calculation of p_a, the amplitude of excitation of the ath mode. We see

[1] H. Bateman, *Electrical and Optical Wave Motion* (Cambridge University Press, 1915).
[2] W. W. Hansen, J. App. Phys. **9**, 654 (1938); W. W. Hansen and R. D. Richtmyer, J. App. Phys. **10**, 189 (1939).
[3] Compare as to method, E. U. Condon, J. App. Phys. **11**, 502 (1940).

that $I_a(t)$ given by (4) measures the effectiveness of the current distribution in exciting the ath mode.

If, as is usual in practice, the current $\mathbf{i}$ is confined to a wire of small cross section with $I(t)$ being the total current in the wire, then

$$I_a(t)=\frac{1}{V}I(t)\int \mathbf{A}_a\cdot\mathbf{ds}. \tag{8}$$

By Stokes' theorem

$$\int \mathbf{A}_a\cdot d\mathbf{s}=\int\int \operatorname{curl}\mathbf{A}_a\cdot\mathbf{dS}=M_a. \tag{9}$$

The quantity M_a is the flux through the current-carrying loop caused by unit amplitude of excitation of the ath mode. It is appropriate, therefore, to call it the mutual inductance of the loop with this mode.

Impedance of Coupling Loop

If the wire loop in which the current flows has resistance R, then the electromotive force needed when current I flows is given by

$$\mathcal{E}=RI+\sum_a M_a\dot{p}_a, \tag{10}$$

where p_a is given in terms of I by

$$\ddot{p}_a+\frac{2\pi\nu_a}{Q_a}\dot{p}_a+(2\pi\nu_a)^2p_a=\frac{4\pi c^2}{V}M_aI(t). \tag{11}$$

Suppose the currents and voltages have a time dependence of frequency ν. Writing $\mathcal{E}$, I, p_a, etc. for the amplitudes of $e^{2\pi i\nu t}$, the equations for the amplitudes are

$$\mathcal{E}=RI+\sum_a 2\pi i\nu M_ap_a,$$

$$\frac{\pi V}{c^2}\left(\nu_a^2-\nu^2+i\frac{\nu\nu_a}{Q_a}\right)p_a=M_aI$$

and therefore, eliminating the p_a between these equations one finds for the effective impedance of the coupling loop

$$Z=R+\sum_a\frac{2\pi i\nu M_a^2}{\frac{\pi V}{c^2}\left(\nu_a^2-\nu^2+i\frac{\nu\nu_a}{Q_a}\right)}. \tag{12}$$

The important thing to notice about (10) and hence about (12) is that there is no self-inductance term. The effects of self-inductance are contained in (12) since the entire field inside the resonator is represented in terms of the p_a. At low frequencies such that $\nu\ll\nu_a$, the second term in (12) simplifies into

$$2\pi i\nu\sum_a\frac{\lambda_a^2M_a^2}{\pi V},$$

which is the inductive reactance due to an effective self-inductance of the loop as modified by the presence of the walls.

If the driving frequency is exactly equal to the resonant frequency of one particular mode, $\nu=\nu_a$ then that particular term in the sum in (12) will be large compared to all others. The resonant amplitude of the ath mode is

$$(p_a)_{\text{resonant}}=-iQ_a\frac{\lambda_a^2M_a}{\pi V}I, \tag{13}$$

where p_a lags $\pi/2$ behind I, as shown by the factor $-i$.

Example

As a specific example, consider the simplest mode of oscillation of a copper cube whose edge is $A=20$ cm. The frequency is $\nu_a=1.06\cdot10^9$ cycle/sec. and $Q_a=33{,}000$. The normalized vector potential is

$$A_{ax}=4\sin(\pi y/A)\sin(\pi z/A),$$

$$A_{ay}=0,\quad A_{az}=0,$$

giving for the magnetic field at unit amplitude

$$\operatorname{curl}\mathbf{A}_a=\frac{4\pi}{A}\left[\mathbf{j}\sin\frac{\pi y}{A}\cos\frac{\pi z}{A}-\mathbf{k}\cos\frac{\pi y}{A}\sin\frac{\pi z}{A}\right].$$

Suppose the coupling loop is a single turn of wire whose area is 1 cm², located near the point on the wall whose (x, y, z) coordinates are $(A/2, 0, A/2)$. Near this point the magnetic field is in the $\mathbf{k}$ direction, and has a magnitude $4\pi/A$. Hence if the plane of the loop is normal to the z axis, the mutual inductance M_a is

$$M_a=4\pi/A=0.628\text{ cm}.$$

From (12) we see that at resonance the coupling of the ath mode contributes a resistive term to the loop's impedance, whose magnitude is

$$R_a = 2\nu_a Q_a \frac{\lambda_a^2 M_a^2}{V}.$$

In (12), $\mathcal{E}$ and I are in electromagnetic units, so to get R_a in ohms, divide by 10^9. Substituting for this example, we get

$$R_a = 2760 \text{ ohms}.$$

The resonant amplitude p_a of this mode is

$$\frac{p_a}{I} = \frac{R_a}{2\pi\nu_a M_a} = 660,$$

where both p_a and I are in the same units.

The electric vector along the line, $y = z = A/2$ is

$$E = \frac{2\pi}{\lambda} \cdot 4p_a \text{ stat. volt/cm},$$

so the line integral of E from $x=0$ to $x=A$ is

$$V_B = EA = \frac{8\pi}{\sqrt{2}} p_a \text{ stat. volts}.$$

The voltage drop in the loop is $R_a I$, so the voltage multiplication is

$$\frac{V_B}{V_L} = \frac{8\pi}{\sqrt{2}} \cdot 300 \cdot \frac{p}{R_a I} = 127.5.$$

For example, if an r. m. s. voltage of 1000 is applied to the loop, the loop current will be 0.36 ampere and the power consumed is 360 watts. The resonant amplitude $p_a = 23.8$ abamperes, so the magnetic field amplitude at the loop is 14.9 gauss. The electric vector along the center line is 6.33 kv/cm, giving a total voltage amplitude along the center line of 127 kv.

Capacitative Coupling

In the preceding, we have assumed the charge to be zero everywhere inside the resonator. The more general case is that in which there is a charge density ρ as well as a current $\mathbf{i}$ in the cavity. In practice this might be done by inserting a short wire through a hole in the wall; the driving electromotive force is then applied between the wire and the wall.

With charge in the cavity it is necessary to introduce a scalar potential φ, as well as the vector potential. The fields are given by

$$\mathbf{H} = \text{curl } \mathbf{A}, \quad \mathbf{E} = -\frac{1}{c}\frac{\partial \mathbf{A}}{\partial t} - \text{grad } \varphi. \tag{14}$$

Substitution in Maxwell's equations gives

$$\begin{aligned} -\frac{1}{c}\frac{\partial}{\partial t} \text{div } \mathbf{A} - \nabla^2 \varphi &= 4\pi\rho, \\ \text{curl curl } \mathbf{A} + \frac{1}{c^2}\frac{\partial^2 \mathbf{A}}{\partial t^2} &= 4\pi\left(\mathbf{i} - \frac{1}{4\pi c}\frac{\partial}{\partial t} \text{grad } \varphi\right). \end{aligned} \tag{15}$$

One may still use the same vector potential solutions as before. For these div $\mathbf{A} = 0$, hence the first equation of (15) becomes

$$-\nabla^2 \varphi = 4\pi\rho.$$

Therefore, at each instant φ is to be determined from the charge distribution exactly as if ρ were independent of the time. The boundary condition is $\varphi = 0$ on the walls.

The equation for $\mathbf{A}$ in (15) is of the same form as before, except that the displacement current associated with φ has to be included in the complete expression for $\mathbf{i}$. When one calculates $I_a(t)$ by (4),

$$I_a(t) = \frac{1}{V}\int\left(\mathbf{i} - \frac{1}{4\pi c}\frac{\partial}{\partial t} \text{grad } \varphi\right) \cdot \mathbf{A}_a dV,$$

it turns out that the term arising from the displacement current vanishes, so the expression for $I_a(t)$ is actually the same as before.

If the current is really confined to a wire which ends in an internal electrode, and I is the total current, then the total rate at which work is done on the field by the current is

$$-c\int \mathbf{i} \cdot \mathbf{E} dV = I\sum_a M_a \dot{p}_a + cI\varphi_0 \tag{16}$$

where φ_0 is the potential of the internal electrode. If C is the capacity of this electrode relative to the walls, reckoned electrostatically, then $\varphi_0 = q/C$ where $I = \dot{q}$ so the electromotive force which

must be applied between the wire and the wall is

$$\mathcal{E}=c\frac{q}{C}+\sum_a M_a\dot{p}_a. \tag{17}$$

Here $\mathcal{E}$ is in electromagnetic units, while q and C are in electrostatic units. Applying (17) to a steady state with frequency ν, we find for the impedance of a capacitative coupling

$$Z=\frac{c^2}{2\pi i\nu C}+\sum_a \frac{2\pi i\nu M_a^2}{\frac{\pi V}{c^2}\left(\nu_a^2-\nu^2+i\frac{\nu\nu_a}{Q_a}\right)}. \tag{18}$$

Here C is the capacity calculated electrostatically and M_a is to be calculated from (9) on the lead-in wire. The excitation of the resonant modes is entirely caused by coupling with the lead-in wire, the capacity of the internal electrode merely makes it possible to put current into the lead-in wire.

To give a specific example, suppose a fine wire enters the center of the base of the same copper box that was considered in the previous section. On its end 1 cm above the base, suppose there is a ball 0.1 cm in radius. The electrostatic capacity to a good approximation is

$$C=0.105 \text{ cm}.$$

The coupling of the wire to the mode considered before is

$$M_a=\int \mathbf{A}_a\cdot d\mathbf{s}=4 \text{ cm}.$$

Hence the input impedance in ohms at resonance, $\nu=\nu_a$,

$$Z=10^{-9}\left[\frac{c^2}{2\pi i\nu C}+\frac{2\nu_a Q_a\lambda_a^2 M_a^2}{V}\right]$$

$$=112{,}000-1280i.$$

The resonant frequency with capacitative coupling is not exactly $\nu=\nu_a$; to get vanishing reactance it is necessary to choose ν enough different from ν_a to balance out the capacitative reactance of the condenser formed by inner electrode and resonator walls.

The Production of Proton Beams

E. S. Lamar, W. W. Buechner and R. J. Van de Graaff
Massachusetts Institute of Technology, Cambridge, Massachusetts

(Received September 14, 1940)

An account is given of further work on capillary ion sources of the diffusion type. Both metal and glass capillaries have been investigated. The performance of the metal sources is affected by surface conditions which are difficult to control. The average proton yield from these sources is about ten percent. It was found that the yield could be increased to about fifty percent by coating the surface with phosphorus pentoxide. Sources constructed of Pyrex have a proton yield of about sixty percent and also greater stability in operation, as well as certain other advantages. Various characteristics of the output of both types of source are described as functions of the source geometry, arc current, and other variables.

Introduction

THE present paper and the one immediately following describe a continuation of previous work on ion sources carried out at the Massachusetts Institute of Technology.[1,2] This field of research owes its importance to the need in many experimental problems for well-focused ion beams of controllable energy and suitable composition. In nuclear physics, for example, there is urgent need for intense beams of protons and deuterons. Although many high voltage generators in use or under construction are capable of delivering currents of several milliamperes, present technique with ion sources and high voltage tubes limits the current available at the target to a small fraction of the generator

[1] Lamar, Samson and Compton, Phys. Rev. **48**, 886 (1935).
[2] Lamar, Buechner and Compton, Phys. Rev. **51**, 936 (1937).

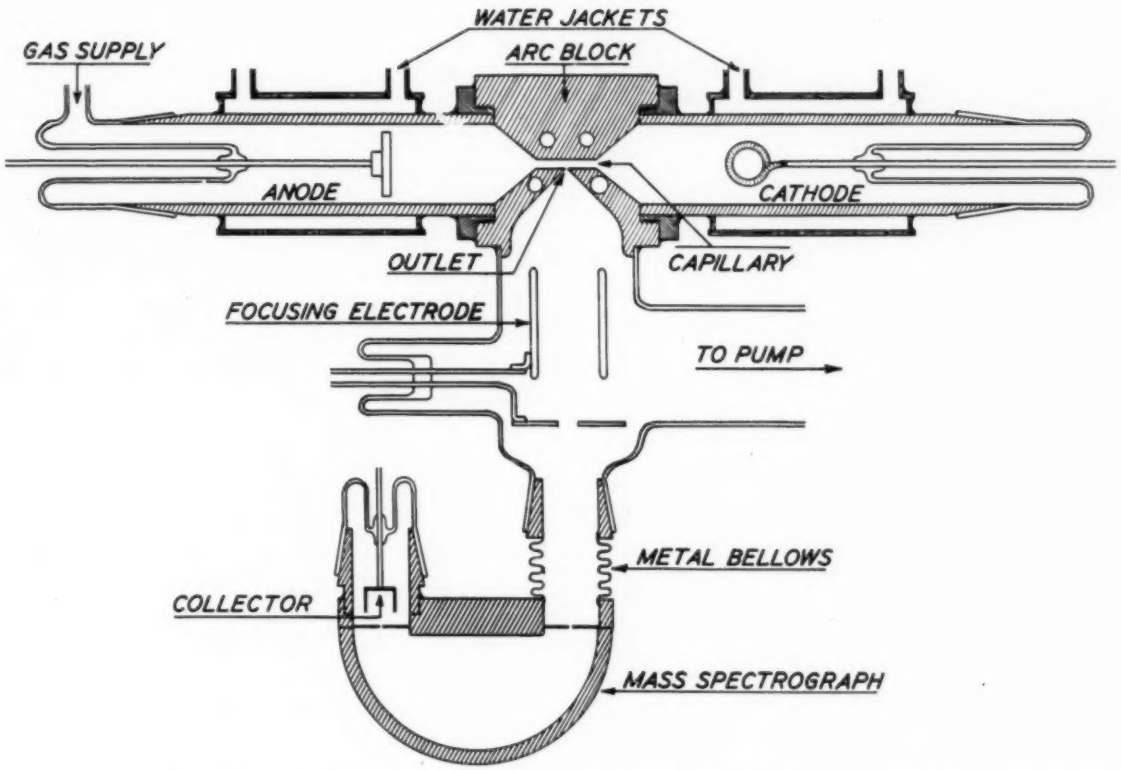

FIG. 1. Typical metal capillary arc together with electrodes external to the arc for collecting and analyzing the ion current.

output. In some cases the output of the ion source itself is low. In others the output, while high, cannot be delivered to the target because of the exacting requirements imposed by the high voltage tube.

Of vital importance to the whole problem is the initial focusing of the ion beam with sufficient accuracy to make possible its passage through the tube to the target with full generator voltage. The collisions of the unfocused or scattered ions with the tube electrodes and walls liberate charged and uncharged particles. The secondary electrons in their transit back up the tube produce in the gas ions which in general are not focused. The neutral gas evolved from the electrodes and walls as a result of bombardment by the unfocused ions contributes to the gases already present and so increases the ionization and the scattering. It is evident, therefore, that the various effects of the unfocused current may become regenerative in increasing the unfocused current reaching each of the many tube electrodes. Current to these electrodes not only represents a loss in useful generator current, but may so alter the potential distribution along the high voltage tube as to cause actual electric breakdown. In view of these considerations it is evident that the useful current from an ion source is not simply the total source output, but is the current which can be delivered in a focused beam sufficiently far from the ion source outlet to insure its subsequent transit down the high voltage tube. The focusing aspect of the ion source problem is considered in detail in the paper immediately following the present one.

It is evident from the preceding paragraph that neutral gas in the high voltage tube contributes to the regenerative processes precipitated by the ion beam and leading to ultimate breakdown. Hence it is important that only a minimum of neutral gas accompany the desired ion current as it leaves the ion source, or in other words, the percent ionization of the gas issuing from the source should be high.

Ion sources for most nuclear investigations are of value chiefly insofar as they produce atomic

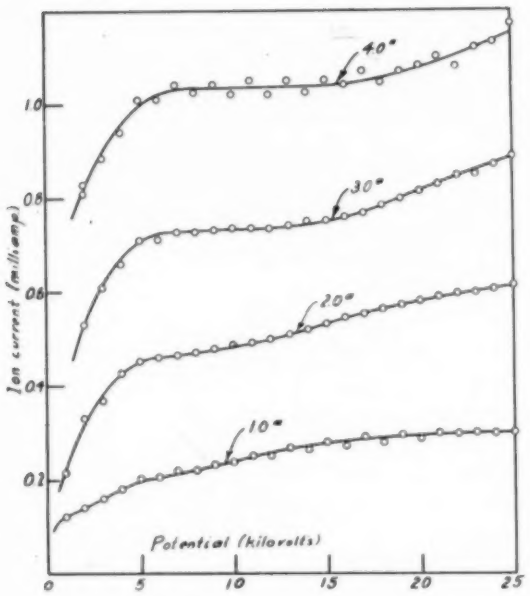

FIG. 2. Output ion current as a function of collecting potential for various values of the total arc current for a typical metal capillary.

ions of hydrogen and deuterium. These atomic ions are produced from their respective molecular species as primary and as secondary products of ionization, and as primary products from the atomic gas. The net probability of atomic ionization from the molecular gas seldom exceeds five percent of that for ionization resulting in the formation of molecular ions. This being the case, it is desirable to increase the relative concentration of neutral atomic gas. Neutral atoms are produced in an electric discharge and disappear by recombination on the discharge tube walls. Surfaces differ greatly in the extent to which they catalyze this recombination. The present paper includes an investigation of various surfaces insofar as they relate to the percentage of atomic ions available from a low pressure hydrogen arc.

Intense ionization can be produced most simply by an electrical discharge operating through a constricted region.[3,4] As will be seen from the next paper, the degree to which an ion beam can be focused depends on the initial energy distribution. The low voltage arc has a lower energy spread among the ions than does any other type of electrical gas discharge. Another consideration, one of special importance with high voltage generators operating in compressed gas, is the limitation in the space available for the ion source and all its auxiliary equipment. The linear dimensions of a low voltage arc can be made small, and the relatively low power required is delivered at voltages which can be conveniently generated in a limited space. Such considerations have led to the present investigation of the low voltage capillary arc as a source of positive ions for use with high voltage equipment.

METAL CAPILLARY ARCS

A diagram of a typical metal capillary arc is presented in Fig. 1, together with electrodes external to the arc for collecting and analyzing the ion current. This general arrangement is described in some detail in an earlier paper.[1] It is essential that the depth of the outlet be negligible in comparison with the outlet diameter since the solid angle available for ion drift decreases rapidly with increasing depth.

In Fig. 2 typical sets of ion currents are presented as functions of collecting potential for various values of the total arc current. The capillary in this case was 4.0 mm in diameter and 4.0 mm long, while the outlet diameter was 0.80 mm. On each of these curves a fairly flat saturation is apparent which is followed by further increase in the ion current. A study of the increase in ion current beyond the saturation as a function of pressure shows that this increase is not caused by ionization in the high vacuum region but is real current from the capillary arc. The particular form assumed by these curves is a logical consequence of the mechanism responsible for the removal of the ions from the discharge. As was discussed in the earlier paper,[1] instead of employing a high voltage probe electrode, the ions are allowed to drift out of the discharge through the outlet provided. Both ions and electrons drift out, the effect of one on the other serving to minimize the usual space charge until the ions are in a region of relatively high vacuum. In somewhat different language, the outlet radius exceeds the thickness of the positive ion space charge sheath covering the

[3] Tuve, Dahl and Van Atta, Phys. Rev. **46**, 1027 (1934).
[4] Tuve, Dahl and Hafstad, Phys. Rev. **48**, 241 (1935).

discharge tube walls so that the arc plasma actually protrudes through the outlet. The focusing field accelerates ions drifting past the plasma edge, and as the field is increased pushes this edge back toward the outlet. As the plasma surface approaches the outlet plane, the collected ion current approaches saturation until all ions drifting through the outlet are collected. Beyond saturation, the plasma surface is pushed into the arc, or in other words, the collecting field penetrates into the outlet, and collects ions which would not otherwise drift through the outlet. This penetration of the collecting field into the arc is responsible for the increase in ion current beyond saturation. It will be shown in the next paper that, whereas the ion current up to and including saturation, is well focused by the ion lens system formed by the outlet cone and the first focusing cylinder, the current beyond saturation is not. Hence, for high collecting potentials, the edge of the outlet acts as an aberration in the ion lens and the ions suffering from this aberration do not contribute to the useful current.

In Fig. 3 the saturation currents obtained from Fig. 2 are presented as a function of arc current. An analysis of this curve yields considerable information concerning the arc both as a discharge and as a source of ions. In the pressure range generally employed (between 0.02 and 0.2 mm), the arc drop is approximately independent of arc current. To a first approximation, therefore, the ion current density to the walls I_p is proportional to the arc current. Furthermore, since the total arc drop remains constant it seems reasonable to assume that so also does the drop across the positive ion space charge sheath covering the capillary wall. If the radius r of the outlet is reduced by the thickness x of the sheath, the saturation ion current i_p is given by

$$i_p=\pi I_p(r-x)^2$$

or, for thin sheaths,

$$i_p=\pi I_p(r^2-2rx). \tag{1}$$

Langmuir and Mott-Smith[5] give the space charge equation for a plane sheath as

$$I_p=5.462(10^{-8})M^{-\frac{1}{2}}V^{\frac{3}{2}}x^{-2}, \tag{2}$$

[5] I. Langmuir and L. M. Mott-Smith, Gen. Elec. Rev. 27, 449, 616, 762 (1924).

where I_p is the ion current density in amperes per square centimeter, M is the molecular weight, V is the drop across the sheath in volts, and x is the sheath thickness in centimeters. Remembering that V is constant and that I_p is proportional to arc current i_a, Eq. (1) becomes

$$i_p=Ai_a-Bi_a^{\frac{1}{2}}, \tag{3}$$

where $Ai_a=\pi r^2 I_p$ and $Bi_a^{\frac{1}{2}}=2\pi r I_p x$.

Equation (3) has been fitted to give the solid line through the points in Fig. 3. The dotted line is a plot of Ai_a, the ion current which would be collected were the area of the outlet not reduced

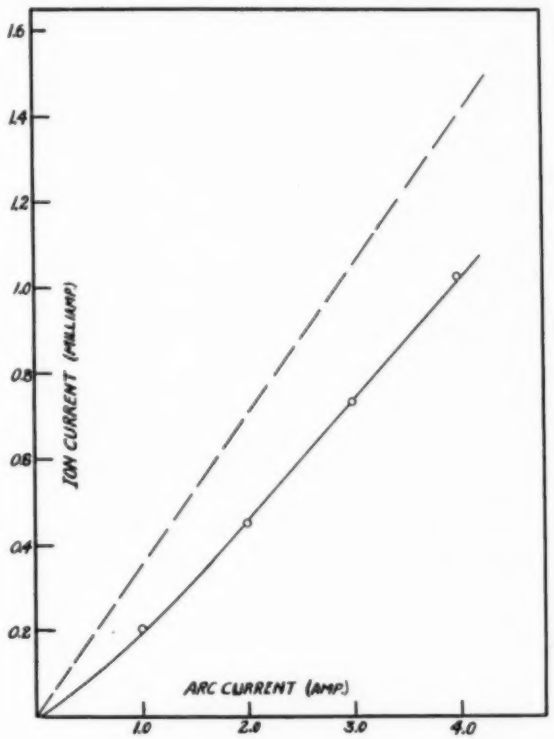

FIG. 3. Saturation output ion current as a function of total arc current for a typical metal capillary.

by that of the sheath. The constants determined from the data have been employed with Eq. (2) to give the potential drop across the sheath. The result for the data presented above is 21 volts. The arc drop was 70 volts and the potential difference between anode and wall was 34 volts. Hence the highest potential an ion can possess when leaving the plasma at the outlet is 13 volts and the lowest is zero for the particular capillary arc in question. Mass analysis under

good vacuum conditions showed no voltage spread which could be resolved by the mass spectrograph. The upper limit set by the spectrograph was 36 volts.

Measurements and computations of a nature similar to those just described for a 4-mm capillary 4 mm long have been made for a number of different capillaries. From these investigations, some generalizations are possible within the errors inherent in the experiments. The potential drop per unit length of capillary is independent of capillary diameter for the capillaries studied, and in the pressure range from 0.02 and 0.2 mm is 1.7 volts per mm. The potential difference between the discharge tube walls and the cathode varies very little with changes in capillary length. For a change from 4 to 20 mm in length, the potential difference between wall and cathode changed from 36 to 39 volts. The potential difference between the anode and the sheath edge at the outlet is 10 volts plus the drop along the capillary from the anode end to the outlet. This gives the maximum possible voltage spread of the ions. With this information it is possible to set the drop across the sheath within narrow limits.

In Fig. 4 the ion current density per ampere arc current is given for a number of capillaries as a function of capillary length. Unfortunately the various sources employed did not cover a sufficiently wide range of geometries to provide accurate information for plotting these curves. Hence they are drawn as dotted rather than as full lines to indicate that the general shape is

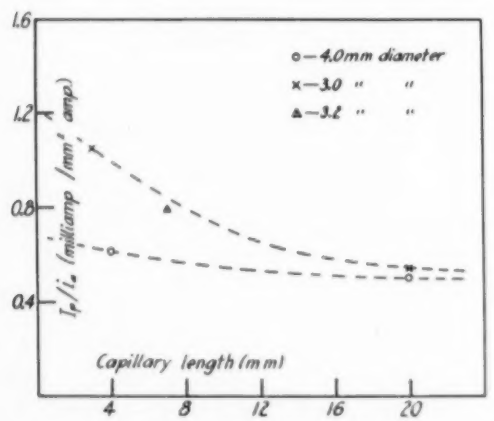

FIG. 4. Saturation output ion current density per unit arc current as a function of capillary length.

determined not entirely by the points themselves, but with the aid of other information indicative of the general trend. It is seen that the ion current density per unit arc current for a 20-mm capillary does not vary rapidly with capillary diameter, whereas for short capillaries it is approximately proportional to the reciprocal of the capillary area. Indeed, it does not seem unreasonable that the total current passing through a long capillary should depend only on the cross section of the capillary exposed to the general discharges on cathode and anode sides, and hence that the values of this current density for different capillary diameters should approach one another as the length is increased. This assumption, together with the two points on each curve, makes it possible to draw the dotted lines with some confidence in their reality. A fifth point has been included for a 7-mm capillary 3.2 mm in diameter. These data indicate that no gain in ion output is to be expected with decreasing capillary diameter for capillaries exceeding 20 mm in length, whereas for short capillaries one might hope to gain in the inverse ratio of the cross-sectional area.

The output of a given metal ion source may vary over a rather wide range and in a somewhat unpredictable manner. For any one day, the source may reach an equilibrium condition such that data taken with it can be reproduced time and time again. However, at some later date the data, although reproducible, will not necessarily agree with that taken at the earlier period. This lack of reproducibility from day to day is greatest for the longest capillaries and is believed, for the reasons which follow, to be due to changes in surface conditions. It will be shown later, by comparison with the glass sources, that part of the arc current, instead of flowing through the capillary, goes from anode to cathode through two discharges in series, the first from anode to wall and the second from wall to cathode. The current carried by this path depends upon the emission of electrons from the anode side of the wall. This emission, presumably by photons, excited atoms, and ions, is sensitive to changes in surface conditions. Since surfaces are notoriously difficult to control, the fraction of the arc current flowing through the capillary, and hence the ion output, may and does vary. The data

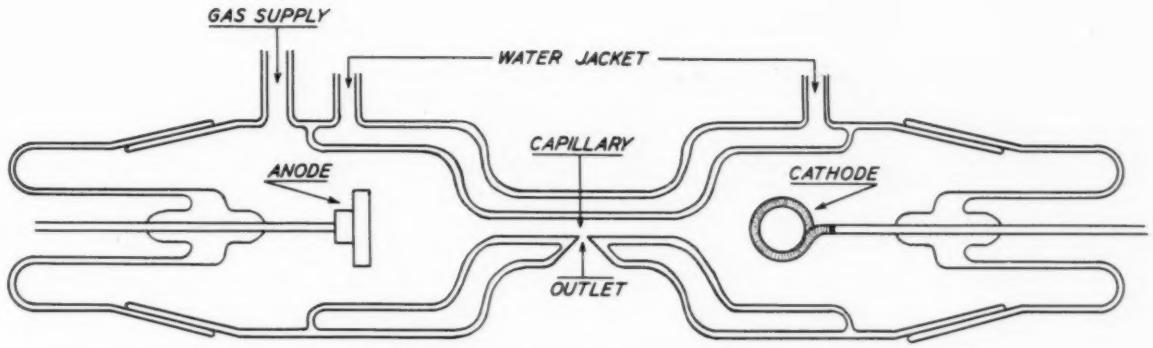

FIG. 5. Water-jacketed Pyrex ion source.

presented thus far are all representative of the most probable condition of the surface.

In order that a metal capillary arc be stable the circuit must be so arranged as to restart the arc should it go out. If the walls are allowed to float and the arc is extinguished, cathode and anode are well shielded electrically one from the other with the result that there is little tendency for the arc to start again. If the walls are tied to the anode through a resistance, a discharge will start on the cathode side and may go through to the anode, thus starting the capillary discharge. This resistance should not be too low, however, since in such a case the discharge from cathode to wall will be favored by the external circuit and the main capillary discharge may never start. Carrying this argument to its logical conclusion shows that if the resistance between anode and wall is zero, so also is the current through the capillary. Resistances ranging from 1000 to 30,000 ohms seem equally satisfactory for use in this connection.

The fraction of the ion output current from a hydrogen discharge carried by protons is also very erratic. This is not surprising since the percentage protons in excess of about five percent depends upon the concentration of neutral atomic hydrogen and hence upon the surface conditions. The lowest proton yield recorded was 5.3 percent and the highest was 21 percent. The average of a large number of mass analyses gave 11 percent for each of several sources ranging in length from 4 to 20 mm and in diameter from 3 to 4 mm. The difficulty connected with proton percentage was overcome by coating the discharge tube walls with a syrupy mixture of phosphorus pentoxide and water and mixing sufficient water vapor with the hydrogen supply to prevent the coating from drying out. This coating has been found by v. Wartenberg and Schultze[6] to be particularly effective in preventing the recombination of atomic hydrogen. With this coating the loss in atomic hydrogen is mainly by diffusion into the cathode and anode regions where recombination takes place on the untreated electrodes. The capillaries employed, therefore, were long in order to reduce the solid angle available for this diffusion. Proton percentages as high as 80 percent have been obtained from metal capillaries by this method, which represents a satisfactory solution so far as proton percentage is concerned. It is difficult and inconvenient, however, in routine operation of a high voltage installation to maintain such a surface in active condition. In addition, it is apparent that this gain in beam purity is at the expense of the total ion output since the output decreases with increasing capillary length. Further discussion of the metal capillary source will be included in later sections where comparisons with glass and with other ion sources can be made.

GLASS CAPILLARY ARCS

As pointed out in an earlier paper,[2] there are certain advantages to be gained from the use of insulating rather than conducting walls for the capillary arc, but to realize all these advantages with a glass capillary, adequate provision for cooling must be made. It was suggested that the

[6] H. v. Wartenberg and G. Schultze, Zeits. f. physik. Chemie **B6**, 261 (1930).

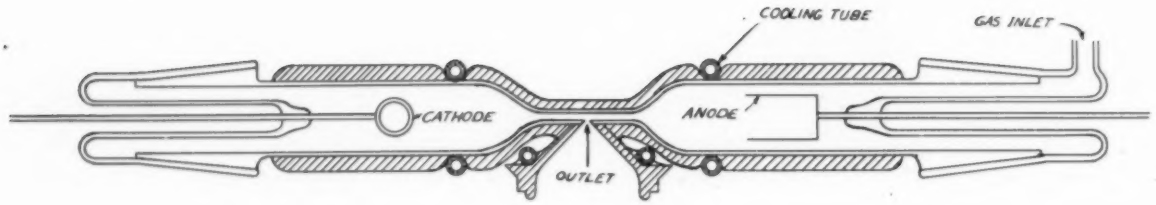

FIG. 6. Copper-coated Pyrex capillary arc.

cooling might be accomplished by surrounding the glass with metal. With this in mind, further work has been done by the authors, and by Getting, and his collaborators[7] at Harvard.

For purposes of general study the water-jacketed Pyrex source shown in Fig. 5 was constructed with a capillary diameter of 3.2 mm. The limiting arc current for this source was 3.0 amperes as compared with 0.3 ampere for the uncooled glass capillary reported earlier. This source, although of interest for the general study, is not sufficiently rugged in construction for practical use. Other schemes for cooling have all involved embedding the glass in a heavy metal exterior. In one a block of type metal was cast around the glass. This, while not as effective thermally as the all-glass construction, was much more rugged mechanically. The capillary arc shown in Fig. 6 was made by electroplating the Pyrex with a heavy coating of copper. This can be done over a silver coating deposited chemically or over a platinum coating obtained from a preparation supplied by the Hanovia Company. The glass must be heated almost to the softening point to insure sticking of the platinum when the tube is placed in the electroplating bath. With either platinum or silver as an electroplating base, the focusing cone and water-cooling tubes must be soldered on while the copper coating is extremely thin in order to prevent breakage by differential expansion. The outlet is ground after all soldering has been completed. The capillary just described, and that reported by Getting and his collaborators[7] in which a Kovar capillary was lined with glass, are both satisfactory solutions of the cooling problem. The authors prefer the copper coating since, with it, most of the glass is encased in and protected by metal and is not subject to breakage at such critical points as the Kovar seals.

With the insulating capillaries, the collecting potential must be applied between collecting system and either cathode or anode, whereas with the metal capillaries the circuit could be completed by the current to the wall. If the capillaries are completely insulating there is no difficulty about collection because the field tends to concentrate at the plasma edge. If the capillary is coated externally with metal and the coating is not continued to the outlet edge, the field tends to concentrate on the sharp metal edge and hence is less effective in pushing the plasma on beyond this edge to the outlet. It is often necessary therefore to supplement the main collecting potential by a relatively small one

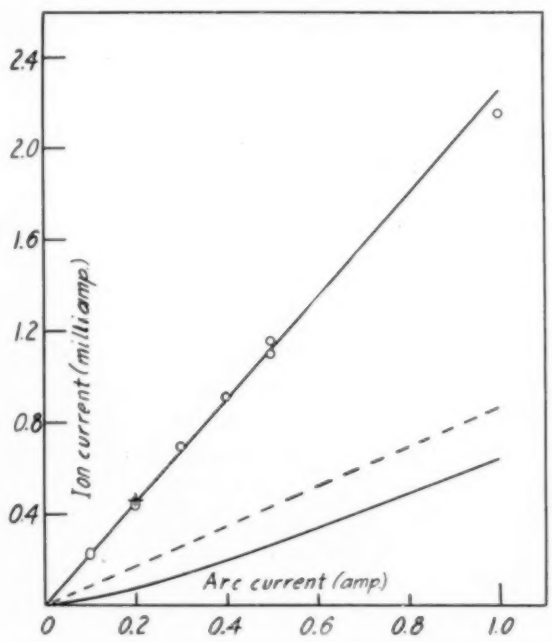

FIG. 7. Saturation ion current as a function of arc current for various Pyrex sources as reduced to standard dimensions.

[7] Getting, Fisk and Vogt, Phys. Rev. **56**, 1098 (1939); I. A. Getting and H. W. Leighton, Rev. Sci. Inst. **11**, 232 (1940).

applied between the metal envelope and either cathode or anode.

The saturation ion current must be greater for an insulating than for a conducting source since in the former case all of the arc current must pass through the capillary. This assumes of course that the arc plasmas are the same for the same capillary current in each case. Each element of wall area of the insulator adjusts its potential so as to collect equal numbers of electrons and ions, whereas the metal wall potential is such that these currents as a whole are equal. This difference in behavior results in a much smaller potential difference across the sheath and hence a much thinner sheath covering the walls of the insulator. Experimentally the reduction of the outlet area by that of the sheath cross section is not apparent in the insulating sources.

From data of the type presented for the metal sources in Fig. 2, a curve of the type presented in Fig. 3 can be drawn for the Pyrex sources. Here the saturation ion current is accurately proportional to the product of capillary current density and outlet area so that the results have all been reduced to a particular geometry taken as standard. The standard which has been adopted is a 3.0-mm diameter capillary having an outlet diameter of 1.0 mm. These data are presented in Fig. 7 and were obtained with capillaries ranging in diameter from 2.0 to 3.5 mm and in outlet diameter from 0.5 to 1.0 mm. A saturation current point obtained by Getting, and his collaborators[7] is included and the agreement with the other data is most satisfactory. These authors reported no simple dependence of useful ion current on total arc current. Conversation with Dr. Getting reveals, however, that their measured ion currents, in most cases, were not saturation values.

TABLE I. *Representative data for ion sources of different types. Column A is for a canal-ray tube, B for a capillary arc of the probe type, C for a metal capillary of the diffusion type, and D for a glass diffusion type capillary.*

	A	*B*	*C*	*D*
Pressure (mm)	0.02	0.03	0.02	0.02
Potential drop (volts)	50,000	100	70	100
Power (watts)	2,000	235	385	135
Max. possible energy spread (volts)	50,000	9000	13	30
Percent protons	30	20	20*	60
Percent atomic ionization	0.12	7.9	2.2†	3.6

* This figure is for the uncoated metal. With coating of P_2O_5 values up to 80 percent have been obtained.

† The currents used in computing this figure were for average capillary conditions as determined from a large number of runs. Under especially clean conditions this value may be as high as 4.4 percent.

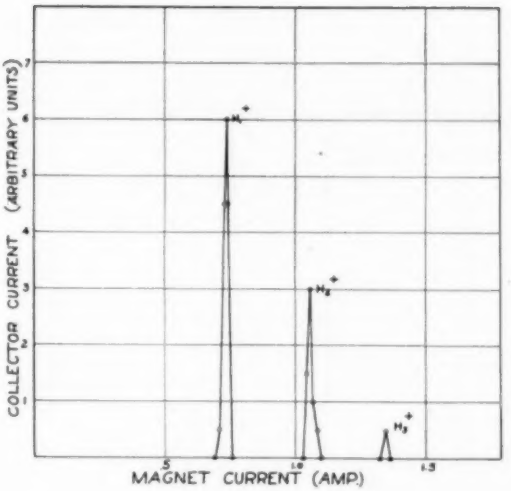

FIG. 8. Typical mass-spectrograph curve for an untreated Pyrex capillary.

The ion output from a standard short metal capillary has been included in Fig. 7 for comparison with the glass. The dotted line is the output which would be realized from the metal capillary were the outlet not reduced by that of the sheath. It is interesting to notice that the most probable condition of the metal capillary is one in which 61.5 percent of the arc current fails to follow the capillary path.

Most insulators are poor catalysts for the recombination of atomic hydrogen, as compared with metals. This is obviously true here since mass analysis shows a proton percentage from the Pyrex ion sources of about 60 percent as compared with 11 percent from the metal sources. A typical mass-spectrograph curve is presented in Fig. 8. This result is in agreement with those of Getting and his collaborators[7] and in particular with those of Hill, Buechner, Clark and Fisk[8] where the mass analysis was carried out at the target end of a high voltage tube. This result was obtained without treating the walls with

[8] Hill, Buechner, Clark and Fisk, Phys. Rev. **55**, 463 (1939).

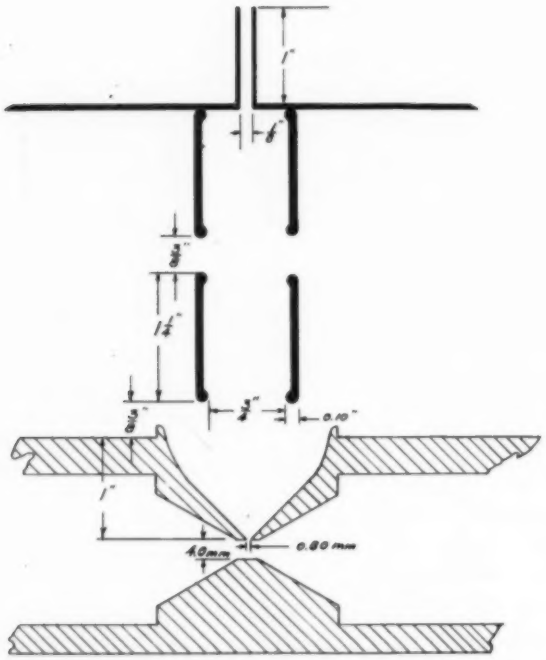

FIG. 9. Electrode and canal arrangement tested and used in the design for an ion gun assembly embodying differential pumping.

water. If treatment is employed the proton percentage can be increased beyond this figure.[2, 6]

CONCLUSIONS

The results of the present investigation are summarized in Table I where two sources representative of other types in general use have been included for comparison. Of course many other types of sources have been reported in the literature. Most of these are either not well suited to high voltage applications or have not been reported in sufficient detail to allow their inclusion in the table. Source *A* is a canal-ray tube of the type reported by Oliphant and Rutherford.[9] Complete data for this type of source has been given by Bouwers, Heyn and Kuntke[10] and has been used in Table I. Source *B* is a constricted discharge employing a probe for removing the ions from the discharge. This type was reported first by Tuve and his collaborators.[3, 4] The later results of Zinn[11] are quoted here. In columns *C* and *D* the present results for metal and for glass capillaries, respectively, with no probe electrode are presented. The significant constants are the gas pressure, the potential drop across the discharge, the maximum possible energy spread of the ions leaving the discharge, the percent protons, and the percent atomic ionization.

It is apparent from the table that the probe type capillary arc gives the highest percent ionization. However, because of the initial spread in energy and in angle of the ions, great difficulty has been experienced in obtaining accurate focus for beams of more than a few microamperes.[4] It is clear, therefore, that had the focused current rather than the total current been used in computing the percent atomic ionization, this figure would have been reduced. It will be shown in the next paper that the currents used in computing the percent atomic ionization in columns *C* and *D* are those which can be well focused rather than the total ion outputs. For example, with the electrode and tube arrangement shown schematically in Fig. 9, a beam of one milliampere has been obtained emerging from the small tube shown. This tube was $\frac{1}{8}$ inch in diameter and 1 inch long, and was placed with its entrance $4\frac{1}{4}$ inches from the source outlet. With a diffusion pump connected to the region between the source and the diaphragm supporting the tube it becomes possible to remove most of the neutral gas before the ion beam enters the high voltage tube and hence to increase the percent total ionization to beyond 90 percent.

It thus appears that capillary arcs employing the automatic space charge neutralization existing in a plasma, together with diffusion for removing the ions from the discharge, provides a suitable solution for the ion source problem for the following reasons: (1) The energy spread of the ions is negligible. (2) The percent atomic ionization compares favorably with that from other sources. (3) The percent protons from the glass source is high. (4) The ease of initial focusing, which makes possible the effective utilization of the source output.

The authors wish to make various acknowledgments in connection with the work described in this paper and the one immediately following. To avoid duplication these are made at the end of the second paper.

[9] M. L. E. Oliphant and Rutherford, Proc. Roy. Soc. **A141**, 259 (1933).
[10] Bouwers, Heyn and Kuntke, Physica **2**, 153 (1937).
[11] W. H. Zinn, Phys. Rev. **52**, 655 (1937).

An Experimental Investigation of Ion Beam Focusing

W. W. Buechner, E. S. Lamar and R. J. Van de Graaff
Massachusetts Institute of Technology, Cambridge, Massachusetts
(Received September 14, 1940)

An experimental investigation has been made of the initial focusing of ions from capillary sources of the diffusion type described in the previous paper. The lens system used consisted of a 90-degree cone at the ion source followed by three coaxial cylinders which were arranged at various potentials up to 25 kilovolts. Since the beams are rendered slightly luminous by traces of gas in the high vacuum region, they have been studied by a photographic method. The beams have also been studied by an electrical scanning method. Both types of investigation were made as functions of the electrode potentials and arc variables and are in good agreement. Based on these observations a focusing and canal arrangement suitable for differential pumping has been tested. This arrangement has been embodied in a design for a projected ion gun assembly.

Introduction

As described in the preceding paper, ions straying from a poorly focused beam and striking the electrodes of a high voltage tube may cause electric breakdown. The necessity for preventing this breakdown often limits the useful ion beam at the target of the high voltage tube to a small fraction of the output of the high voltage source used to operate the tube. Thus, efficient focusing of the ion beam is necessary if the useful current is to be high. With the type of electrostatic focusing customary for high voltage tubes, it is known[1,2] that the potential difference across any electrostatic lens must be greater than the potential difference through which the ions have already fallen if the lens is to be effective. Most high voltage tubes are constructed with equal potential differences between successive electrodes, these serving the dual purpose of distributing the voltage and accelerating the ions. It follows that most of the focusing is done by the first few electrodes, and that the most critical region for focusing is the one in which the ions are brought from rest up to a potential of the order of that established between successive electrodes of the high voltage tube proper. Since the ions are originally produced in some type of electrical discharge the ion source itself must be considered as an integral part of the initial focusing system. It thus appears desirable that the source, together with the initial accelerating system, be constructed as a unit to form an ion gun assembly to direct an accurately focused ion beam into the high voltage tube for further acceleration. As will be shown below, a differential pumping system can be readily provided to remove from the ion gun practically all of the neutral gas diffusing from the source thus preventing this gas from entering the main high voltage tube where its presence in the path of an initially well focused ion beam could indirectly cause breakdown.

In addition to satisfying other requirements discussed in the preceding paper, an ion beam should be parallel or slightly converging as it enters the high voltage tube proper. The degree of convergence should be easily controllable by the initial focusing system in order to allow the possibility of compensating for space charge spreading of the ion beam not overcome by the slight focusing action of the successive lenses in the high voltage tube. Fortunately, while the focusing action of successive lenses decreases with increasing energy of the ion beam, so also does the spreading caused by space charge. Since the focusing action on an ion beam depends on the energy of the ions it is essential that the ions be homogeneous in energy in order that the focal points of the lenses be the same for all. Hence, neither the source nor the initial accelerating system should be such as to introduce an appreciable energy spread among the ions.

The important region of initial focusing does

[1] F. H. Nicoll, Proc. Phys. Soc. London **50**, 888 (1938); M. E. Rose, Phys. Rev. **53**, 392 (1938); R. R. Wilson, Phys. Rev. **53**, 408 (1938); L. H. Thomas, Phys. Rev. **54**, 588 (1938).
[2] Tuve, Dahl and Hafstad, Phys. Rev. **48**, 241 (1935).

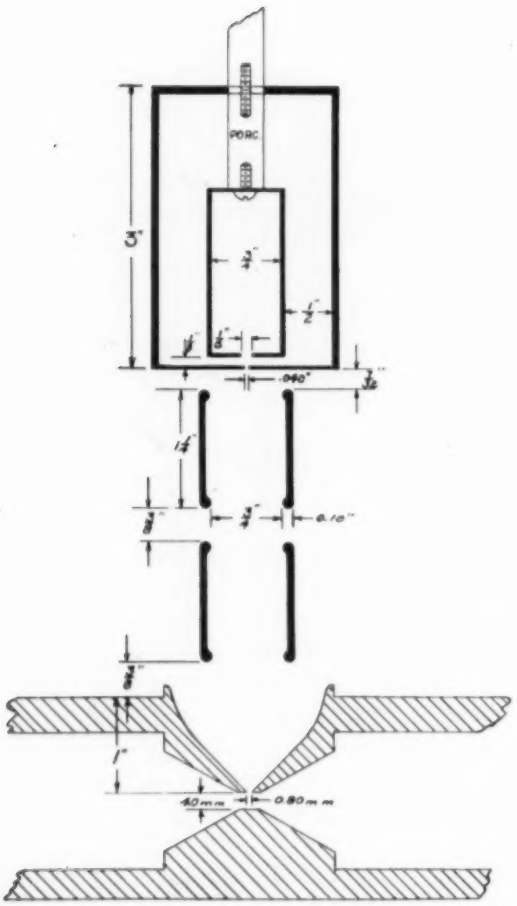

FIG. 1. Collector system for determining the distribution of current in a cross section of the ion beam.

not lend itself readily to any but the most approximate theoretical treatment because of the geometry, because of the considerable space charge in the region of low energy, and because of the initial conditions imposed by the electrical discharge which constitutes the ion source itself. Such factors as these hinder the application to this problem both of theoretical investigations and investigations involving electron beams such as the recent research of Pierce.[3] The present research, therefore, is an experimental investigation of factors essential for the development of an ion gun which would project into the high voltage tube an accurately focused beam with energies up to 25 kilovolts and with substantial elimination of neutral gas diffusing out from the source.

[3] J. R. Pierce, J. App. Phys. **11**, 548 (1940).

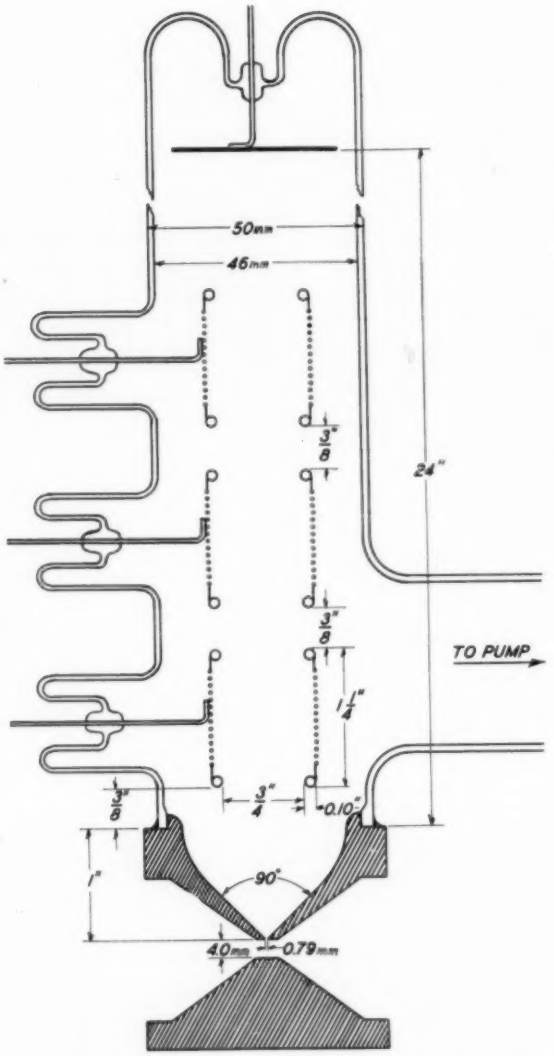

FIG. 2. Cross section of glass accelerating tube for the photographic study of ion beams.

EXPERIMENTAL PROCEDURE AND RESULTS

The authors have used two methods for studying the dependence of beam shape and cross-sectional distribution on the electrode potentials, gas pressure, and beam current in the region near the source: the first employing an electrical scanning apparatus for a particular plane normal to the beam axis, and the second using photography for studying the variation of over-all beam characteristics along the axis.

The first lens of the focusing system was formed by a cylindrical electrode coaxial with a 90-degree cone from the apex of which the ions

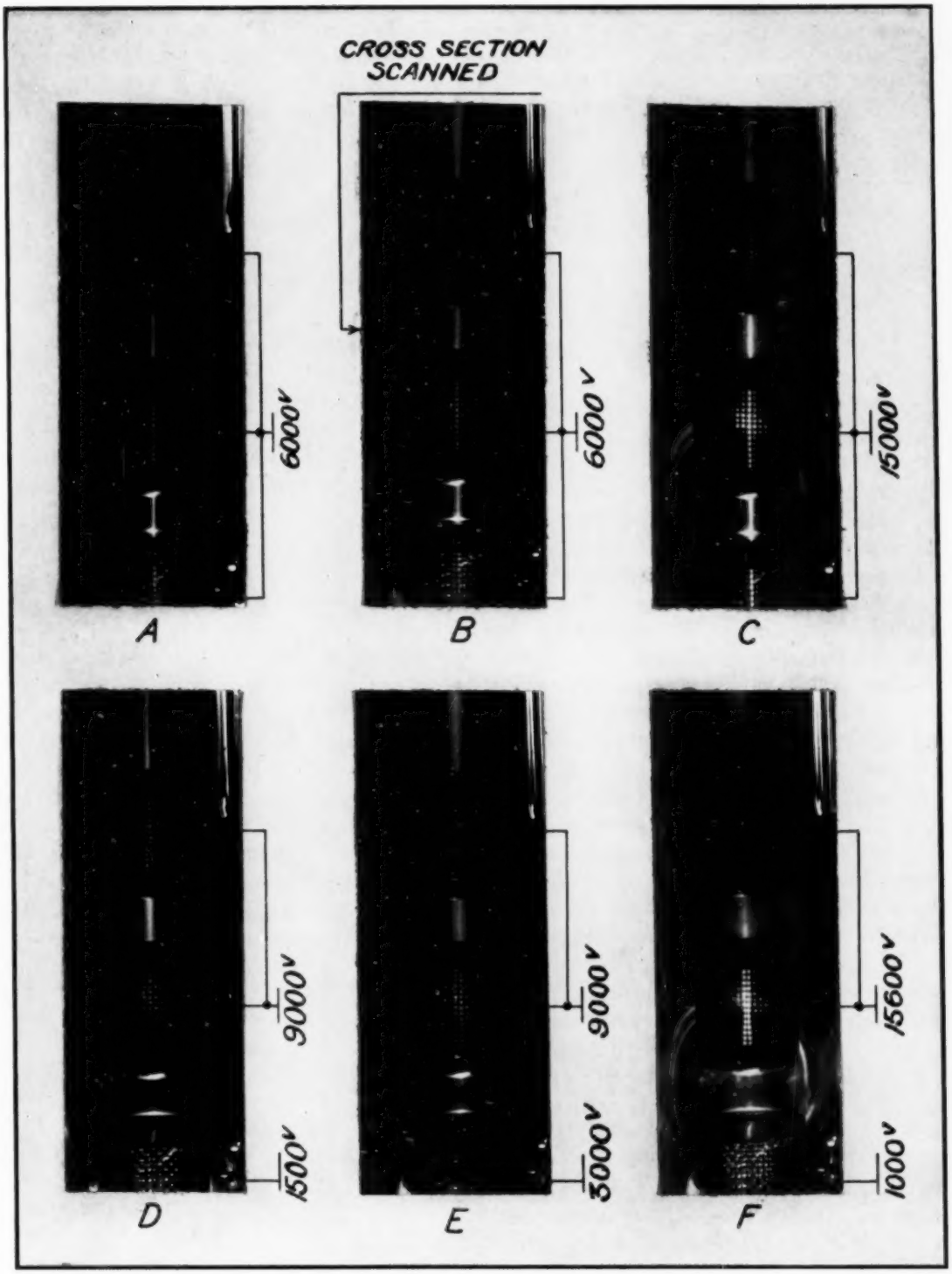

FIG. 3. Photographs of ion beams. Photograph *A* was taken with an arc current of 0.5 ampere for which the saturation output ion current is 90 microamperes. The other photographs were taken with an arc current of 1.5 amperes for which the saturation output ion current is 320 microamperes.

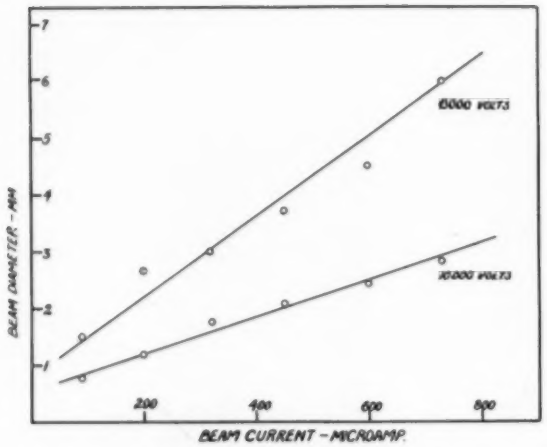

FIG. 4. Beam diameter at the center of the gap between first and second cylindrical electrodes as a function of beam current.

drifted out from the source. Previous work[4] has shown that this lens forms a well-defined beam. The lateral distribution of current in a particular plane was studied electrically with the arrangement shown schematically in Fig. 1. The cross-hatched region is a section of a metal source block of the type described in the preceding paper. Two cylindrical electrodes are shown coaxial with the outlet cone of the source. The assembly, shown beyond the second cylinder, consisted of a steel plate with a 0.04-inch hole and a Faraday collector, which could be moved bodily at right angles to the beam axis, thus giving a means of measuring the current density in the plane of the steel plate, as a function of distance between the center of the 0.040-inch hole and the beam axis. In some of the tests, all accelerating electrodes were at the same potential so that the beam was investigated as a function of the potential difference across the first lens formed by the cone and first cylinder. In other tests potential differences were established between the cone and first cylinder and between the first and second cylinders so that the beam was studied as functions of these two lens parameters.

The electrical method of studying the ion beams is laborious and provides information which is limited to a particular plane normal to the beam axis, whereas the photographic method, once interpreted, provides a most convenient means for obtaining the over-all beam characteristics not only across but along the beam. The method is made possible by the fact that even small traces of gas in the tube render the beam sufficiently luminous to be photographed using emulsions now available. The tube constructed for this study is shown in Fig. 2. The electrode geometry is identical with that for the scanning tube except that a third cylindrical electrode was included. This tube was constructed of glass and the electrodes of nickel gauze except at their ends.

Typical photographs, taken with the beam axis in the plane of the picture, are shown in Fig. 3. The figure is printed with most of the first cylinder showing at the bottom of each of the photographs. In observing the photographs it should be recalled that the cylinders are constructed of metal gauze except at the ends which are solid.

The hydrogen pressure in the accelerating tube when the photographs were made was 1.0×10^{-4} mm. That this pressure was not high enough to distort the beams was shown by a series of photographs taken at different pressures. It was found that in the region studied the beam characteristics were independent of hydrogen pressure up to 1.3×10^{-3} mm. Above this pressure the beams broadened, became diffuse, and finally were indistinguishable from the general background. It is worth mentioning that, as would be expected, slight traces of air in the tube had a much more serious effect than did many times the equivalent pressure of hydrogen, indicating the

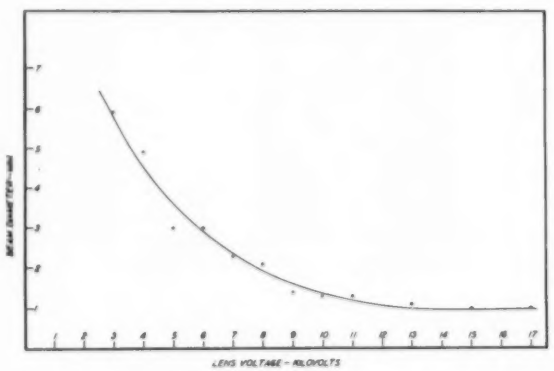

FIG. 5. Beam diameter at the center of the gap between first and second cylindrical electrodes as a function of the single lens voltage for an arc current of 1.5 amperes.

[4] Lamar, Samson and Compton, Phys. Rev. **48**, 886 (1935).

great desirability of good vacuum conditions in high voltage tubes.

Photographs *A*, *B*, and *C*, Fig. 3, were taken with first, second, and third cylinders all connected together, the only lens action being that due to the single potential difference between the cone and the first cylinder. Photographs *A* and *B* were taken with the same potential difference but with different currents. The arc current for *A* was 0.5 ampere which gave an output ion current of 90 microamperes. Photographs *B*, *C*, *D*, *E*, and *F* were all taken with an arc current of 1.5 amperes. Since all the data presented in this paper were taken with the metal source for which information is presented in Figs. 2 and 3 of the preceding paper, the ion currents in the photographs can be estimated from these figures. Photographs *A* and *B* show the dependence of beam diameter on ion current. A number of such photographs have been taken and measured. The results of these measurements are presented in Fig. 4, where the diameter of the beam at the center of the gap between the first and second cylinders is plotted as a function of beam current for two different single lens voltages. It should be mentioned here that these measurements are for the central intense beam. As can be seen from the diagram, the beam diameter between the first and second cylinders is approximately linear with beam current, the intercept being of the same order of magnitude as the diameter of the source outlet.

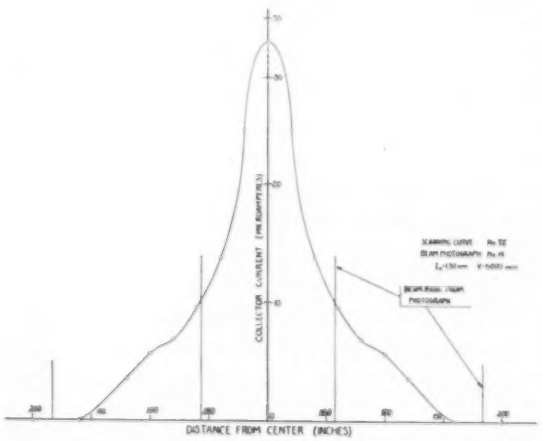

FIG. 6. Current through a 0.040-inch hole as a function of the transverse displacement of the center of the hole from the beam axis, for a single lens.

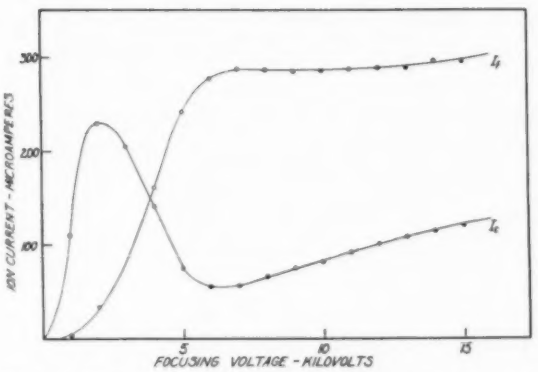

FIG. 7. Ion currents I_f which go through and I_e which fail to go through a $\frac{1}{4}''$ diaphragm hole $4\frac{1}{4}''$ from the source outlet, given as functions of the single lens voltage.

In Fig. 5 the beam diameter between first and second cylinders is presented as a function of the single lens voltage for an arc current of 1.5 amperes. The saturation ion current under these conditions is 320 microamperes and the actual currents at each voltage can be obtained from the data presented in the preceding paper. As can be seen from the diagram, the diameter of the central intense region of the beam decreases with increasing voltage, reaching a relatively constant minimum diameter which is approximately equal to the diameter of the source outlet.

In addition to the central intense region a surrounding trace is present in all the single lens negatives although this trace does not appear on the positive prints of all the beams. At each arc current, for voltages up to and including some critical value, the faint trace is not present in regions of convergence and appears only where the beam is diverging. This trace can be seen in the negatives of the photographs *A* and *B* of Fig. 3. This critical potential is approximately that above which the central beam becomes constant in diameter, and is also that above which the total output ion current breaks away from the saturation plateau as described in the preceding paper.

The faint trace present in regions of divergence is evidenced in Fig. 6, the data for which was taken with the electrical scanning arrangement presented in Fig. 1. Here the current through the 0.040-inch hole is plotted as a function of distance between the center of the hole and the beam axis. The experimental conditions were identical with those under which the photograph of Fig. 3*B* was

taken. On the diagram the diameters of central beam and faint trace in the plane of the scanning hole, as determined from the negative of Fig. 3*B* have been included. The agreement between the two methods of investigation is within the limits of accuracy of the measurements.

When the single lens voltage exceeds the critical value discussed above, the faint trace appears, not only in regions of divergence but in regions of convergence as well. This trace increases in diameter rapidly as the voltage is increased beyond the critical value. The appearance of the faint trace in regions of convergence and its rapid increase in diameter all along the beam is caused by an aberration in the first lens which is present when the focusing field actually penetrates beyond the edge of the source outlet, as was discussed in the preceding paper. The faint trace resulting from this aberration is quite apparent in Fig. 3*C* where the single lens voltage exceeds the critical value mentioned above.

Further evidence for the beam behavior just described is shown in Fig. 7 where the current I_f which goes through a $\frac{1}{4}$-inch hole, and I_e, the current which fails to go through, are plotted as functions of the single lens voltage. The $\frac{1}{4}$-inch hole was located at the end of the second cylinder, and hence was in a region of beam divergence. As the voltage is increased the focused current I_f increases with a corresponding decrease in the unfocused current I_e. The unfocused current I_e does not go to zero because of the faint trace which exists in regions of divergence. After passing through its minimum the unfocused current increases with increasing voltage. In the region of voltage in which this occurs the faint trace is present all along the beam, and the total current is increasing beyond the saturation discussed in the preceding paper. This increase in the unfocused current I_e does not have a counterpart in the focused current I_f since the added current associated with the lens aberration is not focused.

If the beam from a diffusion type ion source is focused by a single lens and allowed to travel on without further acceleration, it gradually diverges because of space charge. This condition is shown in Fig. 8. The dark space near the top of the photograph is caused by a metal clamp around the tube at this point, 52.5 cm from the source outlet. This beam is a continuation of the one shown in Fig. 3*B*, and while it has spread considerably in traveling this distance, the edge is still quite distinct, even though the current is as high as 320 microamperes and the voltage only 6000 volts. The beam diameter at the clamp is 1.0 cm. Of interest in connection with the projection of ion beams in field-free space is the work of Tuve and his collaborators,[2] who have made extensive pioneering investigations of the focusing of ion beams. Using a probe type source they found considerable spreading in projecting beams of much more than 10 microamperes to distances much in excess of 20 cm, particularly with potentials less than 25 kilovolts.

FIG. 8. Photograph of a 6000-volt 320-microampere ion beam taken at some distance along the beam, after a single acceleration near the source outlet. The dark space near the top of the photograph is a metal clamp 52.5 cm from the source outlet. The beam diameter at this point is 1.0 cm.

Obviously even such divergence of the beam as is shown in Fig. 8 is undesirable when dealing with long discharge tubes. The degree of divergence depends on both current and energy. Because of the aberration mentioned above there is, for a particular beam current, a fairly definite voltage across the first lens which cannot be exceeded if all the ions are to be kept in a well-focused beam. This being the case, any energy exceeding this value which is to be given to the ions should be applied by succeeding lenses if the whole beam is to be accurately focused.

Figure 3*D* illustrates the action of such an additional lens. In this case the voltage across the lens formed by cone and first cylinder is 1500 volts. This gives a beam of relatively large diameter which would rapidly diverge if left in a field-free region. This broad beam is subjected to the lens action formed by placing 7500 volts between the first two cylinders. It is evident that this lens has a powerful action for this beam. The degree of convergence of the beam can be varied by changing either lens voltage. This is shown in Fig. 3*E*, which shows the beam obtained with 3000 volts on the first lens and 6000 on the second. The ion current is the same as for Fig. 3*D* and the final energy of the ions is the same in the two cases. Here the beam from the first lens is somewhat stiffer and the beam formed by the second lens is more nearly parallel. It should be mentioned here that the faint trace which appears with the single lens after the beam begins to diverge is substantially eliminated by the proper application of a second lens. It may be nevertheless desirable to provide at intervals diaphragms with axial holes to eliminate further stray ions and thus insure, at least at these intervals, an entirely clean beam.

By making the action of the second lens stronger, the position of minimum diameter or "focus" can be made to move in towards the source. It is apparent that the focusing action might easily be made too strong, and that for a given total potential available and a given distance from the source to the high voltage tube proper, there is an optimum arrangement of potential for introducing into the tube a beam with characteristics suitable for further acceleration. Figure 3*F* shows a case in which the initial focusing has been carried too far with the result that the beam has crossed over. Here the first lens has only 1000 volts while the second has 14.6 kilovolts.

It was found that beams of the type shown in Figs. 3*D*, 3*E*, and 3*F* were little affected by a further difference in potential between the second and third cylinders unless this potential difference was of the order of twice the potential between the second cylinder and the source. It was further found that if the second acceleration of the ions was delayed by using the second and third cylinders as the second lens, the second cylinder being connected electrically to the first, the beams thus formed were decidedly inferior to those obtained with the previous arrangement. Consequently one would expect that best results would be obtained in accelerating the ion beam further, as in a long discharge tube, by locating the source as close to the tube proper as is consistent with good focusing. Otherwise inconveniently high initial voltages might be required in order to introduce a suitable beam into the tube where the main acceleration is to take place. In addition a long beam path along which the ions are traveling at relatively low energy will require especially good vacuum conditions if undue scattering is to be avoided.

Evidence of this sort indicates that it is important to keep the ion beam in a field which will prevent its divergence, and to minimize the distance between the source and the main tube. However, it is possible to apply the initial focusing potentials too quickly. As has been seen, too high a potential on either the first or second lens will lead to an improperly focused beam. That beams of the type represented in Fig. 3*E* are suitable for further acceleration is shown by experience at M.I.T.[5] with a 450-kilovolt tube where practically the entire output of a source was well focused on the target of a 65-inch tube.

As was mentioned in the preceding paper, a one-milliampere beam of ions was projected through a tube $\frac{1}{8}$ inch in diameter and 1 inch long located at the far end of the second cylinder. This was done with a single lens. It appears from what has gone before that it is possible further to improve the focusing by using a double lens. The possibility of removing the major portion of the

[5] Hill, Buechner, Clark and Fisk, Phys. Rev. **55**, 463 (1939).

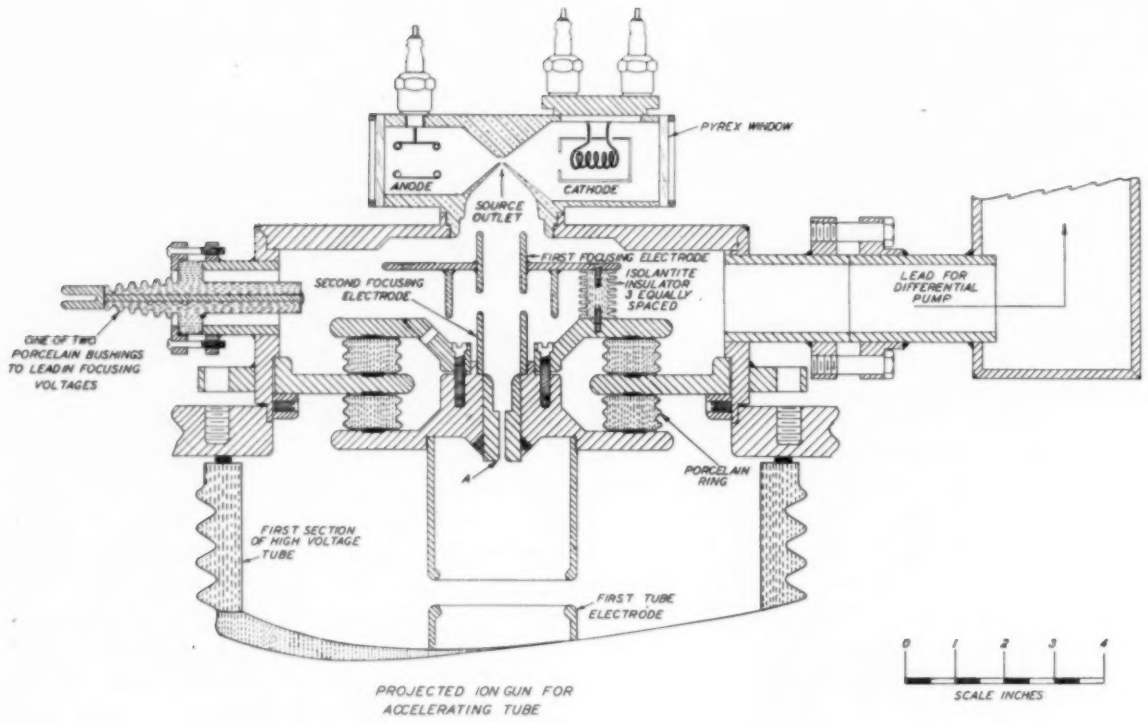

FIG. 9. Design for ion gun.

gas from this intermediate region with a small additional pump is thus apparent. With this arrangement the ion source, initial accelerating system, and differential pumping lead would constitute an ion gun assembly which could project into the high voltage tube a well focused beam of ions free from almost all of the neutral gas diffusing out from the ion source. A design for such an ion gun, with machined surfaces and accurately aligned electrodes, is shown in Fig. 9. The ion gun assembly bolts onto and is removable as a unit from the end plate of the high voltage tube. The small canal "*A*" in Fig. 9 serves the dual purpose of restricting the flow of gas from the gun into the tube and of diaphragming out that part of the ion beam not well focused. With a preliminary test apparatus having the dimensions shown for the initial electrode system and canal, a beam current of 1 milliampere emergent from the canal has been obtained. The $\frac{1}{8}$-inch canal shown has a pumping speed of about 0.15 liter per second for air. If a differential pumping system having a net speed of 10 liters per second for air were connected as shown, 98.5 percent of the gas from the ion source would be removed by the pump and only 1.5 percent would be able to enter the main high voltage tube.

The authors take much pleasure in making various acknowledgments in connection with the work described in this paper and the preceding one. It is a special pleasure to express our appreciation to Dr. Karl T. Compton for his collaboration in the early stages of the ion source research, for his continued interest and inspiration, and for his generous advice. We are glad also to express our appreciation to the members of the high voltage group at the Institute for their suggestions and help in many ways. We wish to thank Mr. J. Clark, especially for his assistance in taking the data, and Mr. A. Sperduto for his experimental assistance in innumerable ways. Finally, the authors are glad to have this opportunity of expressing their gratitude to the Research Corporation and to the Carnegie Corporation of New York for grants supporting this work.

Sparking of Oxide-Coated Cathodes in Mercury Vapor

D. D. KNOWLES AND J. W. MCNALL
Westinghouse Electric and Manufacturing Company, Bloomfield, New Jersey
(Received September 19, 1940)

When an oxide-coated cathode tube of the gas or vapor type passes more than a certain amount of current a spark or cathode spot occurs on the cathode and the tube is damaged. A peak current rating is, therefore, essential for any tube of that type and it becomes necessary to take data on how the sparking current is influenced by cathode temperature, vapor or gas pressure and other factors. By ordinary test methods each spark is so destructive that only one reading can be taken on one tube and the effect of the above factors is confused by the variation in quality of tubes used to obtain the data. The authors have developed a test procedure that so limits the duration of the spark that very little damage to the cathode results. This makes it possible to obtain a large number of readings on each tube and thereby observe effects otherwise obscured. The experimental procedure appears to be a good one for investigations in this field and the results obtained shed some light on the mechanism of sparking.

INTRODUCTION

ELECTRON emission from oxide-coated cathodes in gas or vapor has been the subject of continuous study since its discovery by Wehnelt in 1903, yet many important problems concerned with this emission remain unsolved. One such problem is a phenomenon which may be called sparking. This phenomenon limits the overload capacity of such cathodes and appears in the form of an incandescent spot on the coated cathode resulting in a vaporization or explosion of a part of the coating. Such action causes an irreparable destruction of the cathode or a portion of it.

In this investigation the following terms were used for the different quantities involved. By tube drop the authors mean the voltage drop across the tube from the cathode to anode. The maximum current that a tube can pass without cathode sparking is defined as the sparking current, and the tube drop at that current is the sparking tube drop. The length of time a certain magnitude of current must pass through the tube before sparking occurs will be referred to as the sparking time for that current. Data have been obtained by measuring these quantities for various cathodes, cathode temperatures, and for various pressures of the inert gases and mercury vapor. This discussion will be confined to the case of mercury vapor; a similar discussion for the inert gases will be treated in a later article. Throughout the entire investigation the cathodes employed were those used in commercial rectifiers and thyratrons. They were a crimped, edge-wound konal base metal cathode having a sprayed coating of the standard triple carbonate of the alkaline earth metals barium, calcium, and strontium (Fig. 1).

PROCEDURE

In measuring the tube drop for various magnitudes of continuous anode current, the cathode temperature rises due to the passage of that current so that the tube drop readings are altered by the increase in cathode temperature. This uncontrollable rise in temperature was found undesirable while taking tube drop-current characteristics so a circuit was devised which produced a square wave surge of current of short

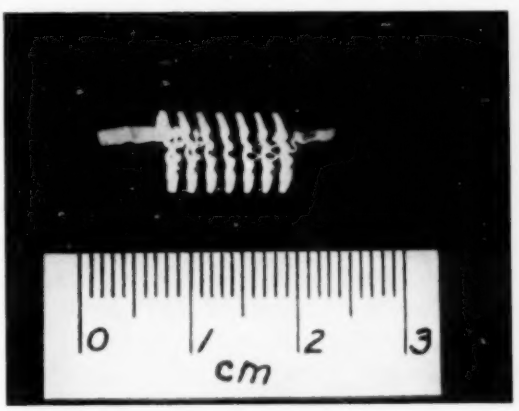

FIG. 1. KU-627 oxide-coated cathode.

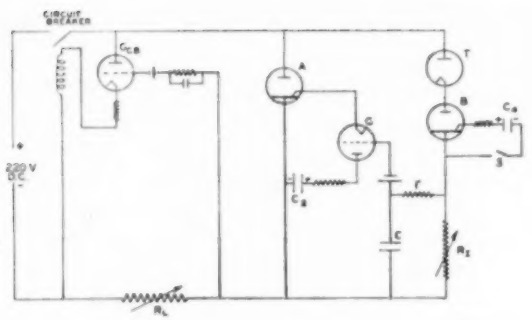

FIG. 2. Surge circuit.

enough duration to eliminate this undesirable heating. A current surge of such short duration was also necessary to prevent the cathode quality from changing while sparking data were being taken. The circuit is shown in Fig. 2.

The direct-current voltage from the supply appears across the ignitron B. The square wave surge of current is started by closing switch S which allows the previously charged condenser C_4 to fire tube B. As soon as tube B becomes conductive, current starts to flow through the tube being tested (T), ignitron B, and resistances R_I and R_L. While this current flows, the voltage drop across R_I charges condenser C through the resistance r. When this condenser becomes charged to a sufficient voltage to overcome the fixed grid bias on the thyratron G (KU-628), this tube becomes conductive and allows the previously charged condenser C_2 to fire ignitron A. At the instant tube A becomes conductive the current through T, B, and R_I transfers to tube A thus terminating the current surge through the tube being tested. The magnitude of the surge current is varied by changing R_I and R_L which, however, are maintained of equal value. By keeping $R_I = R_L$ the voltage drop across R_I remains essentially the same for any magnitude of surge current, thereby providing a constant voltage to charge condenser C through resistance r, all three determining the duration of the current surge. In this investigation a current surge of 0.03-second duration was found convenient. A delayed circuit breaker shown in the left half of the diagram was used to clear the line after the surge.

The values of tube drop and anode current during the surge were determined by means of a magnetic oscillograph which recorded the tube drop and the voltage drop across the calibrated resistance R_I. A reproduction of one of the oscillograms is shown in Fig. 3. This method was used in taking all the data where mercury vapor was used. The vapor pressure of the mercury was controlled by immersing the tube being tested in an oil bath of known temperature.

RESULTS

It was found that for a given tube at a constant cathode temperature and mercury vapor pressure the tube drop is a linear function of the anode current. (Fig. 4). This is in contrast with the near independence of the tube drop with anode current as obtained by the conventional method in which heating of the cathode by the anode current results in a more or less constant value of tube drop as the anode current is increased (Fig. 5).

For other cathode temperatures, the linear characteristic of tube drop *vs.* anode current is still obtained but the slope changes (Fig. 6). For a higher cathode temperature, the slope is less; i.e. the tube drop is less for the same anode current. Likewise, a lower cathode temperature results in a curve of larger slope; i.e. the tube drop is higher for the same anode current.

Different tubes (that is, tubes having cathodes of different qualities) also have linear tube drop *vs.* current characteristics but their slopes are large or small depending upon their relative qualities.

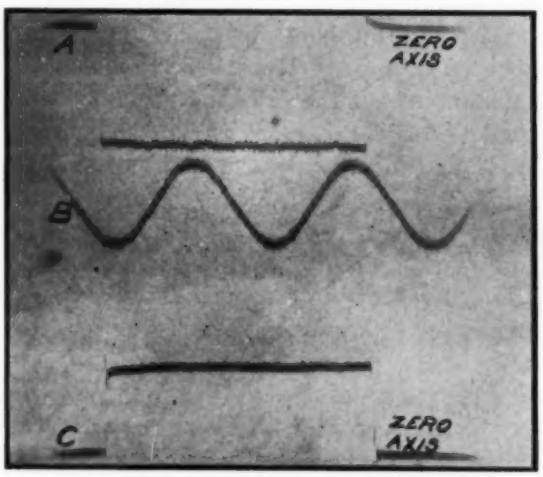

FIG. 3. Typical oscillogram showing: A—voltage drop across R_I; B—60-cycle timing wave; C—tube drop.

By changing the mercury vapor pressure in a tube, with the cathode temperature maintained the same, linear tube drop *vs.* anode current characteristics were again obtained (Fig. 7). In this case, the curves were displaced from one another but their slopes remained fairly constant.

As mentioned previously, for one tube at a given condition the tube drop increased as the anode current was increased. It was found that after the anode current had been increased to a certain value, any further increase resulted in a sparking of the cathode. This sparking could be detected visually and also on the oscillogram by the sudden decrease of the tube drop to a low value of the order expected for a barium arc (Fig. 8). The sparking time could be measured directly from the film by using the 60-cycle timing wave as a reference. When the anode current was increased still further, the tube drop, previous to the formation of the cathode spot, was higher, but the spot formed sooner, i.e., the sparking time was shorter (Fig. 9). From the original definition of the sparking current, namely, that it was the maximum current a tube

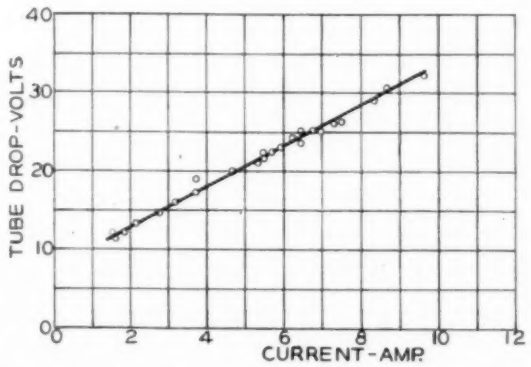

FIG. 4. Typical tube drop *vs.* current curve. KU–627 ~A–9151; tube temperature = 60°C; filament voltage = 2.75.

can pass without cathode sparking, it became evident that it could be determined experimentally by locating the value of anode current corresponding to the vertical asymptote to the sparking time curve. Having determined this value of sparking current, the sparking tube drop could be obtained immediately from the tube drop *vs.* anode current characteristic.

The effect of cathode temperature upon the sparking time curve and the values of sparking

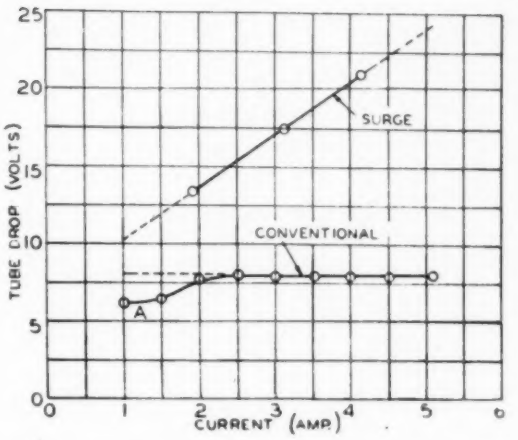

FIG. 5. Tube drop *vs.* current curves for surge and conventional test methods. KI–626~No. 2G72. $E_F = 2.50$ volts; $T_T = 60°C$.

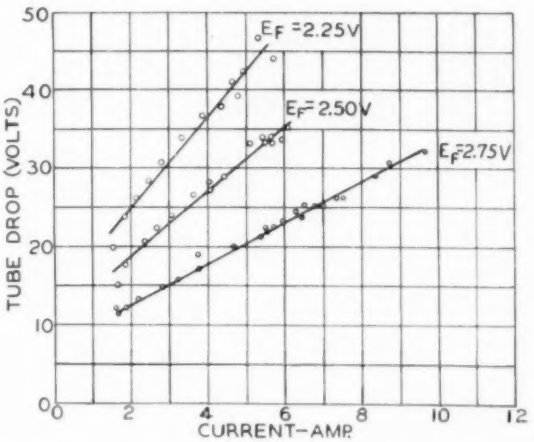

FIG. 6. Effect of filament voltage on tube drop *vs.* current curves. KU–627~A–9151; tube temperature = 60°C.

current and tube drop was also investigated (Figs. 10 and 11). It was found that: (1) An increase in the cathode temperature resulted not only in a tube drop *vs.* current characteristic of smaller slope but also in a larger magnitude of sparking current; (2) for a higher cathode temperature a sparking time curve similar to that for a lower cathode temperature was obtained but was shifted to larger values of anode current; (3) in spite of the fact that a larger value of sparking current was obtained for the higher cathode temperature, the sparking tube drop was somewhat smaller in value than that for a lower cathode temperature.

For another tube having a cathode of different quality, similar characteristics were obtained. If

the cathode had relatively better quality, then a lower slope of tube drop *vs.* tube current characteristic was obtained, a relatively larger value of sparking current was found, and a somewhat smaller value of sparking tube drop was obtained. A cathode of poorer quality had characteristics relatively opposite to those of the better cathode (Fig. 12).

The intersection of the vertical asymptote to a sparking time curve with the corresponding tube drop *vs.* anode current curve determines a sparking point. When several of these sparking points were determined for the same mercury vapor pressure by operating a cathode at different temperatures and by using cathodes of different quality, it was discovered that they formed a smooth curve. The determination of more sparking points definitely established the existence of such a curve (Fig. 13). Because of its method of determination this sparking curve is independent of cathode quality and cathode temperature. In order to determine the effect of cathode area on these various sparking characteristics similar data were taken on tubes having cathodes similar in shape but of a much larger area. The sparking curve for these larger cathodes was similar in shape to that for the smaller cathodes but was shifted towards the higher values of tube current. The two curves, however, resolved into one when the sparking tube drop was plotted against the sparking current per unit area of the cathode instead of against the total sparking current. The sparking curve thus becomes remarkably general in that it is now completely independent of cathode temperature, cathode quality, and cathode area.

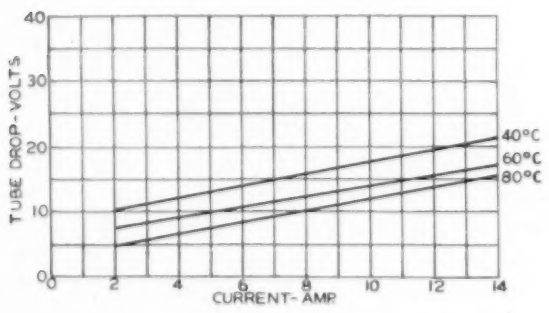

FIG. 7. Effect of condensed mercury vapor temperature on tube drop *vs.* current curves. KU-627~No. 7; E_F = 2.50 volts.

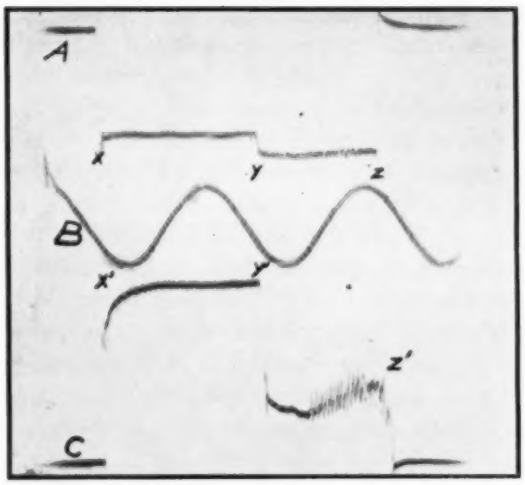

FIG. 8. Oscillogram showing sparking.

The effect of the mercury vapor pressure upon this sparking curve was also investigated. Sparking data were taken for two other mercury vapor pressures corresponding to condensed mercury temperatures of 40°C and 80°C. The sparking curve obtained for each of these two mercury vapor pressures along with the original for 60°C is shown in Fig. 14. These sparking points seemed to be well fitted by a curve of the form $I_s(E_s - E_s') = W_s$ where both E_s' and W_s are constants for a given temperature of condensed mercury. The values of E_s' and W_s for these three sparking curves were determined by a least squares solution, resulting in the following sparking equations:

$I_s(E_s - 17.3)$
$= 25.0$ for a mercury pressure of 6.μ (40°C)

$I_s(E_s - 11.1)$
$= 85.2$ for a mercury pressure of 25μ (60°C)

$I_s(E_s - 12.3)$
$= 15.8$ for a mercury pressure of 89μ (80°C),

where I_s is the sparking current per square inch of cathode area and E_s is the sparking tube drop. Each of these curves is independent of cathode quality, temperature, and area. At any one of these values of mercury vapor pressure a change in the cathode quality, temperature, or area merely slides the sparking point along the appropriate sparking curve.

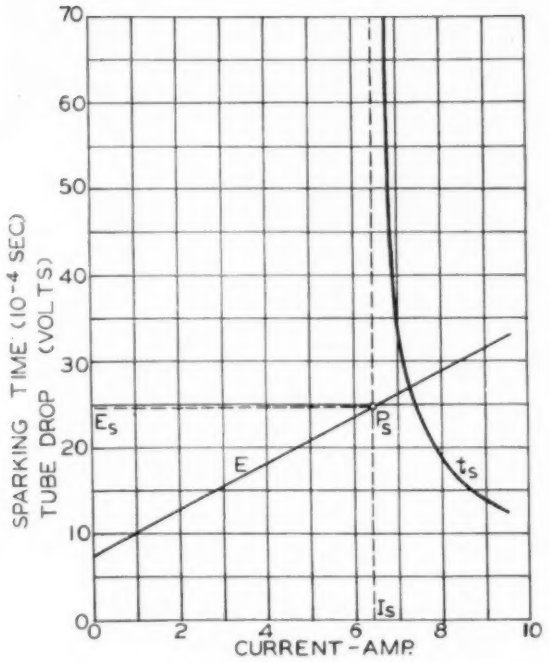

FIG. 9. Experimental method of determining sparking points. KU–627∼A–9151; tube temperature = 60°C; filament voltage = 2.75 v.

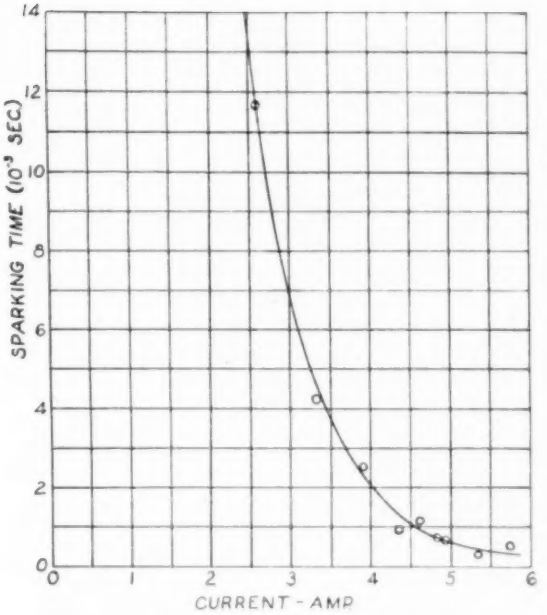

FIG. 10. Sparking time curve. KU–627∼A–9151; $T_{HO} = 60°C$. $E_f = 2.25$ v.

DISCUSSION

Returning to the original linear tube drop *vs.* anode current characteristics it was shown that, for cathodes of the same area operated at the same temperature and for the same vapor pressure of mercury, the slopes of the curves were definite indications of the relative qualities of the cathodes. This fact has since been made use of many times when a determination of the relative qualities of several similar cathodes was desired. Although one purpose of the surge was to eliminate undesirable heating of the cathode by the anode current, it was found that the difference between the tube drop *vs.* anode current characteristic obtained by the surge method and that obtained by the conventional continuous d.c. method was not all due to heating of the cathode. Only a part of the difference could be attributed to heating by the anode current, the remaining part being due to some other cause such as a difference in the degree of activation of the emitting surface for the two cases.

The effect of cathode temperature on the tube drop *vs.* current characteristics is not only reasonable but it is to be expected. An increase in the cathode temperature increases not only the thermionic emission according to Richardson's equation but also the field emission because of the effective lowering of the work function of the

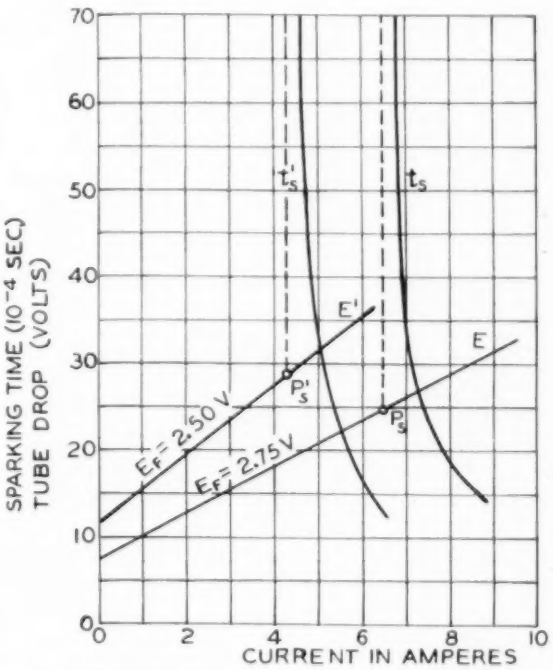

FIG. 11. Effect of filament voltage on sparking time curve and the sparking point. KU–627∼A–9151; tube temperature = 60°C.

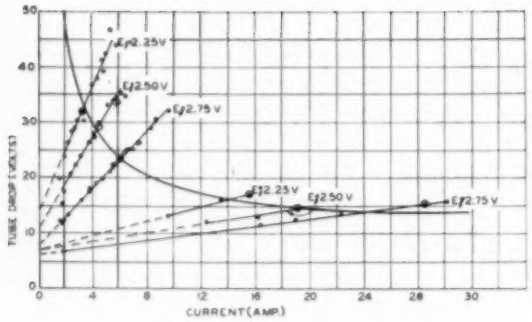

FIG. 12. Tube drop *vs.* current—oxide-coated cathode—mercury vapor~60°C.

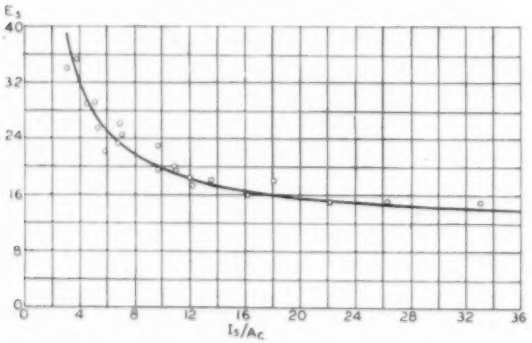

FIG. 13. Sparking tube drop *vs.* sparking current per sq. in. of cathode area. Tube temperature = 60°C; $E_s = 11.5 + 82.8/I_s'$; $I_s'(E_s - 11.5) = 82.8$.

emitting surface. Another possible factor is the increase in electrical conductivity of the coating for a higher temperature. All three of these factors tend to make the tube drop lower for a given value of anode current.

It was mentioned previously that in order to make the sparking points for cathodes of different sizes lie on the same sparking curve it was necessary to use the sparking current per unit area of the cathode instead of the total sparking current. It can be concluded, therefore, that normally either every part or a certain proportion of every part of the cathode area contributes equally to the total emission. This is interesting in view of the fact that after the initiation of sparking, practically all of the

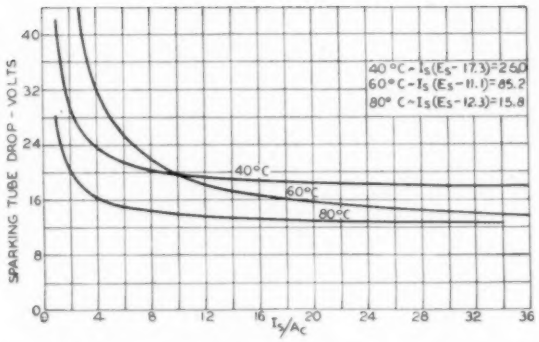

FIG. 14. Effect of condensed mercury vapor temperature on sparking curves.

emission is localized or concentrated at a small spot on the cathode.

In attempting to explain the mechanism of sparking, all of the facts just presented must be considered. In the first place, the sparking time curve is a typical heating curve. Also, the form of the sparking curve equation suggests that for a certain mercury vapor pressure a cathode sparks when it dissipates a definite amount of energy W_s. Thus it seems probable that cathode sparking is a heating phenomenon and is due either to energy dissipated in the emitting coating because of its electrical resistance, or to heating produced by positive ion bombardment, or both. The fact that every part or a certain proportion of every part of the cathode contributes equally towards the total emission seems to rule out the possibility of any gradual localization of the total current. The facts seem to point to an unstable condition somewhat similar to the transition from a glow to an arc.

This paper has dealt exclusively with the sparking of oxide-coated cathodes in mercury vapor. Investigations using the same experimental technique to study sparking in various inert gases indicate that these phenomena can be correlated with the physical and electrical characteristics of the gas or vapor. This phase of the problem will be discussed in a later publication.

General Theory of Three-Dimensional Consolidation*

MAURICE A. BIOT
Columbia University, New York, New York
(Received October 25, 1940)

The settlement of soils under load is caused by a phenomenon called consolidation, whose mechanism is known to be in many cases identical with the process of squeezing water out of an elastic porous medium. The mathematical physical consequences of this viewpoint are established in the present paper. The number of physical constants necessary to determine the properties of the soil is derived along with the general equations for the prediction of settlements and stresses in three-dimensional problems. Simple applications are treated as examples. The operational calculus is shown to be a powerful method of solution of consolidation problems.

INTRODUCTION

IT is well known to engineering practice that a soil under load does not assume an instantaneous deflection under that load, but settles gradually at a variable rate. Such settlement is very apparent in clays and sands saturated with water. The settlement is caused by a gradual adaptation of the soil to the load variation. This process is known as *soil consolidation*. A simple mechanism to explain this phenomenon was first proposed by K. Terzaghi.[1] He assumes that the grains or particles constituting the soil are more or less bound together by certain molecular forces and constitute a porous material with elastic properties. The voids of the elastic skeleton are filled with water. A good example of such a model is a rubber sponge saturated with water. A load applied to this system will produce a gradual settlement, depending on the rate at which the water is being squeezed out of the voids. Terzaghi applied these concepts to the analysis of the settlement of a column of soil under a constant load and prevented from lateral expansion. The remarkable success of this theory in predicting the settlement for many types of soils has been one of the strongest incentives in the creation of a science of soil mechanics.

Terzaghi's treatment, however, is restricted to the one-dimensional problem of a column under a constant load. From the viewpoint of mathematical physics two generalizations of this are possible: the extension to the three-dimensional case, and the establishment of equations valid for any arbitrary load variable with time. The theory was first presented by the author in rather abstract form in a previous publication.[2] The present paper gives a more rigorous and complete treatment of the theory which leads to results more general than those obtained in the previous paper.

The following basic properties of the soil are assumed: (1) isotropy of the material, (2) reversibility of stress-strain relations under final equilibrium conditions, (3) linearity of stress-strain relations, (4) small strains, (5) the water contained in the pores is incompressible, (6) the water may contain air bubbles, (7) the water flows through the porous skeleton according to Darcy's law.

Of these basic assumptions (2) and (3) are most subject to criticism. However, we should keep in mind that they also constitute the basis of Terzaghi's theory, which has been found quite satisfactory for the practical requirements of engineering. In fact it can be imagined that the grains composing the soil are held together in a certain pattern by surface tension forces and tend to assume a configuration of minimum potential energy. This would especially be true for the colloidal particles constituting clay. It seems reasonable to assume that for small strains, when the grain pattern is not too much disturbed, the assumption of reversibility will be applicable.

The assumption of isotropy is not essential and

* Publication assisted by the Ernest Kempton Adams Fund for Physical Research of Columbia University.

[1] K. Terzaghi, *Erdbaumechanik auf Bodenphysikalischer Grundlage* (Leipzig F. Deuticke, 1925); "Principle of soil mechanics," Eng. News Record (1925), a series of articles.

[2] M. A. Biot, "Le problème de la Consolidation des Matières argileuses sous une charge," Ann. Soc. Sci. Bruxelles **B55**, 110–113 (1935).

anisotropy can easily be introduced as a refinement. Another refinement which might be of practical importance is the influence, upon the stress distribution and the settlement, of the state of initial stress in the soil before application of the load. It was shown by the present author[3] that this influence is greater for materials of low elastic modulus. Both refinements will be left out of the present theory in order to avoid undue heaviness of presentation.

The first and second sections deal mainly with the mathematical formulation of the physical properties of the soil and the number of constants necessary to describe these properties. The number of these constants including Darcy's permeability coefficient is found equal to five in the most general case. Section 3 gives a discussion of the physical interpretation of these various constants. In Sections 4 and 5 are established the fundamental equations for the consolidation and an application is made to the one-dimensional problem corresponding to a standard soil test. Section 6 gives the simplified theory for the case most important in practice of a soil completely saturated with water. The equations for this case coincide with those of the previous publication.[2] In the last section is shown how the mathematical tool known as the *operational calculus* can be applied most conveniently for the calculation of the settlement without having to calculate any stress or water pressure distribution inside the soil. This method of attack constitutes a major simplification and proves to be of high value in the solution of the more complex two- and three-dimensional problems. In the present paper applications are restricted to one-dimensional examples. A series of applications to practical cases of two-dimensional consolidation will be the object of subsequent papers.

1. Soil Stresses

Consider a small cubic element of the consolidating soil, its sides being parallel with the coordinate axes. This element is taken to be large enough compared to the size of the pores so that it may be treated as homogeneous, and at the same time small enough, compared to the scale of the macroscopic phenomena in which we are interested, so that it may be considered as infinitesimal in the mathematical treatment.

The average stress condition in the soil is then represented by forces distributed uniformly on the faces of this cubic element. The corresponding stress components are denoted by

$$\begin{matrix} \sigma_x & \tau_z & \tau_y \\ \tau_z & \sigma_y & \tau_x \\ \tau_y & \tau_x & \sigma_z. \end{matrix} \tag{1.1}$$

They must satisfy the well-known equilibrium conditions of a stress field.

$$\begin{aligned} \frac{\partial \sigma_x}{\partial x}+\frac{\partial \tau_z}{\partial y}+\frac{\partial \tau_y}{\partial z}&=0, \\ \frac{\partial \tau_z}{\partial x}+\frac{\partial \sigma_y}{\partial y}+\frac{\partial \tau_x}{\partial z}&=0, \\ \frac{\partial \tau_y}{\partial x}+\frac{\partial \tau_x}{\partial y}+\frac{\partial \sigma_z}{\partial z}&=0. \end{aligned} \tag{1.2}$$

Physically we may think of these stresses as composed of two parts; one which is caused by the hydrostatic pressure of the water filling the pores, the other caused by the average stress in the skeleton. In this sense the stresses in the soil are said to be carried partly by the water and partly by the solid constituent.

2. Strain Related to Stress and Water Pressure

We now call our attention to the strain in the soil. Denoting by u, v, w the components of the displacement of the soil and assuming the strain to be small, the values of the strain components are

$$\begin{aligned} e_x&=\frac{\partial u}{\partial x}, & \gamma_x&=\frac{\partial w}{\partial y}+\frac{\partial v}{\partial z}, \\ e_y&=\frac{\partial v}{\partial y}, & \gamma_y&=\frac{\partial u}{\partial z}+\frac{\partial w}{\partial x}, \\ e_z&=\frac{\partial w}{\partial z}, & \gamma_z&=\frac{\partial v}{\partial x}+\frac{\partial u}{\partial y}. \end{aligned} \tag{2.1}$$

In order to describe completely the macroscopic condition of the soil we must consider an addi-

[3] M. A. Biot, "Nonlinear theory of elasticity and the linearized case for a body under initial stress."

tional variable giving the amount of water in the pores. We therefore denote by θ the increment of water volume per unit volume of soil and call this quantity the *variation in water content*. The *increment of water pressure* will be denoted by σ.

Let us consider a cubic element of soil. The water pressure in the pores may be considered as uniform throughout, provided either the size of the element is small enough or, if this is not the case, provided the changes occur at sufficiently slow rate to render the pressure differences negligible.

It is clear that if we assume the changes in the soil to occur by reversible processes the macroscopic condition of the soil must be a definite function of the stresses and the water pressure i.e., the seven variables

$$e_x \quad e_y \quad e_z \qquad \gamma_x \quad \gamma_y \quad \gamma_z \quad \theta$$

must be definite functions of the variables:

$$\sigma_x \quad \sigma_y \quad \sigma_z \qquad \tau_x \quad \tau_y \quad \tau_z \quad \sigma.$$

Furthermore if we assume the strains and the variations in water content to be small quantities, the relation between these two sets of variables may be taken as linear in first approximation. We first consider these functional relations for the particular case where $\sigma=0$. The six components of strain are then functions only of the six stress components $\sigma_x\ \sigma_y\ \sigma_z\ \tau_x\ \tau_y\ \tau_z$. Assuming the soil to have isotropic properties these relations must reduce to the well-known expressions of Hooke's law for an isotropic elastic body in the theory of elasticity; we have

$$\begin{aligned}
e_x &= \frac{\sigma_x}{E} - \frac{\nu}{E}(\sigma_y+\sigma_z),\\
e_y &= \frac{\sigma_y}{E} - \frac{\nu}{E}(\sigma_z+\sigma_x),\\
e_z &= \frac{\sigma_z}{E} - \frac{\nu}{E}(\sigma_x+\sigma_y),\\
\gamma_x &= \tau_x/G,\\
\gamma_y &= \tau_y/G,\\
\gamma_z &= \tau_z/G.
\end{aligned} \tag{2.2}$$

In these relations the constants E, G, ν may be interpreted, respectively, as Young's modulus, the shear modulus and Poisson's ratio for the solid skeleton. There are only two distinct constants because of the relation

$$G=\frac{E}{2(1+\nu)}. \tag{2.3}$$

Suppose now that the effect of the water pressure σ is introduced. First it cannot produce any shearing strain by reason of the assumed isotropy of the soil; second for the same reason its effect must be the same on all three components of strain $e_x\ e_y\ e_z$. Hence taking into account the influence of σ relations (2.2) become

$$\begin{aligned}
e_x &= \frac{\sigma_x}{E} - \frac{\nu}{E}(\sigma_y+\sigma_x) + \frac{\sigma}{3H},\\
e_y &= \frac{\sigma_y}{E} - \frac{\nu}{E}(\sigma_z+\sigma_x) + \frac{\sigma}{3H},\\
e_z &= \frac{\sigma_z}{E} - \frac{\nu}{E}(\sigma_x+\sigma_y) + \frac{\sigma}{3H},\\
\gamma_x &= \tau_x/G,\\
\gamma_y &= \tau_y/G,\\
\gamma_z &= \tau_z/G,
\end{aligned} \tag{2.4}$$

where H is an additional physical constant. These relations express the six strain components of the soil as a function of the stresses in the soil and the pressure of the water in the pores. We still have to consider the dependence of the increment of water content θ on these same variables. The most general relation is

$$\theta = a_1\sigma_x + a_2\sigma_y + a_3\sigma_z + a_4\tau_x + a_5\tau_y + a_6\tau_z + a_7\sigma. \tag{2.5}$$

Now because of the isotropy of the material a change in sign of $\tau_x\ \tau_y\ \tau_z$ cannot affect the water content, therefore $a_4=a_5=a_6=0$ and the effect of the shear stress components on θ vanishes. Furthermore all three directions x, y, z must have equivalent properties $a_1=a_2=a_3$. Therefore relation (2.5) may be written in the form

$$\theta=\frac{1}{3H_1}(\sigma_x+\sigma_y+\sigma_z)+\frac{\sigma}{R}, \tag{2.6}$$

where H_1 and R are two physical constants.

Relations (2.4) and (2.6) contain five distinct physical constants. We are now going to prove that this number may be reduced to four; in fact that $H=H_1$ if we introduce the assumption of the existence of a potential energy of the soil. This assumption means that if the changes occur at an infinitely slow rate, the work done to bring the soil from the initial condition to its final state of strain and water content, is independent of the way by which the final state is reached and is a definite function of the six strain components and the water content. This assumption follows quite naturally from that of reversibility introduced above, since the absence of a potential energy would then imply that an indefinite amount of energy could be drawn out of the soil by loading and unloading along a closed cycle.

The potential energy of the soil per unit volume is

$$U=\tfrac{1}{2}(\sigma_x e_x+\sigma_y e_y+\sigma_z e_z+\tau_x\gamma_x+\tau_y\gamma_y+\tau_z\gamma_z+\sigma\theta). \quad (2.7)$$

In order to prove that $H=H_1$ let us consider a particular condition of stress such that

$$\sigma_x=\sigma_y=\sigma_z=\sigma_1,$$
$$\tau_x=\tau_y=\tau_z=0.$$

Then the potential energy becomes

$$U=\tfrac{1}{2}(\sigma_1\epsilon+\sigma\theta) \quad \text{with} \quad \epsilon=e_x+e_y+e_z$$

and Eqs. (2.4) and (2.6)

$$\epsilon=\frac{3(1-2\nu)}{E}\sigma_1+\frac{\sigma}{H}, \quad \theta=\sigma_1/H_1+\sigma/R. \quad (2.8)$$

The quantity ϵ represents the volume increase of the soil per unit initial volume. Solving for σ_1 and σ

$$\sigma_1=\frac{\epsilon}{R\Delta}-\frac{\theta}{H\Delta},$$
$$\sigma=\frac{-\epsilon}{H_1\Delta}+\frac{3(1-2\nu)\theta}{E\Delta}, \quad (2.9)$$
$$\Delta=\frac{3(1-2\nu)}{ER}-\frac{1}{HH_1}.$$

The potential energy in this case may be considered as a function of the two variables ϵ, θ. Now we must have

$$\frac{\partial U}{\partial\epsilon}=\sigma_1, \quad \frac{\partial U}{\partial\theta}=\sigma.$$

Hence

$$\frac{\partial\sigma_1}{\partial\theta}=\frac{\partial\sigma}{\partial\epsilon}$$

or

$$\frac{1}{H\Delta}=\frac{1}{H_1\Delta}.$$

We have thus proved that $H=H_1$ and we may write

$$\theta=\frac{1}{3H}(\sigma_x+\sigma_y+\sigma_z)+\frac{\sigma}{R}. \quad (2.10)$$

Relations (2.4) and (2.10) are the fundamental relations describing completely in first approximation the properties of the soil, for strain and water content, under equilibrium conditions. They contain four distinct physical constants G, ν, H and R. For further use it is convenient to express the stresses as functions of the strain and the water pressure σ. Solving Eq. (2.4) with respect to the stresses we find

$$\sigma_x=2G\left(e_x+\frac{\nu\epsilon}{1-2\nu}\right)-\alpha\sigma,$$
$$\sigma_y=2G\left(e_y+\frac{\nu\epsilon}{1-2\nu}\right)-\alpha\sigma,$$
$$\sigma_z=2G\left(e_z+\frac{\nu\epsilon}{1-2\nu}\right)-\alpha\sigma, \quad (2.11)$$
$$\tau_x=G\gamma_x,$$
$$\tau_y=G\gamma_y,$$
$$\tau_z=G\gamma_z$$

with

$$\alpha=\frac{2(1+\nu)}{3(1-2\nu)}\frac{G}{H}.$$

In the same way we may express the variation in water content as

$$\theta=\alpha\epsilon+\sigma/Q, \quad (2.12)$$

where

$$\frac{1}{Q}=\frac{1}{R}-\frac{\alpha}{H}.$$

3. Physical Interpretation of the Soil Constants

The constants E, G and ν have the same meaning as Young's modulus the shear modulus and the Poisson ratio in the theory of elasticity provided time has been allowed for the excess water to squeeze out. These quantities may be considered as the average elastic constants of the solid skeleton. There are only two distinct such constants since they must satisfy relation (2.3). Assume, for example, that a column of soil supports an axial load $p_0 = -\sigma_z$ while allowed to expand freely laterally. If the load has been applied long enough so that a final state of settlement is reached, i.e., all the excess water has been squeezed out and $\sigma = 0$ then the axial strain is, according to (2.4),

$$e_z = -\frac{p_0}{E} \tag{3.1}$$

and the lateral strain

$$e_x = e_y = \frac{\nu p_0}{E} = -\nu e_z. \tag{3.2}$$

The coefficient ν measures the ratio of the lateral bulging to the vertical strain under final equilibrium conditions.

To interpret the constants H and R consider a sample of soil enclosed in a thin rubber bag so that the stresses applied to the soil be zero. Let us drain the water from this soil through a thin tube passing through the walls of the bag. If a negative pressure $-\sigma$ is applied to the tube a certain amount of water will be sucked out. This amount is given by (2.10)

$$\theta = -\frac{\sigma}{R}. \tag{3.3}$$

The corresponding volume change of the soil is given by (2.4)

$$\epsilon = -\frac{\sigma}{H}. \tag{3.4}$$

The coefficient $1/H$ is a measure of the compressibility of the soil for a change in water pressure, while $1/R$ measures the change in water content for a given change in water pressure. The two elastic constants and the constants H and R are the four distinct constants which under our assumption define completely the physical proportions of an isotropic soil in the equilibrium conditions.

Other constants have been derived from these four. For instance α is a coefficient defined as

$$\alpha = \frac{2(1+\nu)}{3(1-2\nu)}\frac{G}{H}. \tag{3.5}$$

According to (2.12) it measures the ratio of the water volume squeezed out to the volume change of the soil if the latter is compressed while allowing the water to escape ($\sigma = 0$). The coefficient $1/Q$ defined as

$$\frac{1}{Q} = \frac{1}{R} - \frac{\alpha}{H} \tag{3.6}$$

is a measure of the amount of water which can be forced into the soil under pressure while the volume of the soil is kept constant. It is quite obvious that the constants α and Q will be of significance for a soil not completely saturated with water and containing air bubbles. In that case the constants α and Q can take values depending on the degree of saturation of the soil.

The standard soil test suggests the derivation of additional constants. A column of soil supports a load $p_0 = -\sigma_z$ and is confined laterally in a rigid sheath so that no lateral expansion can occur. The water is allowed to escape for instance by applying the load through a porous slab. When all the excess water has been squeezed out the axial strain is given by relations (2.11) in which we put $\sigma = 0$. We write

$$e_z = -p_0 a. \tag{3.7}$$

The coefficient

$$a = \frac{1-2\nu}{2G(1-\nu)} \tag{3.8}$$

will be called the *final compressibility*.

If we measure the axial strain just after the load has been applied so that the water has not had time to flow out, we must put $\theta = 0$ in relation (2.12). We deduce the value of the water pressure

$$\sigma = -\alpha Q e_z. \tag{3.9}$$

substituting this value in (2.11) we write

$$e_s = -p_0 a_i. \tag{3.10}$$

The coefficient

$$a_i = \frac{a}{1+\alpha^2 aQ} \tag{3.11}$$

will be called the *instantaneous compressibility*.

The physical constants considered above refer to the properties of the soil for the state of equilibrium when the water pressure is uniform throughout. We shall see hereafter that in order to study the transient state we must add to the four distinct constants above the so-called *coefficient of permeability* of the soil.

4. General Equations Governing Consolidation

We now proceed to establish the differential equations for the transient phenomenon of consolidation, i.e., those equations governing the distribution of stress, water content, and settlement as a function of time in a soil under given loads.

Substituting expression (2.11) for the stresses into the equilibrium conditions (1.2) we find

$$\begin{aligned} G\nabla^2 u + \frac{G}{1-2\nu}\frac{\partial \epsilon}{\partial x} - \alpha\frac{\partial \sigma}{\partial x} = 0, \\ G\nabla^2 v + \frac{G}{1-2\nu}\frac{\partial \epsilon}{\partial y} - \alpha\frac{\partial \sigma}{\partial y} = 0, \\ G\nabla^2 w + \frac{G}{1-2\nu}\frac{\partial \epsilon}{\partial z} - \alpha\frac{\partial \sigma}{\partial z} = 0, \\ \nabla^2 = \partial^2/\partial x^2 + \partial^2/\partial y^2 + \partial^2/\partial z^2. \end{aligned} \tag{4.1}$$

There are three equations with four unknowns u, v, w, σ. In order to have a complete system we need one more equation. This is done by introducing Darcy's law governing the flow of water in a porous medium. We consider again an elementary cube of soil and call V_x the volume of water flowing per second and unit area through the face of this cube perpendicular to the x axis. In the same way we define V_y and V_z. According to Darcy's law these three components of the rate of flow are related to the water pressure by the relations

$$V_x = -k\frac{\partial \sigma}{\partial x}, \quad V_y = -k\frac{\partial \sigma}{\partial y}, \quad V_z = -k\frac{\partial \sigma}{\partial z}. \tag{4.2}$$

The physical constant k is called the *coefficient of permeability* of the soil. On the other hand, if we assume the water to be incompressible the rate of water content of an element of soil must be equal to the volume of water entering per second through the surface of the element, hence

$$\frac{\partial \theta}{\partial t} = -\frac{\partial V_x}{\partial x} - \frac{\partial V_y}{\partial y} - \frac{\partial V_z}{\partial z}. \tag{4.3}$$

Combining Eqs. (2.2) (4.2) and (4.3) we obtain

$$k\nabla^2 \sigma = \alpha\frac{\partial \epsilon}{\partial t} + \frac{1}{Q}\frac{\partial \sigma}{\partial t}. \tag{4.4}$$

The four differential Eqs. (4.1) and (4.4) are the basic equations satisfied by the four unknowns u, v, w, σ.

5. Application to a Standard Soil Test

Let us examine the particular case of a column of soil supporting a load $p_0 = -\sigma_z$ and confined laterally in a rigid sheath so that no lateral expansion can occur. It is assumed also that no water can escape laterally or through the bottom while it is free to escape at the upper surface by applying the load through a very porous slab.

Take the z axis positive downward; the only component of displacement in this case will be w. Both w and the water pressure σ will depend only on the coordinate z and the time t. The differential Eqs. (4.1) and (4.4) become

$$\frac{1}{a}\frac{\partial^2 w}{\partial z^2} - \alpha\frac{\partial w}{\partial z} = 0, \tag{5.1}$$

$$k\frac{\partial^2 \sigma}{\partial z^2} = \alpha\frac{\partial^2 w}{\partial z \partial t} + \frac{1}{Q}\frac{\partial \sigma}{\partial t}, \tag{5.2}$$

where a is the final compressibility defined by (3.8). The stress σ_z throughout the loaded column is a constant. From (2.11) we have

$$p_0 = -\sigma_z = -\frac{1}{a}\frac{\partial w}{\partial z} + \alpha\sigma \tag{5.3}$$

and from (2.12)

$$\theta = \alpha\frac{\partial w}{\partial z} + \frac{\sigma}{Q}.$$

Note that Eq. (5.3) implies (5.1) and that

$$-\frac{1}{a}\frac{\partial^2 w}{\partial z \partial t} = \alpha\frac{\partial \sigma}{\partial t}.$$

This relation carried into (5.2) gives

$$\frac{\partial^2 \sigma}{\partial z^2} = \frac{1}{c}\frac{\partial \sigma}{\partial t}, \tag{5.4}$$

with

$$\frac{1}{c} = \alpha^2\frac{a}{k} + \frac{1}{Qk}. \tag{5.5}$$

The constant c is called the *consolidation constant*. Equation (5.4) shows the important result that the water pressure satisfies the well-known equation of heat conduction. This equation along with the boundary and the initial conditions leads to a complete solution of the problem of consolidation.

Taking the height of the soil column to be h and $z=0$ at the top we have the boundary conditions

$$\sigma = 0 \quad \text{for } z=0,$$
$$\frac{\partial \sigma}{\partial z} = 0 \quad \text{for } z=h. \tag{5.6}$$

The first condition expresses that the pressure of the water under the load is zero because the permeability of the slab through which the load is applied is assumed to be large with respect to that of the soil. The second condition expresses that no water escapes through the bottom.

The initial condition is that the change of water content is zero when the load is applied because the water must escape with a finite velocity. Hence from (2.12)

$$\theta = \alpha\frac{\partial w}{\partial z} + \frac{\sigma}{Q} = 0 \quad \text{for } t=0.$$

Carrying this into (5.3) we derive the initial value of the water pressure

$$\sigma = p_0 \Big/ \left(\frac{1}{\alpha a Q} + \alpha\right) \quad \text{for } t=0 \quad \text{or} \quad \sigma = \frac{a-a_i}{\alpha a} p_0, \tag{5.7}$$

where a_i and a are the instantaneous and final compressibility coefficients defined by (3.8) and (3.11).

The solution of the differential equation (5.4) with the boundary conditions (5.6) and the initial condition (5.7) may be written in the form of a series

$$\sigma = \frac{4}{\pi}\frac{a-a_i}{\alpha a} p_0 \left\{ \exp\left[-\left(\frac{\pi}{2h}\right)^2 ct\right] \sin\frac{\pi z}{2h} + \frac{1}{3}\exp\left[-\left(\frac{3\pi}{2h}\right)^2 ct\right] \sin\frac{3\pi z}{2h} + \cdots \right\}. \tag{5.8}$$

The settlement may be found from relation (5.3). We have

$$\frac{\partial w}{\partial z} = \alpha a \sigma - a p_0. \tag{5.9}$$

The total settlement is

$$w_0 = -\int_0^h \frac{\partial w}{\partial z} dz = -\frac{8}{\pi^2}(a-a_i)hp_0 \sum_0^\infty \frac{1}{(2n+1)^2} \exp\left\{-\left[\frac{(2n+1)\pi}{2h}\right]^2 ct\right\} + ahp_0. \tag{5.10}$$

Immediately after loading ($t=0$), the deflection is

$$w_i = -\frac{8}{\pi^2}(a-a_i)hp_0 \sum_0^\infty \frac{1}{(2n+1)^2} + ahp.$$

Taking into account that

$$\sum_0^\infty \frac{1}{(2n+1)^2} = \frac{\pi^2}{8}, \quad w_i = a_i hp_0, \tag{5.11}$$

which checks with the result (3.10) above. The final deflection for $t=\infty$ is

$$w_\infty = ahp_0. \tag{5.12}$$

It is of interest to find a simplified expression for the law of settlement in the period of time immediately after loading. To do this we first eliminate the initial deflection w_i by considering

$$w_s = w_0 - w_i = \frac{8}{\pi^2}(a-a_i)hp_0 \sum_0^\infty \frac{1}{(2n+1)^2}\left\{1-\exp\left[-\left(\frac{(2n+1)\pi}{2h}\right)^2 ct\right]\right\}. \tag{5.13}$$

This expresses that part of the deflection which is caused by consolidation. We then consider the rate of settlement.

$$\frac{dw_s}{dt} = \frac{2c(a-a_i)}{h} p_0 \sum_0^\infty \exp\left\{-\left[\frac{(2n+1)\pi}{2h}\right]^2 ct\right\}. \tag{5.14}$$

For $t=0$ this series does not converge; which means that at the first instant of loading the rate of settlement is infinite. Hence the curve representing the settlement w_s as a function of time starts with a vertical slope and tends asymptotically toward the value $(a-a_i)hp_0$ as shown in Fig. 1 (curve 1). It is obvious that during the initial period of settlement the height h of the column cannot have any influence on the phenomenon because the water pressure at the depth $z=h$ has not yet had time to change. Therefore in order to find the nature of the settlement curve in the vicinity of $t=0$ it is enough to consider the case where $h=\infty$. In this case we put

$$n/h = \xi, \quad 1/h = \Delta\xi$$

and write (5.14) as

$$\frac{dw_s}{dt} = 2c(a-a_i)p_0 \sum_0^\infty \exp\left[-\pi^2(\xi+\tfrac{1}{2}\Delta\xi)^2 ct\right]\Delta\xi$$

for $h=\infty$. The rate of settlement becomes the integral

$$\frac{dw_s}{dt} = 2c(a-a_i)p_0 \int_0^\infty \exp\left(-\pi^2\xi^2 ct\right)d\xi = \frac{c(a-a_i)p_0}{(\pi ct)^{\frac{1}{2}}}. \tag{5.15}$$

The value of the settlement is obtained by integration

$$w_s = \int_0^t \frac{dw_s}{dt} dt = 2(a-a_i)p_0\left(\frac{ct}{\pi}\right)^{\frac{1}{2}}. \tag{5.16}$$

It follows a parabolic curve as a function of time (curve 2 in Fig. 1).

6. Simplified Theory for a Saturated Clay

For a completely saturated clay the standard test shows that the initial compressibility a_i may be taken equal to zero compared to the final compressibility a, and that the volume change of the soil is equal to the amount of water squeezed out. According to (2.12) and (3.11) this implies

$$Q=\infty, \quad \alpha=1. \tag{6.1}$$

This reduces the number of physical constants of the soil to the two elastic constants and the permeability. From relations (3.5) and (3.6) we deduce

$$H=R=\frac{2G(1+\nu)}{3(1-2\nu)} \tag{6.2}$$

and from (5.5) the value of the consolidation constant takes the simple form

$$c=k/a. \tag{6.3}$$

Relation (2.12) becomes

$$\theta=\epsilon. \tag{6.4}$$

The general differential equations (4.1) and (4.4) are simplified,

$$\begin{aligned} G\nabla^2 u+\frac{G}{1-2\nu}\frac{\partial\epsilon}{\partial x}-\frac{\partial\sigma}{\partial x}=0,\\ G\nabla^2 v+\frac{G}{1-2\nu}\frac{\partial\epsilon}{\partial y}-\frac{\partial\sigma}{\partial y}=0,\\ G\nabla^2 w+\frac{G}{1-2\nu}\frac{\partial\epsilon}{\partial z}-\frac{\partial\sigma}{\partial z}=0, \end{aligned} \tag{6.5}$$

$$k\nabla\sigma^2=\frac{\partial\epsilon}{\partial t}. \tag{6.6}$$

By adding the derivatives with respect to x, y, z of Eqs. (6.5), respectively, we find

$$\nabla\epsilon^2=a\nabla\sigma^2, \tag{6.7}$$

where a is the final compressibility given by (3.8).

From (6.6) and (6.7) we derive

$$\nabla\epsilon^2=\frac{1}{c}\frac{\partial\epsilon}{\partial t}. \tag{6.8}$$

Hence the volume change of the soil satisfies the equation of heat conduction.

Equations (6.5) and (6.8) are the fundamental equations governing the consolidation of a completely saturated clay. Because of (6.4) the initial condition $\theta=0$ becomes $\epsilon=0$, i.e., at the instant of loading no volume change of the soil occurs. This condition introduced in Eq. (6.7) shows that at the instant of loading the water pressure in the pores also satisfies Laplace's equation.

$$\nabla\sigma^2=0. \tag{6.9}$$

The settlement for the standard test of a column of clay of height h under the load p_0 is given by (5.13) by putting $a_i=0$.

$$w_s=\frac{8}{\pi^2}ahp_0\sum_0^\infty\frac{1}{(2n+1)^2}\times\left\{1-\exp\left[-\left(\frac{(2n+1)\pi}{2h}\right)^2 ct\right]\right\}. \tag{6.10}$$

From (5.16) the settlement for an infinitely high column is

$$w_s=2ap_0\left(\frac{ct}{\pi}\right)^{\frac{1}{2}}. \tag{6.11}$$

It is easy to imagine a mechanical model having the properties implied in these equations. Consider a system made of a great number of small rigid particles held together by tiny helical springs. This system will be elastically deformable and will possess average elastic constants. If we fill completely with water the voids between the

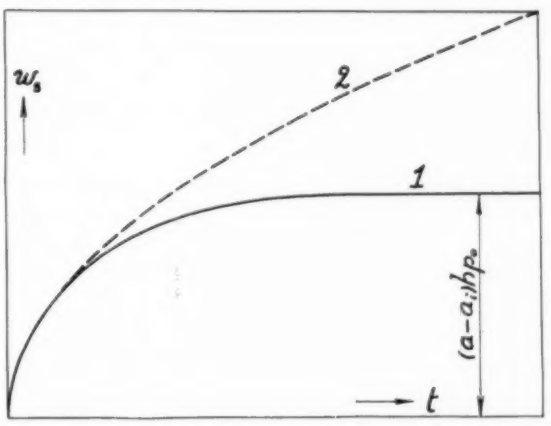

Fig. 1. Settlement caused by consolidation as a function of time. Curve 1 represents the settlement of a column of height h under a load p_0. Curve 2 represents the settlement for an infinitely high column.

particles, we shall have a model of a completely saturated clay.

Obviously such a system is incompressible if no water is allowed to be squeezed out (this corresponds to the condition $Q=\infty$) and the change of volume is equal to the volume of water squeezed out (this corresponds to the condition $\alpha=1$). If the systems contained air bubbles this would not be the case and we would have to consider the general case where Q is finite and $\alpha\neq 1$.

Whether this model represents schematically the actual constitution of soils is uncertain. It is quite possible, however, that the soil particles are held together by capillary forces which behave in pretty much the same way as the springs of the model.

7. Operational Calculus Applied to Consolidation

The calculation of settlement under a suddenly applied load leads naturally to the application of operational methods, developed by Heaviside for the analysis of transients in electric circuits. As an illustration of the power and simplicity introduced by the operational calculus in the treatment of consolidation problem we shall derive by this procedure the settlement of a completely saturated clay column already calculated in the previous section. In subsequent articles the operational method will be used extensively for the solution of various consolidation problems. We consider the case of a clay column infinitely high and take as before the top to be the origin of the vertical coordinate z. For a completely saturated clay $\alpha=1$, $Q=\infty$ and with the operational notations, replacing $\partial/\partial t$ by p, Eqs. (5.1) become

$$\frac{1}{a}\frac{\partial^2 w}{\partial z^2}=\frac{\partial \sigma}{\partial z}, \quad k\frac{\partial^2 \sigma}{\partial z^2}=p\frac{\partial w}{\partial z}. \tag{7.1}$$

A solution of these equations which vanishes at infinity is

$$w=C_1 e^{-z(p/c)^{\frac{1}{2}}},$$
$$\sigma=C_2-\frac{1}{a}\left(\frac{p}{c}\right)^{\frac{1}{2}} C_1 e^{-z(p/c)^{\frac{1}{2}}}. \tag{7.2}$$

The boundary conditions are for $z=0$

$$\sigma_z=-1=\frac{1}{a}\frac{\partial w}{\partial z}, \quad \sigma=0.$$

Hence

$$C_1=a\left(\frac{c}{p}\right)^{\frac{1}{2}}, \quad C_2=1.$$

The settlement w_s at the top ($z=0$) caused by the sudden application of a unit load is

$$w_s=a\left(\frac{c}{p}\right)^{\frac{1}{2}}\cdot 1(t).$$

The meaning of this symbolic expression is derived from the operational equation[4]

$$\frac{1}{p^{\frac{1}{2}}}1(t)=2\left(\frac{t}{\pi}\right)^{\frac{1}{2}}. \tag{7.3}$$

The settlement as a function of time under the load p_0 is therefore

$$w_s=2ap_0\left(\frac{ct}{\pi}\right)^{\frac{1}{2}}. \tag{7.4}$$

This coincides with the value (6.11) above.

[4] V. Bush, *Operational Circuit Analysis* (John Wiley, New York, 1929), p. 192.

Field Emission X-Ray Tube

CHARLES M. SLACK AND LOUIS F. EHRKE
Research Department, Lamp Division, Westinghouse Electric and Manufacturing Company, Bloomfield, New Jersey
(Received November 9, 1940)

It has been found possible to draw currents of the order of several thousand amperes from cold metals by field emission in vacuum. This principle has been put to use in the design of a condenser discharge x-ray tube for high speed radiography. An auxiliary electrode spaced close to the cathode and connected to the anode through a high resistance serves to initiate the discharge which is then transferred to the anode. This auxiliary electrode is made in the form of a focusing electrode. Radiographs of bullets and the internal workings of other high speed objects are now made possible.

IT has been found that currents of several thousand amperes can be obtained in highly evacuated tubes by the application of high field gradients to cold metallic electrodes. This article is concerned with the utilization of these currents in the development of an x-ray tube for taking radiographs of rapidly moving objects.

HISTORICAL

Since the first use of x-rays for radiographic purposes, a large part of the effort of tube and equipment manufacturers has been directed toward shortening the exposure time. This resulted some ten years ago in commercial tubes and equipment capable of taking pictures in one-twentieth to one-sixtieth of a second, sufficiently fast to stop motion of practically all internal parts of the body. The development of the "flash" technique in light pictures has further stimulated this search for faster radiographic exposures. Steenbeck,[1] Kingdon and Tanis[2] and Oosterkampf[3] have contributed much toward this goal. The first two used a mercury pool discharge tube making possible very high currents, but having the limitations of a single position plus the necessity for cooling to low temperatures to reduce the vapor pressure of mercury. Oosterkampf[3] was able to obtain 20 amp. emission by suddenly raising the cathode temperature of an ordinary tube close to the melting point, a rather dangerous commercial procedure.

[1] Max Steenbeck, *Wissenschaftliche Veroffentlichungen aus den Siemens-Werken* (Julius Springer, Berlin, 1938), Vol. 17, Chapter 4, pp. 363–380.
[2] K. H. Kingdon and H. E. Tanis, Jr., Phys. Rev. **53**, 128 (1938).
[3] W. J. Oosterkampf, Phillips Tech. Rev. p. 22 (Jan. 1940).

DEVELOPMENT OF THE FIELD EMISSION TUBE

While studying the flash-back problem in vacuum x-ray tubes using a condenser discharge, it was noted that a single flash-back was sufficient to discharge the condensers and apparently did so in an extremely short time.

It was decided to study this effect further and to measure the magnitude of the currents involved. They were found to be much higher than anticipated, perhaps amperes rather than milliamperes. Since one ampere emission is the practical limit of the tungsten filament for commercial x-ray tubes, it was thought worth while to study this erratic type of field emission further in the hopes that it might be controlled and put to a useful rather than a destructive purpose.

With a single point tungsten cathode placed approximately 1 mm from a flat anode (Fig. 1) it was found possible to draw several thousand amperes from a condenser charged to 50,000 volts. Some x-rays were produced but, in general, the behavior was quite erratic. If the point was too close to the anode, a metallic arc was formed which allowed such large currents to pass that most of the energy was dissipated in the circuit rather than the tube. As the wire was moved farther back, the peak current diminished and the production of x-rays increased, but the initiation of the discharge became erratic, the tube often failing to fire altogether. Many shapes and types of material were tried, but the results were very much the same.

This difficulty was overcome by the introduction of a third electrode (Fig. 2) spaced close to the cathode and connected to the anode through a high resistance. This electrode served to concen-

FIG. 1. Simple point to plane.

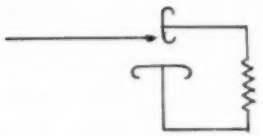

FIG. 2. Point to plane and transfer to second plane.

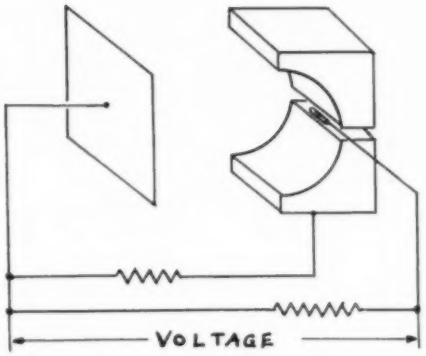

FIG. 3. Arrangement of x-ray tube electrodes transfer to anode.

trate a high field at the cathode and initiate the discharge which is then forced, by the voltage drop across the high resistance, to transfer to the anode. As soon as this auxiliary electrode has performed its job of starting the discharge, it assumes a potential very close to that of the cathode and consequently if shaped correctly (as in Fig. 3 for instance), may be utilized in focusing the electrons on the desired region of the anode.

APPLICATION OF FIELD EMISSION TO THE PRODUCTION OF SHORT EXPOSURE X-RAYS

An x-ray picture being a simple shadowgraph, the size and shape of the focus of the electrons on the anode, from which the x-rays originate, are extremely important and the projection of this area in the direction of the x-ray beam should be kept as small as possible. Fortunately, x-rays do not obey Lambert's cosine law, so that very little is lost by working near grazing incidence to the target. This means that a rectangular shaped focal spot, the projection of which is a square, is the optimum from the radiographic and loading standpoint. The length of the rectangle is determined by the field angle required. Ordinarily a 40-deg. field is sufficient. This means that the rectangle may be approximately three times as long as it is broad, with a corresponding increase in loading.

By placing the flattened cathode inside a trough (see Fig. 3) of the auxiliary electrode, we have been able to obtain a semblance of a rectangular focus and believe that with more work along this line, satisfactory focusing can be obtained. Even when the electron beam is fairly well spread over the whole of the target, good definition may be obtained in one direction by working near grazing incidence.

The energy of the impacting electrons on the target is dissipated in four different ways: (1) x-radiation, 0 to 0.1 percent depending on voltage, the higher the voltage the higher the efficiency; (2) light and heat radiation from focal spot 1 to 5 percent depending on exposure time; (3) vaporization of tungsten 0 to 3 percent; (4) heating of the tungsten at and near the focal spot 90 to 98 percent.

It is obvious from these considerations that conduction of heat to the surrounding tungsten must be depended upon to play the major role in heat dissipation and since the amount of conducted heat from a given area depends on the time and difference in temperature, it is to be seen that the dissipating ability of a focal area will decrease with the shorter exposure times. It is fortunate that it varies as the square root of the time according to the formula.[3]

$$W_m = T_m(\pi K C t)^{\frac{1}{2}}/2.$$

W_m = is the loading in total energy permitted per unit area which will raise the surface temperature an amount T_m. K is the thermal conductivity; C is the heat capacity and t the time of exposure.

For tungsten, the values are approximately as follows: $T_m = 3400°$K, $K = 1.6$ watts per cm per degree C; $C = 2.7$ watts per sec. per cu. cm per degree C.

On this basis, using a condenser of 0.02 microfarad charged to 100 kv and assuming a discharge time of 1 microsecond, a focal spot area of approximately 16 sq. cm would be required to

prevent the vaporization of tungsten. In the tubes so far constructed, an effective focal area of from one-fourth to one-eighth this value has been used and while some vaporization does occur, it is estimated that several thousand exposures could be made before the vaporized tungsten film would be sufficient to absorb appreciably the x-rays produced. The failure of the formula in this particular case may be due to a number of causes. The two most important probably are: (1) The total discharge time of the condenser may be several times that of the x-ray exposure since the intensity of x-rays falls off rapidly with the voltage. (2) A considerable portion of the electrons are reflected from the focal spot giving up their energy elsewhere. These considerations indicate that for extremely short exposures, the definition of the radiograph can never equal the best obtainable with longer exposure times.

Operation of the Tube

The manner of operation of the tube can best be seen by reference to circuit diagram (Fig. 4). The condensers are charged by means of transformer *A* and series rectifiers to a voltage somewhat below that necessary to breakdown gap *F*. Simultaneously, condenser *D* is charged to about 1000 volts. When the circuit is broken at *B*, the

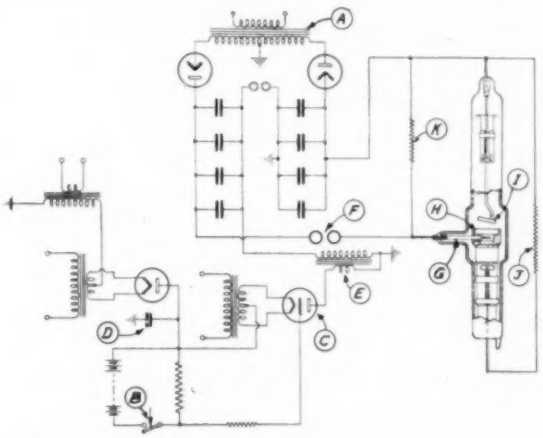

Fig. 4. Circuit diagram showing operation of tube.

charge on the grid of the thyratron *C* leaks off, enabling *D* to discharge through the primary of the induction coil *E*, which gives a sufficient impulse to the high voltage circuit to cause *F* to flash over.

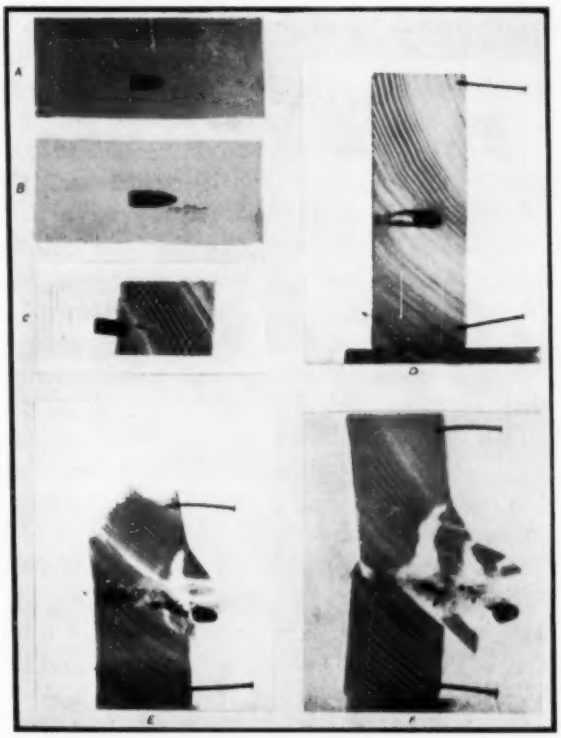

Fig. 5. Bullet series. *A*—.22 long rifle bullet in free flight. Velocity 1300 ft./second. No measurable blur. *B*—.220 Swift in free flight. Velocity 4100 ft./second. Amount of blur is measure of exposure time. *C*—.22 long rifle entering ash block. Note triggering wire. *D*—Partly through block. Note action of fibers tending to close hole made by bullet. *E*—Bullet emerges from block—block starts to break up. Bullet has been deflected by grain structure. *F*—Both block and bullet are considerably broken up.

When this occurs, an incipient discharge is initiated between *G* and *H* within the shield and the main discharge then passes from *H* to *I* with the resultant production of x-rays.

The formation time for the discharge inside the tube must be of the same order or even less than that required for a spark in air since a gap placed across *K* will jump a considerably greater distance without the tube connected than with it in the circuit. Also, a very small spacing is sufficient between the external connections to *G* and *H* to prevent a spark in air, though the whole condenser voltage would be here momentarily were it not for the field emission breakdown between these electrodes within the tube.

The time constant of the trigger circuit is about 20 microseconds, and the time for complete discharge through the tube about 1 microsecond.

The time delay of the trigger circuit is estimated by the distance a bullet travels after breaking the circuit at *B* and the discharge time is judged by the blurring of the bullet image.

The time delay may be increased to any desired value by adding capacity or increasing the resistance of the grid leak of the thyratron *C*.

No measurable blur could be obtained with the use of a .22 long rifle bullet in free flight (Fig. 5*A*), speed about 1200 ft. per second. However, a .220 Swift bullet with a speed of 4000 ft. per second, showed an average blur corresponding to somewhat less than 1 microsecond in time (*B*).

This indicates a discharge current of some 2000 amperes and a rough check on this value was obtained by measuring the voltage drop across a 5-ohm straight wire resistance by means of a micrometer spark gap. The error produced by the self-inductance of the wire with such rapidly changing currents could be estimated by using wires of different diameters and lengths, keeping the resistance constant.[2]

A series of pictures showing a Remington .22 long rifle bullet at different stages of penetration through similar blocks of hard ash is shown in Figs. 5*C*, *D*, *E*, *F*. It is interesting to note the destruction of the bullet and the rapidity with which the wood seals the hole left by the bullet.

Conclusions

It is always difficult to attempt to estimate the future possibilities of such a device; however, some indication as to its future applications may be gleaned from the results already obtained. We have been limited, with our present equipment, to about 100,000 volts and 0.02 mf which enables us, with good intensifying screens, to penetrate about 4″ of tissue, 4 cm of aluminum or from 1 to 2 mm of steel. The penetration goes up rapidly with the voltage, however, and it is believed that with 2 or 3 hundred kilovolts, it should be possible to obtain distinguishable radiographs through an inch or more of steel equivalent. This voltage is a great deal higher than that necessary for long time exposures and consequently there will be considerable loss in contrast. Fortunately, this loss of contrast can be tolerated in most commercial applications because of the great differences in opacity of materials and it is believed that a great deal of valuable information might be obtained in the study of the distortion of rapidly moving machine parts as well as the penetration of bullets in various materials.

The development of a tube for such voltages and energies offers certain difficulties, none of which at the present time seem insurmountable. It will be necessary to regulate the focal size to prevent excessive vaporization of tungsten and to so control the spacing as to prevent the formation of metallic ions in sufficient numbers to cause the discharge to degenerate into an arc. This last phenomenon need only be prevented during the early part of the discharge, since the x-rays generated at voltages below two-thirds that of the maximum are of little use because of their relatively low penetrating power.

We would like to thank Mr. C. E. Dawley who has aided in many phases of this work and to also express our appreciation to Dr. H. C. Rentschler, Director of the Laboratory, for his advice and helpful cooperation.

I HAVE learned from long experience to have more faith in the scientist than he has in himself. Experience and faith tell me that—given time, facilities, and freedom to follow where imagination leads—the scientist will do all he hopes to do, and more.

David Sarnoff in "Science and Security"

Announcing . . . A New Emulsion

for Eastman Spectroscopic Plates

ANOTHER EMULSION—TYPE 103—has been added to the series of *Eastman Spectroscopic Plates*. It has somewhat higher speed and lower contrast than the Type I emulsion, and a grain structure approximating that of the Type III emulsion.

The new Type 103 emulsion is available both unsensitized and with the regular sensitizings for *Eastman Spectroscopic Plates*, excepting the extreme red and infrared classes. Further information will be forwarded promptly upon request.

EASTMAN KODAK COMPANY

Research Laboratories Rochester, N. Y.

Two Outstanding Science Dictionaries

GERMAN-ENGLISH SCIENCE DICTIONARY

By LOUIS DE VRIES, Iowa State College. With the Collaboration of Members of the Graduate Faculty. 473 pages, 5 x 7. $3.00

Widely praised by teachers everywhere, this unique dictionary contains 48,000 terms needed by the student in chemistry, physics, mathematics, biology, and related sciences. In addition to the scientific and technical terms, the dictionary includes many idioms and literary terms.

"Attention should be called to this much-needed valuable little dictionary for aid in reading scientific German, especially in fields outside one's own. . . . There has been a crying need for just such a volume to serve general science. . . ."

Professor HAROLD K. FINK, California Institute of Technology, in *Science*

FRENCH-ENGLISH SCIENCE DICTIONARY

By LOUIS DE VRIES. With the Collaboration of Members of the Graduate Faculty. 546 pages, 5 x 7. $3.50

This volume contains 43,000 terms covering the same fields as the *German-English Science Dictionary*. The French irregular verb is effectively presented by giving many forms of the present, past, and future tenses, past participle, etc. A feature of the book is the inclusion of some 500 common idioms.

"It seems to me an excellent work, handy and compact, yet sufficiently complete for graduate-student use. . . . I am recommending the book to my graduate students."

Professor G. WAKEHAM, University of Colorado

Send for copies on approval

McGRAW-HILL BOOK COMPANY, INC.

330 West 42nd Street New York, N. Y.

Innovations in Instruments

Scientific Blackout

You won't have to pull down the shades or turn out the lights if the blackout of war ever comes to America, according to General Electric scientists who are concentrating on United States defense problems. These scientists are working on a combination of light and glass which will allow daylight in through windows during the day, but which will keep light from shining out at night. Pitting one color against another, they have found that a combination of blue-painted windows and sodium lighting achieves the desired effect, according to H. A. Breeding, physicist at the Schenectady lighting laboratory. The paint to be used, Breeding states, is ordinary paint treated with a special blue dye, experiments on which are still proceeding. Windows treated with this special blue paint will admit daylight, but, if homes and factories equipped with these blue windows are lighted inside with sodium lights, not a flash of light will escape to the outside.

Boiler System Corrosion Control

In steam boilers, particularly high pressure ones, the control of dissolved oxygen is of great importance. De-aeration of feed water to protect the system from corrosion is an established practice, but cyclical events which admit oxygen to the feed water may continue indefinitely and undetected if a continuous record is not available. Possibly the most sensitive industrial instrument to be put in use by operators of large steam plants is the Cambridge Dissolved Oxygen Recorder. The sensitivity of this instrument, manufactured by the Cambridge Instrument Company, Inc., Grand Central Terminal, New York City, is such that dissolved oxygen in feed water can be measured to one part in 400,000,000. Until this instrument was developed, the only means of determining dissolved oxygen was a chemical method requiring considerable time and producing only "spot" determinations. The Cambridge Dissolved Oxygen Recorder, however, is completely automatic and provides a continuous indication and record of dissolved oxygen entering the boiler.

New Color for Fluorescent Lamps

Soft white, a new color for Mazda fluorescent lamps, has been announced recently by the commerical engineering department of the Westinghouse Lamp Division, Bloomfield, New Jersey. The latest addition to the seven available fluorescent colors is a combination of daylight and pink phosphors--approximately two parts daylight to one part pink. Soft white lamps are obtainable in 15, 20, 30, and 40 watt sizes. Richer in red light, the new color makes vegetables, meats, and other foods look better than do standard white or daylight colors. Soft white is also flattering to all skin colorings and is therefore adapted to use in night clubs, hotels, etc.

New Vacuum Tubes

Announcement of several new tubes marketed recently by the RCA Manufacturing Company, Inc., RCA Radiotron Division, Harrison, New Jersey, follows:

3S4; intended for use in the output stage of light-weight a.c./d.c./battery-operated portable equipment. This new tube has essentially the same characteristics as the miniature type 1S4 but is designed with a filament having a center tap to permit either a series-filament or a parallel-filament operating arrangement. The series arrangement requiring only 50 milliamperes has been provided especially for equipment utilizing a source of rectified power for the filament supply.

815; new push-pull beam power amplifier designed for radio amateur use at ultra-high frequencies. Its exceptional efficiency and high power sensitivity permit full power input with low driving power, according to the manufacturers. A single 815 is useful in push-pull class C telegraph service where it is capable of handling a power input of 75 watts with less than $\frac{1}{4}$ watt of driving power at frequencies as high as 150 megacycles; it is also adapted for use as a modulator and as a multiplier. Mechanical features of the 815 include its balanced and compact structure of twin beam units, close electrode spacing, short internal leads to minimize lead inductance and resistance, and a "micanol" wafer octal base. The heaters of the tube are arranged for either 12.6- or 6.3-volt operation.

826; transmitting triode designed especially for use at ultra-high frequencies. It may be used as an oscillator, r.f. power amplifier, and frequency multiplier at maximum ratings at frequencies as high as 250 megacycles and at reduced ratings at frequencies up to 300 megacycles. Maximum plate dissipation of the 826 is 60 watts in class C telegraph service. The 826 features a double-helical filament center-tapped within the tube so that effects of filament inductance can be minimized. In addition, two short heavy leads are brought out from the grid and from the plate to individual terminals in order to reduce the inductance of these internal connections. All terminals are placed at one end of the bulb so that short leads can be used in neutralizing circuits.

866-A/866; a half-wave, mercury vapor rectifier to supersede the RCA types 866-A and 866. It is designed to withstand high peak inverse voltage and to conduct at relatively low applied voltage. This new tube employs a ceramic cap insulator and is constructed in a dome-top bulb. An edgewise wound ribbon filament made of a new alloy material is said to provide a large emission reserve and improved life. Two 866-A/866's operating in a full-wave rectifier are capable of delivering to the input of a choke-input filter a rectified voltage of 3180 volts at 0.5 ampere with good regulation.

BROAD PLATEAU GEIGER-MUELLER TUBES

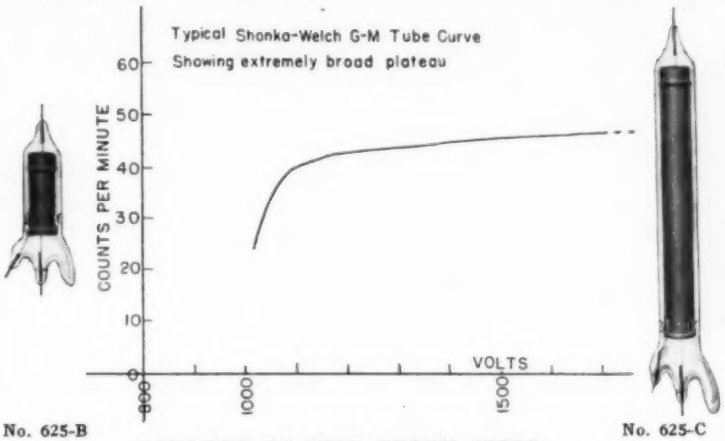

No. 625-B

No. 625-C

By
Professor Francis R. Shonka
DePaul University
Chicago

SALIENT FEATURES:

Extremely Wide Plateau.

Eliminates the need for highly stabilized voltage supply.

High Efficiency and Reliability.

OFFERED IN TWO STOCK SIZES:

No. 625B—short tube, 60 mm long.....each, $25.00
No. 625C—long tube, 180 mm long.....each, $30.00

Special sizes available on order.

For full information, write

W. M. Welch Scientific Company

Established 1880

1515 Sedgwick Street Chicago, Illinois, U.S.A.

WELCH

Catalog lists over 10,000 items for Science Laboratories

IMPROVED "SPOTLIGHT" GALVANOMETERS

Rubicon MULTIPLE REFLECTION galvanometers have recently been improved through a redesign of the optical system. The definition of the line-image is now so sharp that readings can be estimated to .1 of a millimeter division.

These sturdy, self-contained galvanometers are available with sensitivities as high as .0006 microampere per millimeter. The scales, which are 100 mm. long, are remarkably proportional. Send for Bulletin 320.

RUBICON COMPANY

ELECTRICAL INSTRUMENT MAKERS

Ridge Ave. at 35th Street Philadelphia, Pa.

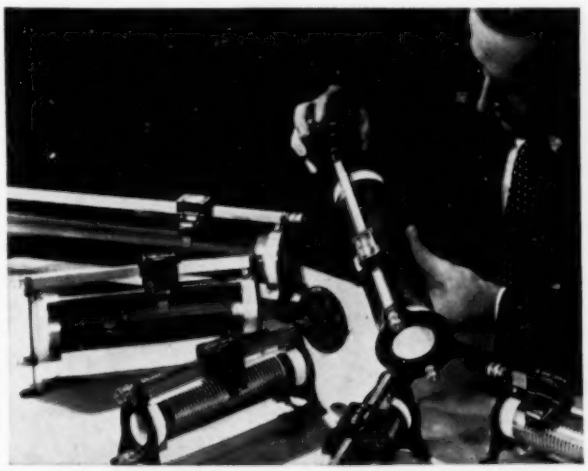

JAGABI "LUBRI-TACT" LABORATORY RHEOSTATS

Lubricated sliding contact. Four sizes, seventy-six different ratings carried in stock.

Also Compression Carbon Rheostats.

Bulletin 1620-R.

JAMES G. BIDDLE CO.

ELECTRICAL AND SCIENTIFIC INSTRUMENTS

1211-13 ARCH STREET PHILADELPHIA, PA.

1625; transmitting beam power amplifier, similar to RCA-807. The 1625 has a 12.6-volt heater and a 7-pin base, and is therefore particularly suitable for use in aircraft radio transmitters. High power sensitivity makes this new tube especially useful in frequency multiplier service where high harmonic output is essential; it may also be used as a crystal oscillator and buffer amplifier in medium power transmitters with an input up to a half-kilowatt. The 1625 can be operated at maximum ratings at frequencies as high as 60 megacycles and at reduced ratings at frequencies as high as 125 megacycles; its maximum plate dissipation rating is 30 watts (ICAS).

1626; transmitting triode of the indirectly heated type with 12.6-volt heater, designed especially for r.f. oscillator service and particularly suitable for use in aircraft radio transmitters. The maximum plate dissipation is 5 watts. This tube may be operated at maximum ratings at frequencies as high as 30 megacycles, and at reduced ratings at frequencies as high as 90 megacycles.

Complex Computing Machine

An electrical calculating machine which will carry out computations with complex numbers, and which can be operated from a distance over a telegraph circuit, has been devised and is installed in the Bell Telephone Laboratories in New York City. This machine was described and demonstrated by Dr. G. R. Stibitz of the Bell Telephone Laboratories before the September meeting of the Mathematical Association of America at Dartmouth College, Hanover, New Hampshire. Figure 1 shows the keyboard and printer, and Fig. 2 the relays and crossbar switches of the complex computer, which is constructed entirely of standard telephone apparatus with computing elements consisting of relays and crossbar switches such as are used to connect subscribers in the most modern type of dial exchange.

FIG. 1. Keyboard and printer of the Bell Telephone Laboratories' complex computing machine.

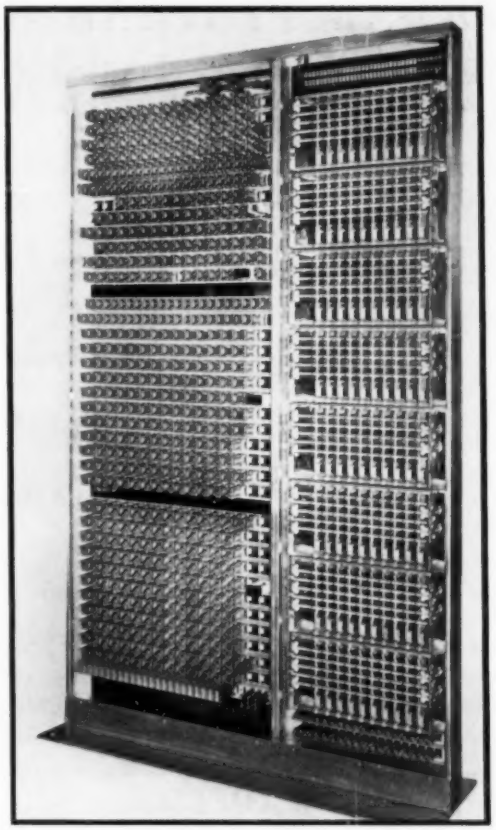

FIG. 2. Relays and crossbar switches.

The operator sits at a teletypewriter, which may be located at any convenient place, and presses keys to record the numbers and the operation to be performed on them; i.e., whether they are to be divided, multiplied, etc. In the recent demonstration the teletypewriters and keyboard were installed in Hanover and connected to the calculating machine in New York by a two-way telegraph circuit; thus the calculations were carried out on a machine 200 miles away from the calculator. In this demonstration, the multiplication of two eight-digit complex numbers required about 40 seconds, measured from the time the first key was pressed until the answer was printed on the teletypewriter.

Junior VoltOhmyst

The Rider VoltOhmyst circuit, providing a push-pull electronic d.c. voltmeter-ohmmeter with a resistance range ratio for engineering and servicing requirements, has been applied to a compact, lower cost instrument known as the RCA Junior VoltOhmyst, recently put on the market by the RCA Manufacturing Company, Inc., Camden, New Jersey. This instrument is useful for servicing radio and television receivers, transmitters, aircraft radio, sound amplification and reinforcement systems,

Send for this Complete Catalog

6 New Polaroid* Laboratory Products
Price Reductions as Great as 70%

This catalog announces new prices —and presents a new and complete line of Polaroid Laboratory Products: new standard Polaroid Polarizing Filters and Quarter-wave Plates; new kits, complete with accessories and instructional literature, including one for general all-round use, another adapted to the optical disc, and two for use on a common horizontal projection lantern with the new Polaroid Projector Polariscope — all important in giving students an insight into polarized light and its growing applications in everyday life.

For your copy of this catalog write your laboratory supply house or Division 42

POLAROID CORPORATION
730 Main Street, Cambridge, Mass.

*T. M. Reg. U. S. Pat. Off.

THERMOCOUPLES for special uses

We manufacture many thermocouples with much higher electromotive force than is obtainable with the standard platinum-rhodium vs platinum couple.

A few typical couples are:

COUPLE	E. M. F., microvolts per °C in range 0-100°C.
Pt-Ir vs Au-Pd	47
Chromel P vs Au-Pd	63
Silver vs Bismuth	76
Bismuth-Tin vs Bismuth	126

These are for use at moderate temperatures only and the e.m.f's, cannot be guaranteed. They are supplied in all wire sizes.

Complete information will be furnished on request.

BAKER & CO., INC.
PLATINUM
113 Astor Street Newark, N. J.

RECERTIFICATION *of* STANDARD CELLS

Industry is continually demanding more and more accuracy from science. With proper treatment your Eppley precision type standard cells will meet this demand, but we wish to point out that according to authoritative sources the emf of cadmium cells should be redetermined at intervals of not more than two years.

In this connection we are pleased to offer the services of a finely equipped laboratory and a competent personnel. Our saturated standards, maintained in closely controlled oil baths, are regularly compared with the national standards at the National Bureau of Standards in Washington.

We will be pleased to examine and report on the condition of your cells without charge. For recertification a charge of Three Dollars ($3.00), plus postage and insurance is made. Approximately two weeks should be allowed for recertification.

EPLAB
THE EPPLEY LABORATORY, INC.
SCIENTIFIC INSTRUMENTS
NEWPORT, R.I.
U. S. A.

facsimile and other types of equipment. Its features are similar to the laboratory type RCA 163 VoltOhmyst, with the addition of an isolated a.c. voltmeter circuit.

The input resistance for measuring d.c. voltages is constant at 11,000,000 ohms, allowing voltages to be read in high resistance circuits. On the 3-volt scale this gives a meter with a sensitivity of 3,666,666 ohms per volt. The d.c. voltmeter circuit has six ranges: 0 to 3, 10, 30, 100, 300, and 1000 volts. The isolated a.c. voltage measurements are read on five scales: 0 to 10, 30, 100, 300, and 1000, with a sensitivity of 1000 ohms per volt.

Electronic Developments Demonstrated at Conference

First public demonstration of beam transmission of power with the Klystron, newly developed electronic tube for generation of ultra-high-frequency radio waves, was made before a meeting of more than 125 eastern educators October 18 at the Westinghouse Lamp Division, Bloomfield, New Jersey. The tube demonstrated generates radio waves 40 centimeters long at a power output of about 150 watts. A high degree of stability is achieved by the use of cavity resonators, a new principle in communication engineering.

Other instruments and discoveries demonstrated and discussed at the Conference included the following:

Recently devised ultra-high speed x-ray tubes, developed by Drs. Charles M. Slack and L. F. Ehrke of the Westinghouse Lamp Division Research Laboratories. These make possible x-ray pictures taken in one one-millionth of a second. Pictures may be taken at the proper angle for stereoscopic vision, a development of particular importance in studying interior structures.

Newest discoveries in bactericidal ultraviolet, presented to the Conference by Dr. Harvey C. Rentschler, Director of Research of the lamp laboratories. A motion picture of the Sterilamp's "death rays" in action killing dreaded typhoid germs was shown.

Advances in fluorescent lighting, discussed by Dr. J. W. Marden, Assistant Director of Research in the Westinghouse lamp laboratories. Dr. Marden showed four unique fluorescent lamps made in the shape of blue donkeys and pink elephants, laboratory curiosities indicative of the work now going on to develop fluorescent lamps in all shapes and sizes.

A 10,000-watt water-cooled mercury vapor lamp which has a light-emitting heart the size of a pencil, shown by Samuel G. Hibben, Westinghouse Director of Applied Lighting. This lamp is one-fifth as bright as the surface of the sun.

Instrument Booklets

"Radio-frequency characteristics of decade resistors," an article illustrated with photographs and graphs, is contained in the December, 1940, issue of *The General Radio Experimenter*, published by the General Radio Company, 30 State Street, Cambridge, Massachusetts.

"Alchemy in action" heads an account of the Conference on Applied Nuclear Physics and is followed by "Harvest home," a brief history of research in agriculture and introduction of recommended procedures on the farms of Ohio, in the November issue of *Science and Appliance*. The December issue of this leaflet features an article on "Better Christmas greens," and another on "Live with a dog and like it." *Science and Appliance* is a publication of The Ohio State University Research Foundation.

Announcement of the addition of the Pope Collection of Alchemical and Historical Pictures to the Fisher Collection in Pittsburgh, is made in the Vol. 12, No. 2 issue of *The Laboratory*, publication of the Fisher Scientific Company, Pittsburgh, Pennsylvania. The Sir William Jackson Pope Collection was the most complete of its kind abroad and was well known to both artists and scientists in England and on the Continent; it was brought from England this fall.

The American Society of Heating and Ventilating Engineers, 51 Madison Avenue, New York City, has compiled a booklet, *Outline of Research Facilities and Bibliography of Research Reports*, listing engineering data available through the Society's various channels of publication, and organized and experienced research laboratory facilities for investigating special heating, ventilating and air conditioning engineering problems. "For those engineers and technicians who are now coordinating the national effort through the numerous channels of the Government defense program this brochure is presented for assistance in quickly locating technical data and research information on various phases of heating, ventilating and air conditioning," according to the statement of A. E. Stacey, Jr., a member of the Society's Committee on Research.

Defending its 87-year-old record on national defense, the Bausch and Lomb Optical Company, Rochester, New York, issued recently a 16-page booklet, *Bausch and Lomb and Our National Defense*. It contains laudatory letters from Secretaries Stimson and Knox of the War and Navy Departments and forms a refutation of attacks on the Company's loyalty and patriotism engendered by the indictment which charged restraint of trade in military optical instruments.

A 28-page catalog issued recently by Leeds and Northrup Company lists everything needed to check thermocouple pyrometers. It illustrates and describes portable equipment for plant tests under actual operating conditions, and also the laboratory apparatus to standardize it. A copy of this catalog may be obtained by writing Leeds and Northrup Company, 4934 Stenton Avenue, Philadelphia, Pennsylvania, and requesting Catalog E-33A-503.

LOW REFLECTION SURFACES

We are now prepared to produce low reflecting surfaces on a commercial basis by the high-vacuum distillation of metallic fluorides.*

By reducing the usual 4% reflection loss at each glass-air surface, a substantial improvement can be made in the light transmission and image forming characteristics of any optical system.

NATIONAL RESEARCH CORPORATION
100 BROOKLINE AVENUE
BOSTON, MASS.

* U. S. Pat. 2,207,656

Linde
RARE GASES AND MIXTURES
NEON
ARGON
HELIUM
KRYPTON
XENON
MIXTURES

. . . Spectroscopically Pure
. . . Easily removed from bulb without contamination

Scientific uses for Linde rare gases include—
1. The study of electrical discharges.
2. Work with rectifying and stroboscopic devices.
3. Metallurgical research.
4. Work with inert atmospheres, where heat conduction must be increased or decreased.

Many standard mixtures are available. Special mixtures for experimental purposes can be supplied upon request.

The word "Linde" is a trade-mark of
The Linde Air Products Company
Unit of Union Carbide and Carbon Corporation
30 East 42nd Street New York, N. Y. UCC Offices in Principal Cities

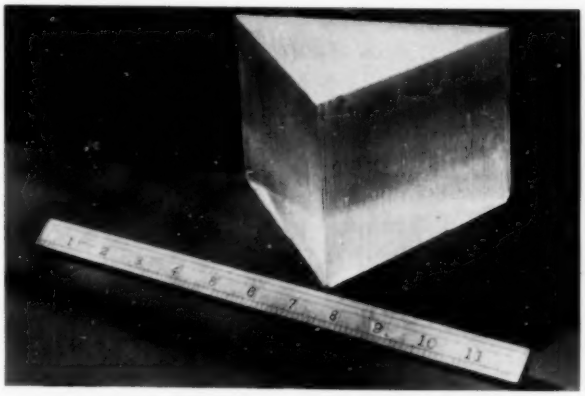

An eight pound rock salt prism blank cut from a twenty-five pound single crystal

May we send you a reprint of the recent publication—

SYNTHETIC OPTICAL CRYSTALS

published in Industrial and Engineering Chemistry Vol. 32, page 1478, November 1940.....Write to

THE HARSHAW CHEMICAL CO.
SPECIAL PRODUCTS DIVISION CLEVELAND, OHIO

TIME STANDARD
Tuning Fork Controlled

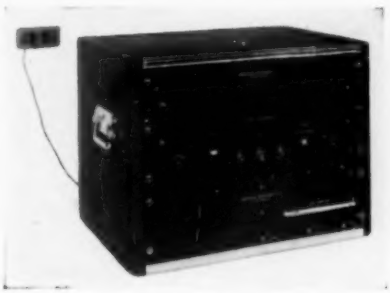

A complete, self-contained, stable, fixed-frequency power oscillator for the following uses:
★ Driving galvanometers for oscillographs, oscillograph cameras, etc.
★ Driving synchro-chronographs.
★ A time standard for adjusting watches, clocks, motors, generators, etc.
★ A source of modulating current for signal generators and radio beacons.
★ A source of constant frequency sine-wave voltage for all types of a-c. bridge circuits.
★ Geophysical and structural explorations.
★ Wherever an alternating-current of constant and known frequency is desired.

Fully Described in Bulletin AP 2089

AMERICAN INSTRUMENT CO.
8010 GEORGIA AVENUE · SILVER SPRING, MARYLAND

New, Simple, Handy, **OHMITE**
Ohm's Law Calculator

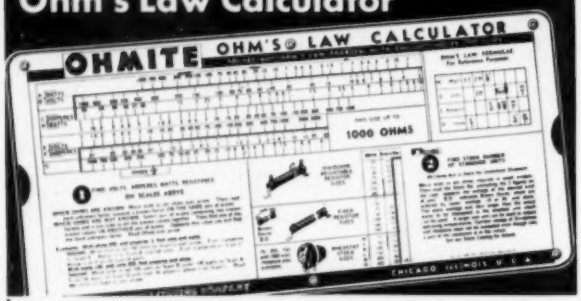

Solves any Ohm's Law Problem with one setting of the slide!

● All values are direct reading. Covers the current and wattage range for motors, generators, lamps, electrical apparatus and other applications up to 100 amperes or 1000 watts. Convenient Stock Unit Selector tells the stock number of the resistor or rheostat you may need Size 4-1/8" x 9". Send for it today — write on company letterhead giving name and position, and enclose 10c in coin to cover cost of handling.

OHMITE MANUFACTURING COMPANY
4889 Flournoy Street, Chicago, U. S. A.

Be Right with **OHMITE**
RHEOSTATS • RESISTORS • TAP SWITCHES

Serving the **REFRIGERATION INDUSTRY**

HYDRON
METALLIC BELLOWS
produced hydraulically
BY
CLIFFORD MANUFACTURING CO.
564 E. FIRST STREET, BOSTON
BOSTON CHICAGO DETROIT LOS ANGELES
PRODUCERS OF BELLOWS EXCLUSIVELY
SERVING AUTOMATIC CONTROL MANUFACTURERS
COMPLETE ENGINEERING SERVICE

INDEX TO ADVERTISERS

Name	*Page*
AMERICAN INSTRUMENT COMPANY ..... Ion Type X-Ray Tube. Powder Spectrum Diffraction Cameras. Scientific Instruments and Supplies.	ix
BAKER & COMPANY, INC. ..... Platinum, palladium, gold, and silver, and their alloys, in wire and sheet form. Laboratory ware and special apparatus.	vii
JAMES G. BIDDLE COMPANY ..... "Jagabi" Rheostats; Adam Hilger and Kipp & Zonen Optical Instruments; "Pointolite" Lamps; Electrical Testing and Speed-measuring Instruments.	v
CENTRAL SCIENTIFIC COMPANY .....Cover 4 Manufacturers of Cenco Physical Apparatus and Instruments to meet all requirements of University, College and High School Physics Laboratories. Specializing in high vacuum pumps and development of instruments and apparatus for various sciences.	
CLIFFORD MFG. COMPANY ..... Hydron metallic bellows for temperature and pressure control devices. Data for engineers.	x
EASTMAN KODAK COMPANY ..... Purified Organic Chemicals for research purposes; Plates for Photography, Photomicrography, Spectroscopy, Photometry, Astronomy; Wratten Light Filters; Cameras and Films.	iii
THE EPPLEY LABORATORY, INC. ..... Standards of e.m.f. (standard cells). Precision electrical instruments; potentiometers, bridges, temperature bridges, volt boxes. Thermopiles and pyrheliometers.	vii
GENERAL RADIO COMPANY ..... Manufacturers of electronic measuring instruments; vacuum-tube voltmeters, amplifiers and oscillators; wave analyzers, noise meters and analyzers, stroboscopes; laboratory standards of capacitance, inductance and frequency; impedance bridges, decade resistors and condensers; air condensers and variable inductors; rheostats, Variacs, transformers; other laboratory accessories.	ii
HARSHAW CHEMICAL COMPANY ..... Optical Lithium Fluoride grown in single crystal to predetermined size. Industrial Chemicals.	ix
LEEDS & NORTHRUP COMPANY ..... Manufacturers of Galvanometers, Resistors, Bridges, Condensers, Inductances, Potentiometers, Testing Sets; Temperature Measuring, Recording and Controlling Apparatus; Instruments for Measuring and Controlling Conductivity of Electrolytes and Hydrogen Ion Concentrations.	i
THE LINDE AIR PRODUCTS COMPANY ..... Oxygen, Argon, Helium, Krypton, Neon, Xenon, Rare Gas Mixtures, Nitrogen, Hydrogen, Calcium Carbide, Acetylene, equipment for Oxy-Acetylene welding and cutting.	ix
MCGRAW-HILL BOOK COMPANY, INC.	iii
NATIONAL RESEARCH CORPORATION ..... Specialists in industrial applications of high vacuum in the fields of physics and chemistry; research, design, consulting; low reflecting glass surfaces, special products produced under low pressure.	ix
OHMITE MANUFACTURING COMPANY ..... Manufacturers of close control rheostats, fixed and adjustable power resistors, precision and non-inductive resistors, attenuators, tapswitches and R.F. chokes.	x
POLAROID CORPORATION ..... Polaroid experimental kit for demonstrating Polarized light. Hand book.	vii
RUBICON COMPANY ..... Galvanometers, electrometers, potentiometers, Wheatstone and Kelvin bridges, resistance boxes, hydrogen ion and conductivity apparatus.	v
W. M. WELCH SCIENTIFIC COMPANY ..... Scientific instruments—laboratory apparatus. Catalog lists 10,000 items.	v